FAKULTÄT FÜR MEDIZIN

LEHRSTUHL FÜR KINDER- UND JUGENDMEDIZIN

GENERATION OF EWING'S SARCOMA ANTIGENS CHM1- AND EZH2-SELECTIVE AND HLA-A*0201-RESTRICTED T-CELL RECEPTOR TRANSGENIC T CELLS

Franziska Blaeschke

Vollständiger Abdruck der von der Fakultät für Medizin der Technischen Universität München zur Erlangung des akademischen Grades eines

Doktors der Medizin

genehmigten Dissertation.

Vorsitzender: Univ.-Prof. Dr. E. J. Rummeny

Prüfer der Dissertation:

1. Univ.-Prof. Dr. S. Burdach

2. Univ.-Prof. Dr. U. A. D. Behrends

Die Dissertation wurde am 10.06.2015 bei der Technischen Universität eingereicht und durch die Fakultät für Medizin am 06.04.2016 angenommen.

“TO MYSELF I AM ONLY A CHILD PLAYING ON THE BEACH,

WHILE VAST OCEANS OF TRUTH LIE UNDISCOVERED BEFORE ME”

(Isaac Newton)

1 Abbreviations

ACT	Adoptive T cell therapy
AEC	3-Amino-9-ethyl-carbazole
AES	Advanced Ewing’s sarcoma
ALL	Acute lymphoblastic leukemia
Allo-SCT	Allogeneic stem cell transplantation
APC	Allophycocyanin
APC	Antigen-presenting cell
Auto	Autologous
BCP	1-Bromo-3-Chloro-Propan
BM	Bone marrow
Bp	Base pair
BSA	Bovine serum albumin
CAIX	Carbonic anhydrase IX
CAR	Chimeric antigen receptor
CB	Cord blood
CD	Cluster of differentiation
cDNA	Copy deoxyribonucleic acid
CDR	Complementarity-determining regions
CEA	Carcinoembryonic antigen
CHM1	Chondromodulin 1
CLL	Chronic lymphocytic leukemia
CM	Central memory
CR	Complete remission
CTA	Cancer testis antigen
CTL	Cytotoxic T lymphocyte
DC	Dendritic cell
DEPC	Diethylpyrocarbonat
DLI	Donor lymphocyte infusion
DMEM	Dulbecco's modified eagle's medium
DMF	Dimethylformamide
DMSO	Dimethyl sulfoxide

DNA	Deoxyribonucleic acid
dNTP	Deoxynucleoside triphosphate
DPBS	Dulbecco's phosphate-buffered saline
E/T	Effector/ target
Eff	Effector
ELISpot	Enzyme-linked immunosorbent spot
ERG	ETS-related gene
ES	Ewing’s sarcoma
ESFT	Ewing’s sarcoma family tumor
ET	Ewing tumor
ETS	E26 transformation-specific
ETV1	ETS translocation variant 1
Euro-EWING 99	European Ewing tumor working initiative of national groups
EWS	Ewing’s sarcoma oncogene
EZH2	Enhancer of Zeste, Drosophila, Homolog 2
FACS	Fluorescent activated cell sorting
FBS	Fetal bovine serum
FCS	Fetal calf serum
FISH	Fluorescent in situ hybridization
FITC	Fluorescein isothiocyanate
FLI1	Friend leukemia integration
FLU	Influenza peptide
Forw	Forward
FT	Foetal tissue
GFP	Green fluorescent protein
GM-CSF	Granulocyte macrophage colony-stimulating factor
GMP	Good manufacturing practice
Gp100	Glycoprotein 100
GvHD	Graft-versus-host disease
GvT	Graft versus tumor
HBSS	Hank's balanced salt solution
HEPES	Hydroxyethylpiperazine-ethanesulfonic acid

HLA	Human leukocyte antigen
ICE	Ifosfamide, Carboplatin, Etoposide
IFN	Interferon
IgG	Immunoglobulin G
IL	Interleukin
LCL	Lymphoblastoid cell line
LDH	Lactate dehydrogenase
LIPI	Lipase I
mAb	Monoclonal antibody
MACS	Magnetic activated cell sorting
MART1	Melanoma antigen recognized by T cells 1
ME	Melphalan, Etoposide
MEM	Minimum essential medium
Meta-EICESS	Meta European intergroup cooperative Ewing's sarcoma study
MHC	Major histocompatibility complex
mRNA	Messenger ribonucleic acid
MSC	Mesenchymal stem cell
Mu	Murinized
NEAA	Non-essential amino acid
NGS	Next generation sequencing
NTC	Non-template control
Opt	Optimized
PB	Peripheral blood
PBMC	Peripheral blood mononuclear cell
PcG	Polycomb
PCR	Polymerase chain reaction
PE	Phycoerythrin
Pen Strep	Penicillin, Streptomycin
PFA	Paraformaldehyde
PGE2	Prostaglandin E2
PNET	Primitive neuroectodermal tumor
PR	Partial remission
Rev	Reverse

RNA	Ribonucleic acid
RT-PCR	Real-time polymerase chain reaction
SCT	Stem cell transplantation
StC	Stem cell
TAA	Tumor-associated antigen
TAP	Transporter associated with antigen processing
TC	Docetaxel, Cyclophoshamide
TCR	T-cell receptor
TI	Docetaxel, Ifosfamide
TIL	Tumor-infiltrating lymphocyte
TNF	Tumor necrosis factor
TSA	Tumor-specific antigen
TT	Topotecan, Treosulfan
VIDE	Vincristine, Ifosfamide, Doxorubicin, Etoposide
VIE	Vincristine, Ifosfamide, Etoposide

2 INTRODUCTION

2.1 EWING'S SARCOMA

INTRODUCTION. The Ewing's sarcoma (ES) is a highly malignant tumor of the bone or soft tissue. Histologically, ES are assigned to the heterogeneous group of pediatric small round cell tumors, furthermore consisting of neuroblastoma, rhabdomyosarcoma, lymphoma and others (Delattre, Zucman et al. 1994). Holding an incidence of three per one million in children younger than 15 years, ES constitute the group of second most common primary bone malignancies in childhood and adolescence after osteosarcoma. The median age of patients with ES is 15 years, male patients are more often diagnosed than female patients (rate of 3:2). 95 % of patients with ES are Caucasian, the incidence of ES in the African or Asian population is ten fold fewer. The reason for this phenomenon can be found in the process of evolution. Intron six of ES-pathognomonic EWS gene was observed to expand progressively until five million years ago. As a result of recombination between Alu sequences, the length of EWS gene more recently was decreased by more than 2000 base pairs. This effect was only seen in certain populations (such as the African population) and goes along with the lowest incidences of ES (Zucman-Rossi, Batzer et al. 1997).

HISTOLOGY AND ORIGIN. James Ewing first described ES in 1921 as "diffuse endothelioma of bone" (Ewing 1972). In the meanwhile microarray analyses proved that ES do not only display endothelial features but also neuroectodermal and mesenchymal characteristics (Staege, Hutter et al. 2004) Early evidence hinted on a neuroectodermal origin of the ES stem cell (Cavazzana, Miser et al. 1987). In contrast, it was shown that the fusion protein EWS-FLI1 itself holds the capability to induce neuroectodermal differentiation. Thus, it was speculated that the neuroectodermal features may simply be caused by EWS-FLI1 expression (Ross, Smyth et al. 2013). Further studies identified mesenchymal stem cells (MSC) as strong candidates for the cellular

progenitor of ES (Riggi, Suva et al. 2009) (Takashima, Era et al. 2007) (Tirode, Laud-Duval et al. 2007) (Potikyan, France et al. 2008) (Riggi, Cironi et al. 2005). Nevertheless, until now, the cell of origin remains a matter of debate. Taken together, strong evidence exists that the ES stem cell originates from a more undifferentiated cell of the endothelial, neuroectodermal or even chondro-osseous lineage which is arrested at transition to the mesenchymal endothelial development (Richter, Plehm et al. 2009) (Hauer, Calzada-Wack et al. 2013)

It was shown that EWS-FLI1 can induce transformation of bone marrow-derived MSC and transform them to ES-like tumors (Riggi, Suva et al. 2008) (Potikyan, France et al. 2008). However, when human MSC were infected with a virus containing the EWS-FLI1-specific translocation, a full transformation to ES was not detectable in mouse models (Miyagawa, Okita et al. 2008).

For this reason, specific other mutations seem to be inevitable for ES growth, such as the inactivation of p53 and other tumor suppressor genes (Mackintosh, Madoz-Gurpide et al. 2010) (Lessnick, Dacwag et al. 2002) (Neilsen, Pishas et al. 2011).

GENETICS. ES are defined by the presence of chromosomal translocations between the EWS gene on chromosome 22 and genes of the ETS oncogene family (Burchill 2003) (Mackintosh, Madoz-Gurpide et al. 2010). EWS is supposed to be a ribonucleic acid- (RNA-) binding protein belonging to the TET family. It is expressed ubiquitously and stable throughout the cell cycle and the transcribed messenger ribonucleic acid (mRNA) presents a long half-life (Mackintosh, Madoz-Gurpide et al. 2010). These features may identify EWS as a housekeeping gene, the protein itself is supposed to function as a transcription factor. In contrast, ETS genes are a group of oncogenes characterized by a special DNA binding domain, the ETS domain (Delattre, Zucman et al. 1992) (Sharrocks 2001). Oncogenes such as ERG, EWS and TEL were allocated to this family (Mackintosh, Madoz-Gurpide et al. 2010) (Jedlicka 2010).

The most common rearrangement is seen in 85 % of patients and constitutes a translocation between EWS and FLI1 oncogene, t(11;22)(q24;q12) (Delattre,

Zucman et al. 1994) (Zucman, Melot et al. 1993). This abnormality results in the production of the fusion protein EWS-FLI1. EWS-FLI1 acts as a regulator of transcription and regulates the expression of a variety of genes (Chaturvedi, Hoffman et al. 2012). In contrast, affecting 15 % of the patients, the second most frequent translocation t(21;22)(q22;q12) is responsible for the fusion of EWS with the ERG protein. Rearrangements of EWS with other members of ETS oncogene family (such as ETV1, E1AF and FEV) are also described. Genetic variability of ES is determined not only by the binding partner of EWS but also by the location of the translocation breakpoint (Mackintosh, Madoz-Gurpide et al. 2010). Besides the fact that these rearrangements between EWS and ETS genes are pathognomonic for ES, many other mutations are found in this tumor entity (such as p53 and ras mutations) (Huang, Illei et al. 2005).

CLINCAL PRESENTATION AND DIAGNOSIS. Although some ES (15 %) arise in the extra-skeletal soft tissue, most ES originate from the bone. They are typically found in the diaphysis of long bones, the pelvis or the axial skeleton and ribs (Bernstein, Kovar et al. 2006).

Regarding the clinical presentation, pain and swelling are often reported as a first symptom. Because ES share many morphological and immune-phenotypic characteristics with other tumor entities, chromosome analyses are inevitable for diagnosis. The detection of the typical chromosomal translocations by polymerase chain reaction (PCR) and fluorescence *in situ* hybridization (FISH) constitutes the ES-specific criterion. The most reliable immunohistochemical marker for ES is CD99, as it is found in 99 % of ES - although it is also expressed by other tissues and therefore not specific for ES (Llombart-Bosch, Machado et al. 2009) (Pinto, Dickman et al. 2011).

PROGNOSIS. 25 % of ES are initially metastatic often involving lung, bone and bone marrow. The presence of metastases at the time-point of diagnosis is the most significant independent adverse prognostic factor. Bone or bone marrow metastases are accompanied with a worse prognosis than lung metastases. While patients with localized disease show a disease-free survival

rate of approximately 70 % after multimodal therapy, patients with metastatic disease at diagnosis hold an overall survival rate of less than 30 % (Hawkins, Felgenhauer et al. 2002) (Burdach, Thiel et al. 2010). The overall survival rate of patients with residual or recurrent ES is 10 % (Kovar, Alonso et al. 2012) (Kelleher and Thomas 2012). Taken together, the worst risk-group is formed by patients with primary bone or bone marrow (BM) metastases and early (< 24 months after diagnosis), multiple or multifocal relapse (in our context defined as >= 3 bone metastases or BM infiltration) (Cotterill, Ahrens et al. 2000) (Paulussen, Ahrens et al. 1998, Paulussen, Ahrens et al. 1998) – the so-called advanced ES (AES) (Burdach and Jurgens 2002, Burdach, Meyer-Bahlburg et al. 2003) (Burdach 2004). Other negative prognostic factors are bulky primary tumors exceeding 100 cm^3, patient's age older than 15 years at diagnosis, tumors of axial skeleton, high serum lactate dehydrogenase (LDH) levels at diagnosis and poor response to induction therapy. The degree of neuroectodermal differentiation does not seem to have any prognostic value (Rodriguez-Galindo, Spunt et al. 2003).

THERAPY. Successful treatment of ES patients requires a combination of systemic chemotherapy and local treatment (Thacker, Temple et al. 2005) (Bernstein, Kovar et al. 2006). Surgery is used as a local control for appropriate patients (Haeusler, Ranft et al. 2010) (Bacci, Ferrari et al. 2004). Patients with unresectable tumors or patients who would suffer from decreased functionality after resection, can profit from radiation therapy, although the risk of secondary neoplasms has to be taken into account (Dunst and Schuck 2004) (Donaldson 2004) (Schuck, Hofmann et al. 1998).

Standard frontline chemotherapy of ES consists of a combination of Vincristine, Ifosfamide, Doxorubicin and Etoposide (VIDE) (Juergens, Weston et al. 2006). Cyclophosphamide can be used in addition, as well as Dactinomycin (Paulussen, Craft et al. 2008). Unfortunately, the current frontline chemotherapy used for patients with localized disease provides only minimal benefit for patients with AES.

Therefore, patients with AES are introduced into different studies such as the Euro-EWING 99 (European Ewing tumor working initiative of national groups)

(Ladenstein, Potschger et al. 2010) or the Meta-EICESS (Meta European intergroup cooperative Ewing's sarcoma study) protocol. The Meta-EICESS protocol (see 7.8) consists of high-dose chemotherapy (Burdach and Jurgens 2002), as well as myeloablation (Burdach, Jurgens et al. 1993), possible subsequent autologous stem cell rescue and – if necessary and possible - a haplo-identical allogeneic stem cell transplantation (allo-SCT) (Thiel, Wawer et al. 2011) (Burdach, Thiel et al. 2010) (Burdach, van Kaick et al. 2000) (Koscielniak, Gross-Wieltsch et al. 2005) (Lucas, Schwartz et al. 2008) (Rosenthal, Bolotin et al. 2008). After allo-SCT and depending on the outcome and possible graft-versus-host disease (GvHD), other therapeutic strategies such as donor lymphocyte infusion or targeted therapy are considered (Hawkins, Felgenhauer et al. 2002).

After introduction of high-dose chemotherapy and SCT into the therapeutic protocols of AES patients, 5-year overall survival increased to 30 % - a number also demonstrating the urgent need of other therapeutic approaches (Lissat, Chao et al. 2012). In this context, one promising approach is the advancement of immunotherapy for ES patients, such as the adoptive T-cell therapy.

2.2 Adoptive T-cell therapy

Introduction. Within the last decades, immunotherapy and especially adoptive T-cell therapy (ACT) emerged as a potential therapeutic strategy in the treatment of cancer. Already in the early 1970ies, Burnet et al found the human immune system not only being able to recognize infectious-mediated particles, but also tumor cells (Burnet 1971). A milestone in the adoptive T-cell therapy was the finding that donor lymphocyte infusions are able to cause graft-versus-leukemia (GVL) effects in bone marrow-transplanted patients (Kolb, Schattenberg et al. 1995). In different solid tumor entities, the tumor mass was found to be invaded by T cells, the so-called tumor-infiltrating lymphocytes (TIL) (Husby, Hoagland et al. 1976). Evidence occurred that TIL exist in many tumor entities (such as colorectal cancer, melanoma, breast cancer, ovarian cancer and the Ewing's sarcoma). They are able to specifically react against tumor

cells and often even go along with a better prognosis (Deschoolmeester, Baay et al. 2010) (Haanen, Baars et al. 2006) (Baxevanis, Dedoussis et al. 1994) (Stumpf, Hasenburg et al. 2009) (Khong, Wang et al. 2004) (Berghuis, Santos et al. 2011). Until now, one approach of ACT uses TIL, which can be isolated and expanded *ex vivo* without regarding the antigen they are directed against. After the patient underwent lymphodepletion, the expanded TIL are re-infused to the patient (autologous setting). In this setting, Rosenberg et al showed durable cancer regression in patients suffering from metastatic melanoma after re-infusion of expanded melanoma-infiltrating T cells (Rosenberg, Yang et al. 2011). In the meantime, some other research groups were able to confirm the fact that the adoptively transferred TIL can cause long-time regression in patients with metastatic melanoma (Radvanyi, Bernatchez et al. 2012) (Itzhaki, Hovav et al. 2011) (Ellebaek, Iversen et al. 2012). Nevertheless, until now, melanoma constitutes the only tumor entity for which TIL have shown clinical effectiveness. Of course, this approach requires a pre-existing tumor mass and the presence of TIL in the tumor environment.

To overcome this frontier, Stauss et al introduced a method which is independent from the presence of TIL and instead uses T cells which were primed *in vitro* with specific antigens (Amrolia, Reid et al. 2003). In literature, for this purpose two groups of antigens are described: tumor-associated antigens (TAA) are peptides being overexpressed in the appropriate tumor entity in comparison to normal body tissue. While TAA can show little expression in normal tissues though, tumor-specific antigens (TSA) are more specific for the tumor and therefore demonstrate no expression in any of the tested normal tissues. Antigens of both groups can potentially be used as target antigens for T-cell therapy. After finding a suitable antigen, the method of Stauss includes the priming of T cells with the peptide by use of pulsed dendritic cells (DC) and the *in vitro* expansion of the now peptide-specific and HLA-restricted T cells. Afterwards, these T cells can be given to the patient in an autologous or allogeneic setting (Amrolia, Reid et al. 2003).

For ES, our group showed that these un-modified T cells are not successful in the autologous setting but mediate regression of tumor growth in a $Rag2^{-/-}\gamma_c^{-/-}$ mouse model when injected in the allogeneic setting (Thiel, Pirson et al. 2011). However, inclusion of these unmodified T cells into current therapy protocols is

limited due to high production complexity, low cell numbers and fading specificity of the T-cell clones after several generations. In order to overcome these obstacles and to facilitate good manufacturing practice (GMP) accredited off-the-shelf products in the future, several approaches were performed based on genetic modification of T cells. This modification is either done by introduction of a chimeric antigen receptor (CAR) (Sotomayor, Borrello et al.) or by transferring a specific T-cell receptor (TCR) into primary T cells.

CAR-MODIFIED T CELLS. CAR are hybrid receptors consisting of a cell surface molecule and a single-chain variable fragment taken from Fab fragment or a monoclonal antibody. These chimeric antigen receptors are artificially bound to the T-cell surface and are then capable of recognizing antigens without human leucocyte antigen (HLA) restriction. Within the last decades, CAR-modified T cells were constantly improved. Whereas the first generation did only contain one activation domain and therefore damaged the T-cell function, second and third generation CAR comprise two or three signaling domains and create more persisting immune responses (Davila, Brentjens et al. 2012). Recently, even forth generation CAR were described being capable of IL-12 secretion without prior conditioning (Chmielewski, Kopecky et al. 2011, Pegram, Lee et al. 2012). Until now, CAR were produced against a variety of cell surface antigens such as cluster of differentiation (Larkin, Lao et al.) 19, ERBB2 and CAIX. CD19 seems to constitute a very promising antigen in the treatment of B-cell leukemia and lymphoma as it is overexpressed in these malignancies and not found in normal body tissues except the B-cell line (Davila, Kloss et al. 2013). CD19-directed CAR-modified T cells were already found to eradicate B-cell tumors when injected into systemic tumor-bearing mice (Brentjens, Latouche et al. 2003). The first lymphoma patient who was successfully treated with CD19-specific CAR-modified T cells was published by Kochenderfer et al (Kochenderfer, Wilson et al. 2010). In the meantime, CD19-specific T cells caused clinical responses not only in patients with extensive lymphoma (Kochenderfer, Dudley et al. 2012), but also in some patients with chronic lymphocytic leukemia (CLL) (Kalos, Levine et al. 2011) (Porter, Levine et al. 2011) and acute lymphoblastic leukemia (ALL) (Brentjens, Davila et al. 2013) (Grupp, Kalos et al. 2013). In many of these cases, transient but severe side effects occurred due to elevated serum cytokine levels that in some cases

required a cytokine blockade with anti-TNF-α. To date, CD19-directed CAR-modified T cells are already included into a phase I/ II clinical study for refractory B-cell malignancies such as CLL and ALL (Xu, Zhao et al. 2013, Ramos, Savoldo et al. 2014). Since CAR do not recognize their antigens in an HLA-restricted manner, CAR-modified T cells are applicable for every patient without regarding major histocompatibility complex (MHC) haplotypes. On the other side, possible unspecific toxicity has to be taken into account, especially when CAR-modified T cells are infused in an allogeneic setting (Casucci and Bondanza 2011) (Cheadle, Gornall et al. 2014).

TCR-TRANSGENIC T CELLS. This thesis concentrates on the generation of TCR-modified cytotoxic T cells. The human TCR is very similar to the Fab fragment of immunoglobulins. TCR are a heterodimer of two different polypeptide chains termed α- and β-chain. Apart from these αβ-T-cell receptors, a γδ-receptor exists (5 % of T cells) but its role for immune response is not clear yet. The extracellular portion of both chains, the α- and the β-chain, contains a constant and a variable region (see Figure 1) (Kenneth Murphy 2008).

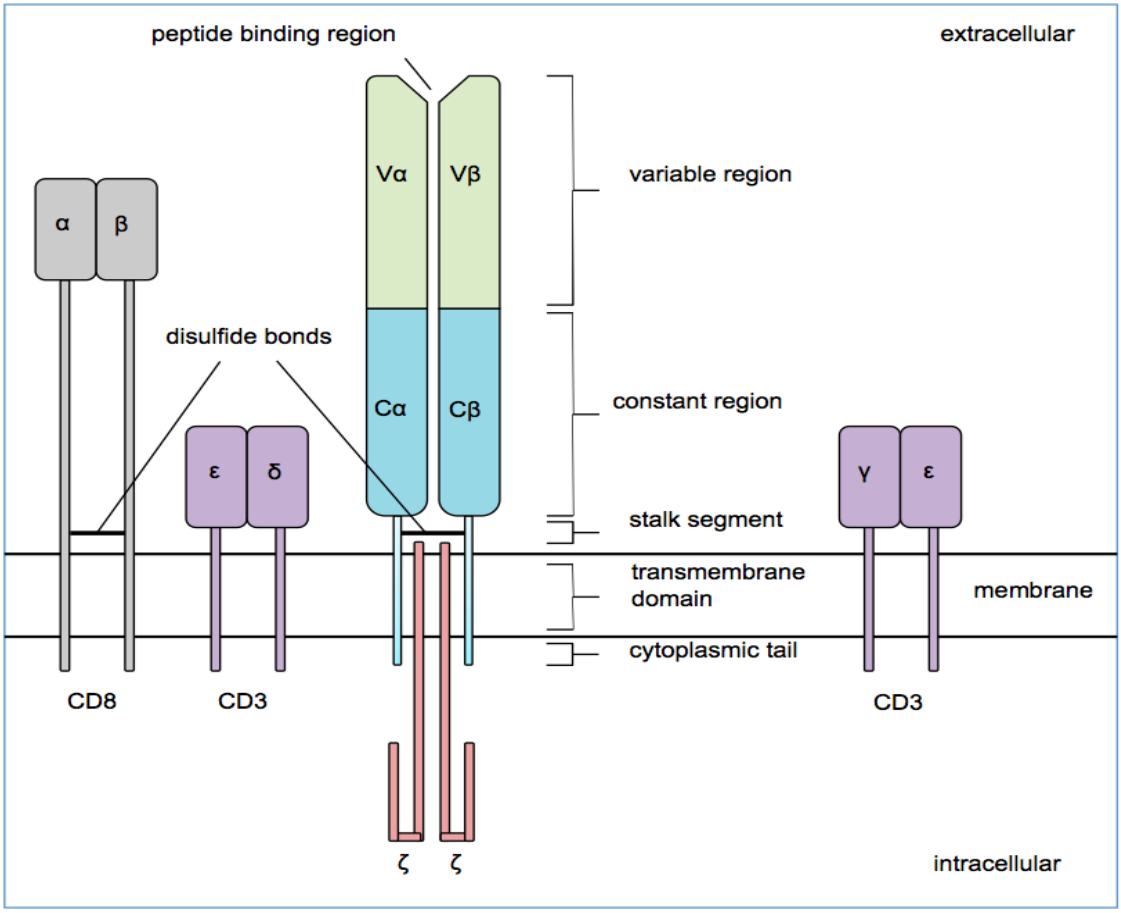

FIGURE 1 Schematic representation of human αβ-TCR complex with CD8. αβ-TCR consist of an α- and a β-chain. Each chain contains a variable region (Vα/β - with the peptide binding domain), a constant region (Cα/β), a stalk segment, a transmembrane domain and a cytoplasmic tail. Chains are linked via a disulfide bond between the stalk segments. Associated to the TCR are a ζ-homodimer and the invariant CD3 heterodimers consisting of an ε- and a δ- or γ-fragment. CD8 functions as the specific co-receptor for cytotoxic T cells and contains an α- and a β-chain which are also linked via a disulfide bond. (Figure modified from Janeway's Immunobiology (Kenneth Murphy 2008).)

The peptide-binding domain is located in the variable part of the receptor. Apart from the constant and variable region, each chain also includes a short stalk segment (analogous to the immunoglobulin hinge region), a transmembrane region and a cytoplasmic tail. The α- and the β-chain are linked via a disulfide bond in the hinge region. In cytotoxic T cells, the co-receptor of the TCR is CD8. Together with CD8, the TCR complex (consisting of the TCR itself, the ζ-chains and CD3 molecules) recognizes antigens being presented on MHC class I molecules.

Regarding the deoxyribonucleic acid (DNA)/ RNA encoding for the human TCR, the α-chain locus consists of a variable (V), a joining (J) and a constant region (C). The β-chain locus shows an additional diversity (D) region between V and J gene segments. While V, J and D regions encode for the variable domain of the TCR, the C domain is translated into the constant part of the TCR. Both chains also include three hypervariable so-called complementarity-determining regions (CDR) which constitute one reason for the huge TCR repertoire we find in the human immune system (see Figure 2). Another reason for this diversity can be seen in the development of the T cell, as the gene segments are joined by somatic recombination. The TCR α-chain was built by VJC-rearrangement, whereas the TCR β-chain was generated by VDJC-rearrangement (Kenneth Murphy 2008).

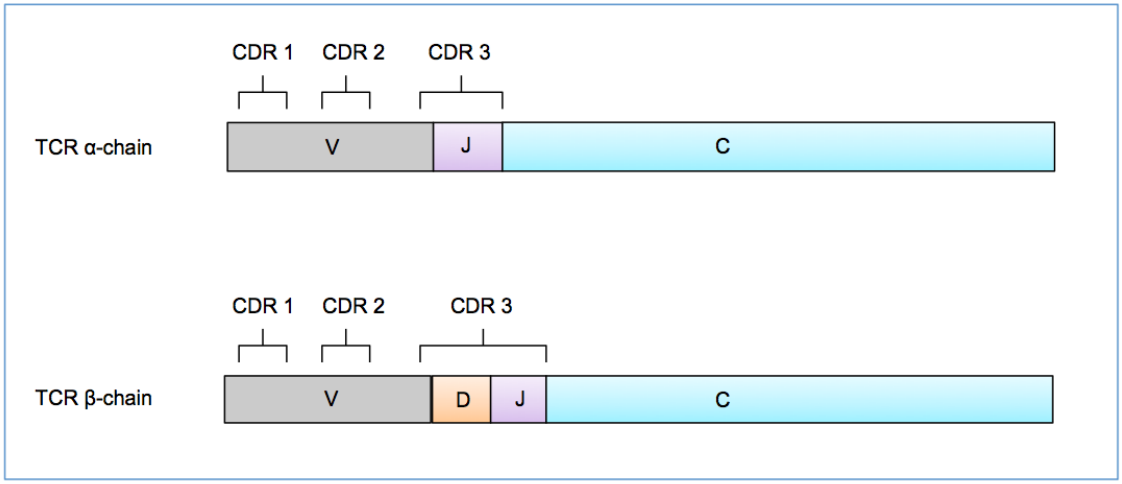

FIGURE 2 **Schematic representation of TCR RNA sequence.** The RNA sequence of the TCR α-chain consists of a variable (V), a joining (J) and a constant (C) region, whereas the TCR β-chain shows an additional diversity (D) region. The complementarity-determining regions (CDR) 1 and 2 are found in the variable chains, CDR 3 contains a part of V, the whole J and – if present – the whole D region. (Figure modified from Janeway's Immunobiology (Kenneth Murphy 2008))

The DNA/ RNA sequence of TCR which are specific for a tumor-associated antigen plays a crucial role in the process of generating TCR-transgenic T cells. In first approaches, the DNA sequence of MART-1- (melanoma-antigen-recognized-by-T-cells-1) specific TCR was identified and retrovirally transduced into primary T cells by the group around Rosenberg in 2006 (Morgan, Dudley et al. 2006). After autologous injection of these TCR-transgenic T cells after maximal lymphodepletion, the group was able to show high levels of circulating engineered T cells and regression of metastatic melanoma lesions in two out of

15 patients suffering from metastatic melanoma. Nevertheless, they observed the phenomenon of reduced expression of the transgene in patients after a while – a common effect in transgenic cells which was already known by this time (Kohn, Hershfield et al. 1998). Apart from that, surprisingly, they also noticed a discordance between the percentage of MART-1 multimer-binding cells (0.8 %) and cells expressing the according Vβ-chain (8.1. %), most likely because the transgenic TCR chains were mispairing with the endogenous TCR chains of the T cells (Morgan, Dudley et al. 2006).

By reason of these findings, effort was spent on the optimization of TCR inserts for retroviral transduction:

Very soon, studies showed that codon-optimization of the insert leads to higher expression rates of the construct (Scholten, Kramer et al. 2006). Additionally, a complete or minimal murinization of the constant regions of the TCR can be performed meaning that either the whole human constant regions are exchanged with the murine constant chains (complete murinization) or only nine amino acids are exchanged (minimal murinization) (Sommermeyer and Uckert 2010). It was found that murinization can also increase expression rates and supplementary prevents mispairing of transgenic TCR chains with endogenous TCR chains of the T cell (Cohen, Zhao et al. 2006).

In the meantime, TCR-transgenic T cells were produced for a variety of antigens such as gp100 (glycoprotein 100), CEA (carcinoembryonic antigen) and NY-ESO-1 (Johnson, Morgan et al. 2009) (Parkhurst, Joo et al. 2009). As an example, CEA-targeting TCR-transgenic T cells were infused into three patients with metastatic colorectal cancer by the Rosenberg group. One of these patients showed a partial tumor response whereas unluckily all three of them developed a dose-limiting colitis (Parkhurst, Yang et al. 2011). In contrast, NY-ESO-1-specific TCR-transgenic T cells showed tumor responses in patients with metastatic melanoma as well as in patients with synovial cell sarcoma (Robbins, Morgan et al. 2011). In this study, none of the patients developed autoimmune toxicities – most probably due to fact that NY-ESO-1 is a cancer testis antigen (CTA) and therefore is not expressed in any normal adult tissue besides the testis (which is MHC-negative) (Hinrichs and Rosenberg 2014).

In contrast to CAR-modified T cells, TCR-transgenic T cells recognize the antigen in an HLA-restricted manner – meaning that they are able to only react against intracellular tumor antigens being processed and presented on MHC complexes on the cell surface. In a small study, we found HLA-A*24 significantly increased in ES patients (Thiel, Wolf et al. 2012). Nevertheless, for this thesis, we focused on HLA-A*0201-restricted T cells as HLA-A*0201 is the most common HLA allele in the European population (Gonzalez-Galarza, Christmas et al. 2011).

3 HYPOTHESIS

The hypothesis of this thesis is: “ES-selective CHM1- (Chondromodulin 1) and EZH2- (Enhancer of Zeste, Drosophila, Homolog 2) specific TCR-transgenic T cells are able to delay ES growth *in vitro* and *in vivo* and may serve to render future donor lymphocyte infusions more effective and less toxic”.

To prove this hypothesis, TCR-transgenic T cells were produced including several steps:

In preliminary work of our group, CHM1 was found to be a ES-specific antigen, whereas EZH2 is a ES-associated antigen (Staege, Hutter et al. 2004) (Richter, Plehm et al. 2009). In subsequent experiments EZH2- and CHM1-specific T cells were identified, expanded and tested for their specificity by flow cytometry-based multimer staining and ELISpot analysis. EZH2- and CHM1-specific T cells showed a specific and HLA-A*0201-restricted reactivity against peptide-loaded T2-cells as well as ES cell lines *in vitro.* Unmodified CHM1-specific T cells were even able to delay ES growth *in vivo* when injected into $Rag2^{-/-}\gamma_c^{-/-}$ mice (Thiel, Pirson et al. 2011). Due to problems with fading specificity after several generations and because of very small cell numbers and a high production complexity, we decided to produce T cells being transgenic for their TCR and directed against EZH2 or CHM1 in a good manufacturing practice (GMP) accredited off-the-shelf manner.

First, the existing clones were to be proved monoclonal and the TCR needed to be identified. These steps were performed using a specific PCR and subsequent sequencing. In a variety of different conditions and with or without several optimizations, the TCR sequence was cloned into retroviral vectors. In a next step, primary T cells – either derived from whole blood or from cord blood (CB) – were transduced with the vector, separated by fluorescent activated cell sorting (FACS) or magnetic bead staining and expanded *in vitro*. Special effort was spent on the development of central memory (T_{CM}) or effector T-cell phenotype (T_{Eff}) tested by flow cytometry-based staining with specific antibodies (T_{CM} here defined as > 80 % $CD62L^+$, T_{Eff} defined as < 5 % $CD62L^+$). After several weeks of culture, the transgenic T cells were tested for their peptide-

and HLA-A*0201-specificity in multimer staining and ELISpot analyses where CHM1-specific TCR-transgenic T cells showed specific reactivity against ES cell lines. The presence of the transgenic TCR sequence was proven by PCR. Finally, the effect of transgenic T cells on ES growth was tested in a mouse model using humanized $Rag2^{-/-}\gamma_c^{-/-}$ mice. Unfortunately, we were not able to show tumor regression caused by CHM1-specific TCR-transgenic T cells in this humanized mouse model – neither when holding a central memory nor an effector phenotype, neither with nor without DC vaccination. Although effort needs to be spent on optimizing the mouse model and experimental conditions, this work might lay the foundation for the introduction of TCR-transgenic T cells into therapeutic protocols for ES patients after allo-SCT in the future.

4 MATERIALS

4.1 TECHNICAL EQUIPMENT

Bacteria shaker Certomat BS-T	Sartorius, Göttingen, Germany
Balance EW 300-LM	Kern & Sohn GmbH, Balingen-Frommern, Germany
Balance (analytical) 770	Kern & Sohn GmbH, Balingen-Frommern, Germany
BD IMag™ Cell separation system	Becton Dickinson and Company, New Jersey, USA
Cell counting chamber Neubauer	Brand, Wertheim, Germany
Centrifuge Biofuge fresco	Heraeus, Hanau, Germany
Centrifuge Multifuge 3 S-R	Heraeus, Hanau, Germany
Centrifuge Sorvall RC6	Thermo Fisher Scientific, Ulm, Germany
Controlled-freezing box	Nalgene, Rochester, USA
Electrophoresis chamber Easy cast	Thermo Fisher Scientific, Ulm, Germany
Electroporator Gene Pulser Xcell™	BioRad, Richmond, CA, USA
ELISpot reader AID iSpot Reader Unit	AID GmbH, Straßberg, Germany
FACS Aria Cell Sorter	Becton Dickinson and Company, New Jersey, USA
Flow cytometer FACSCalibur™	Becton Dickinson and Company, New Jersey, USA
Freezer (- 20 °C) cool vario	Siemens, Munich, Germany
Freezer (- 80 °C) Hera freeze	Heraeus Holding, Hanau, Germany

Fridge (+ 4 °C) cool vario	Siemens, Munich, Germany
Heating block Thermomixer Comfort	Eppendorf, Hamburg, Germany
Ice machine AF 100	Scotsman Ice Systems, Vernon Hills, IL, USA
Incubator BBD 6220	Heraeus, Hanau, Germany
Liquid nitrogen tank L-240 K series	Taylor-Wharton, Theodore, USA
Micropipets (0,5 – 10 µl, 10 – 100 µl, 20 – 200 µl, 100 – 1000 µl)	Eppendorf, Hamburg, Germany
Microscope Axiovert 100	Zeiss, Jena, Germany
Microscope DMIL LED	Leica Camera AG, Solms, Germany
Microwave oven	Siemens, Munich, Germany
MidiMACS Separator	Miltenyi Biotech, Bergisch Gladbach, Germany
MilliQ System TKA GenPure	TKA GmbH, Niederelbert, Germany
MiniMACS Separator	Miltenyi Biotech, Bergisch Gladbach, Germany
Multichannel pipette (10 – 100 µl)	Eppendorf, Hamburg, Germany
NanoPhotometer	Implen, Munich, Germany
Pipetting assistant Easypet	Eppendorf, Hamburg, Germany
Power transformator PowerPac™	BioRad, Richmond, CA, USA
Sterile Bench	Heraeus, Hanau, Germany
Thermal cycler iCycler	BioRad, Richmond, CA, USA
Thermocycler	Eppendorf, Hamburg, Germany
UV transilluminator Gene Genius	Syngene, Cambridge, UK

Vortexer Vortex-Genie2	Scientific Industries, Bohemia, NY, USA
Water bath	GFL, Burgwedel, Germany

4.2 CONSUMABLE SUPPLIES

Cell culture flasks	TPP, Trasadingen, Switzerland
Cell strainer	Becton Dickinson and Company, New Jersey, USA
Cryo tubes	Greiner-bio One GmbH, Frickenhausen, Germany
Falcons	Greiner-bio One GmbH, Frickenhausen, Germany
Filters (sterile) Minisart	Sartorius, Göttingen, Germany
Gloves latex	Meditrade Medicare, Kufstein, Austria
Gloves nitrile	Sempermed, Vienna, Austria
LS columns	Miltenyi Biotech, Bergisch Gladbach, Germany
Nanophotometer Pearl	Implen, Muenchen, Germany
MultiScreen Filterplates (ELISpot)	Millipore, Billerica, MA, USA
MS columns	Miltenyi Biotech, Bergisch Gladbach, Germany
Parafilm	Brand, Wertheim, Germany
Pasteur pipets	Roth, Karlsruhe, Germany
Pipet tips ARTR Aerosol resistant tips	Thermo Fisher Scientific, Ulm, Germany
Plates for cell culture (96, 24, 12, 6	Becton Dickinson and Company, New

wells)	Jersey, USA
Round bottom FACS tubes	Becton Dickinson and Company, New Jersey, USA
Scalpels	Braun, Tuttlingen, Germany
Serological pipets Cellstar®	Greiner-bio One GmbH, Frickenhausen, Germany
Tubes (1.5 ml and 2 ml)	Eppendorf, Hamburg, Germany
Real-Time PCR plates	Eppendorf, Hamburg, Germany

4.3 Chemicals and reagents

100 mM dNTP Set	Invitrogen, Life Technologies, Darmstadt, Germany
1-Bromo-3-Chloro-Propan (BCP)	Sigma-Aldrich, St. Louis, Missouri, USA
1 kb plus DNA ladder	Invitrogen, Life Technologies, Darmstadt, Germany
2-Propanol	Roth, Karlsruhe, Germany
3-Amino-9-ethylcarbazole	Sigma-Aldrich, St. Louis, Missouri, USA
5 % trypsine	Gibco, Life Technologies, Darmstadt, Germany
6 x DNA loading dye	Fermentas, St. Leon-Rot, Germany
MEM NEAA 100 x	Gibco, Life Technologies, Darmstadt, Germany
Agar	Sigma-Aldrich, St. Louis, Missouri, USA
Agarose	Invitrogen, Life Technologies, Darmstadt, Germany

4.3. Chemicals and reagents

AIM V medium	Gibco, Life Technologies, Darmstadt, Germany
Ampicillin	Merck, Darmstadt, Germany
Anti PE Microbeads	Miltenyi Biotech, Bergisch Gladbach, Germany
AutoMACS™Rinsing Solution	Miltenyi Biotech, Bergisch Gladbach, Germany
Anti Human CD14 Magnetic Particles	Becton Dickinson and Company, New Jersey, USA
β2-Microglobuline from human urine	Sigma-Aldrich, St. Louis, Missouri, USA
$CD34^+$ Progenitor Cell Isolation Kit	Miltenyi Biotech, Bergisch Gladbach, Germany
CD8 MicroBeads, human	Miltenyi Biotech, Bergisch Gladbach, Germany
$CD8^+$ T Cell Isolation Kit human	Miltenyi Biotech, Bergisch Gladbach, Germany
D(+)-Glucose	Merck, Darmstadt, Germany
DEPC Water	Ambion, Darmstadt, Germany
Desoxyribonuclease A	Invitrogen, Life Technologies, Darmstadt, Germany
DMEM medium	Gibco, Life Technologies, Darmstadt, Germany
DMSO	Sigma-Aldrich, St. Louis, Missouri, USA
DPBS (10 x)	Gibco, Life Technologies, Darmstadt, Germany

Erythrocyte Lysis Buffer	Pharmacy of Klinikum rechts der Isar
Ethanol	Roth, Karlsruhe, Germany
Ethidium Bromide	Sigma-Aldrich, St. Louis, Missouri, USA
FACS™ Clean	Becton Dickinson and Company, New Jersey, USA
FACS™ Flow	Becton Dickinson and Company, New Jersey, USA
FACS™ Rinse	Becton Dickinson and Company, New Jersey, USA
Fetal bovine serum (FBS)	Biochrom, Berlin, Germany
Ficoll-Paque	GE Healthcare, Uppsala, Sweden
G418	Invitrogen, Life Technologies, Darmstadt, Germany
Glycerol	Sigma-Aldrich, St. Louis, Missouri, USA
GM-CSF	ImmunoTools, Friesoythe, Germany
HBSS 1 x	Gibco, Life Technologies, Darmstadt, Germany
HEPES	Sigma-Aldrich, St. Louis, Missouri, USA
Hepes Buffer (1M)	Biochrom, Berlin, Germany
Human Serum Type AB	Lonza, Basel, Switzerland
Hydrogene peroxide solution	Sigma-Aldrich, St. Louis, Missouri, USA
IFNg	R&D Systems, Minneapolis, Minnesota, USA
IL-1β	ImmunoTools, Friesoythe, Germany
IL-2	R&D Systems, Minneapolis, Minnesota,

	USA
IL-4	R&D Systems, Minneapolis, Minnesota, USA
IL-6	R&D Systems, Minneapolis, Minnesota, USA
IL-12	ImmunoTools, Friesoythe, Germany
IL-15	ImmunoTools, Friesoythe, Germany
IL-21	ImmunoTools, Friesoythe, Germany
Isopropanol	Sigma-Aldrich, St. Louis, Missouri, USA
L-glutamine	Gibco, Life Technologies, Darmstadt, Germany
MACS® BSA Stock Solution	Miltenyi Biotech, Bergisch Gladbach, Germany
Max Efficiency® Stbl2	Invitrogen, Life Technologies, Darmstadt, Germany
Multimers for EZH2 and CHM1	Kindly provided by Prof. Dr. Dirk Busch, Institute for Medical Microbiology, Immunology and Hygiene, Technical University Munich, Germany
Native Pfu Polymerase	Agilent Technologies, Böblingen, Germany
N,N-Dimethylformamide	Roth, Karlsruhe, Germany
Pen Strep	Gibco, Life Technologies, Darmstadt, Germany
Peptides EZH2^{666} and CHM1^{319}	Thermo Fisher Scientific, Ulm, Germany
Peptone	Invitrogen, Life Technologies, Darmstadt,

	Germany
Paraformaldehyde (PFA)	Merck, Darmstadt, Germany
PGE_2	Cayman Chemical Company, Ann Arbor, Michigan, USA
Pro5 Fluorotag R-PE	ProImmune, Oxford, UK
Propidium iodide staining solution	Becton Dickinson and Company, New Jersey, USA
Protamine sulfate	Sigma-Aldrich, St. Louis, Missouri, USA
Restriction Enzymes	Fermentas, St. Leon-Rot, Germany
RetroNectin	TaKaRa, Saint-Germain-en-Laye, France
RPMI 1640 medium	Gibco, Life Technologies, Darmstadt, Germany
S.O.C medium	Invitrogen, Life Technologies, Darmstadt, Germany
Sodium pyruvate	Gibco, Life Technologies, Darmstadt, Germany
T4-Ligase	Fermentas, St. Leon-Rot, Germany
Taq DNA polymerase	Invitrogen, Life Technologies, Darmstadt, Germany
TNF-α	R&D Systems, Minneapolis, Minnesota, USA
TransIT® 293	Mirus, Madison, WI, USA
Tri Reagent Solution	Ambion, Darmstadt, Germany
Trypan blue	Gibco, Life Technologies, Darmstadt, Germany

Tween 20	Sigma-Aldrich, St. Louis, Missouri, USA
Unlabeled Pro5® MHC class I Pentamers	ProImmune, Oxford, UK
X-vivo 15 medium	Lonza, Walkersville, Maryland, USA
Yeast extract	Thermo Fisher Scientific, Ulm, Germany

4.4 Kits

EndoFree Plasmid Maxi Kit	Qiagen, Hilden, Germany
Strataprep DNA Gel Extraction Kit	Agilent Technologies, Böblingen, Germany
MAX Efficiency® Stbl2™ Competent Cells	Invitrogen, Life Technologies, Darmstadt, Germany
Nucleo Spin Plasmid	Macherey-Nagel, Düren, Germany
High Capacity Reverse Transcription Kit	Applied Biosystems, Life Technologies, Darmstadt, Germany
One Shot TOP10 chemically competent cells	Invitrogen, Life Technologies, Darmstadt, Germany
AccuPrime® Taq DNA Polymerase System	Invitrogen, Life Technologies, Darmstadt, Germany
IOTest® Beta Mark Kit	Beckman Coulter, Krefeld, Germany

4.5 ELISPOT REAGENTS

4.5.1 CAPTURE ANTIBODIES

Antibody	Working concentration	Manufacturer
Anti-h-IFN-γ mAb 1-D1K, purified	10 µg/ml	mABTech, Nacka Strand, Sweden
Anti-h-IL-2 mAb IL2-I/249	10 µg/ml	
Anti-h-Granzyme B mAb GB10, purified	10 µg/ml	mABTech, Nacka Strand, Sweden

4.5.2 DETECTION ANTIBODIES

Antibody	Working concentration	Manufacturer
Anti-h-IFN-γ mAb 7-B6-1, biotinylated	2 µg/ml	mABTech, Nacka Strand, Sweden
Anti-h-IL-2 mAb IL2-II, biotinylated	0.5 µg/ml	mABTech, Nacka Strand, Sweden
Anti-h-Granzyme B mAb GB11, biotinylated	2 µg/ml	mABTech, Nacka Strand, Sweden

4.5.3 Enzymes and buffers

Streptavidin-Horse Radish Peroxidase	mABTech, Nacka Strand, Sweden
3-Amino-9-ethyl-carbazole (AEC)	Sigma-Aldrich, St. Louis, Missouri, USA
Anti-h-Granzyme B mAb GB11, biotinylated	mABTech, Nacka Strand, Sweden

Acetate buffer: 37.5 ml H_2O dest. + 3.75 ml 0.2 N acetic acid + 8.8 ml 0.2 N sodium acetate

AEC solution: 1 AEC tablet (20 mg) in 2.5 ml Dimethylformamide (DMF) + 47.5 ml acetate buffer

Development solution: 10 ml AEC solution + 30 µl 30 % H_2O_2 per plate

4.6 Flow cytometry antibodies

Specificity	Format	Clone	Manufacturer
CD3	FITC/APC	HIT3A	Becton Dickinson and Company, New Jersey, USA
CD4	FITC/PE	RPA-T4	Becton Dickinson and Company, New Jersey, USA
CD8	FITC/PE/APC	RPA-T8	Becton Dickinson and Company, New Jersey, USA
CD19	PE	HIB19	Becton Dickinson and Company, New Jersey, USA
CD34	PE	8G12	Becton Dickinson and Company,

			New Jersey, USA
CD38	APC	HIT2	Becton Dickinson and Company, New Jersey, USA
CD45	FITC	HI30	Becton Dickinson and Company, New Jersey, USA
CD62L	APC	Dreg 56	Becton Dickinson and Company, New Jersey, USA
CD83	APC	HB15e	Becton Dickinson and Company, New Jersey, USA
CD86	FITC	2331 (FUN-1)	Becton Dickinson and Company, New Jersey, USA
Mouse IgG1	FITC/PE/APC	X40	Becton Dickinson and Company, New Jersey, USA

4.7 Peptides

Gene	HLA-Allele	Sequence	Position
CHM1	A*0201	VIMPCSWWV	319
EZH2	A*0201	YMCSFLFNL	666

4.8 VECTORS

4.8.1 PMSCVNEO-CONSTRUCTS

The vector pMSCVneo was purchased from Clontech, Mountain View, California, USA. pMSCVneo_EZH2_mu_opt and pMSCVneo_CHM1_mu_opt were generated with the help of GeneArt, Life Technologies, Regensburg. (Vector maps modified from material provided by GeneArt, Life Technologies, Regensburg).

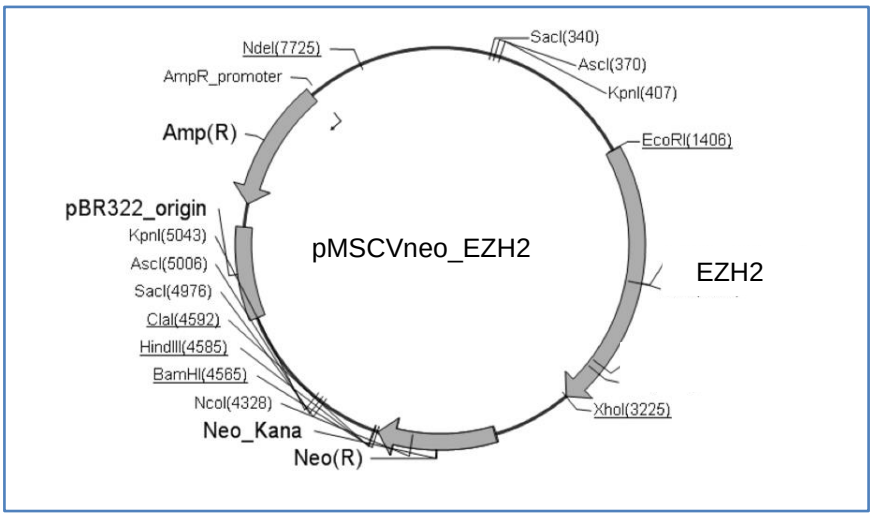

FIGURE 3 Vector map of pMSCVneo_EZH2.

Restriction sites within the insert not shown.

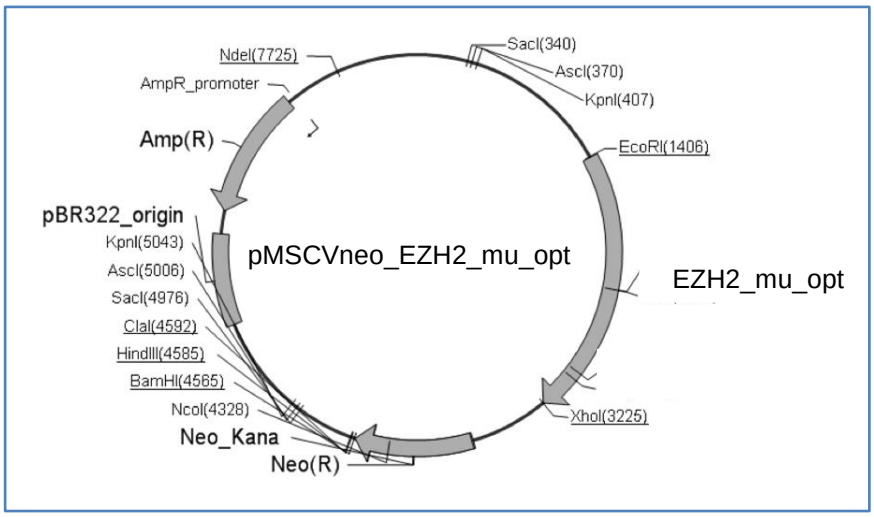

FIGURE 4 Vector map of pMSCVneo_EZH2_mu_opt.

Restriction sites within the insert not shown.

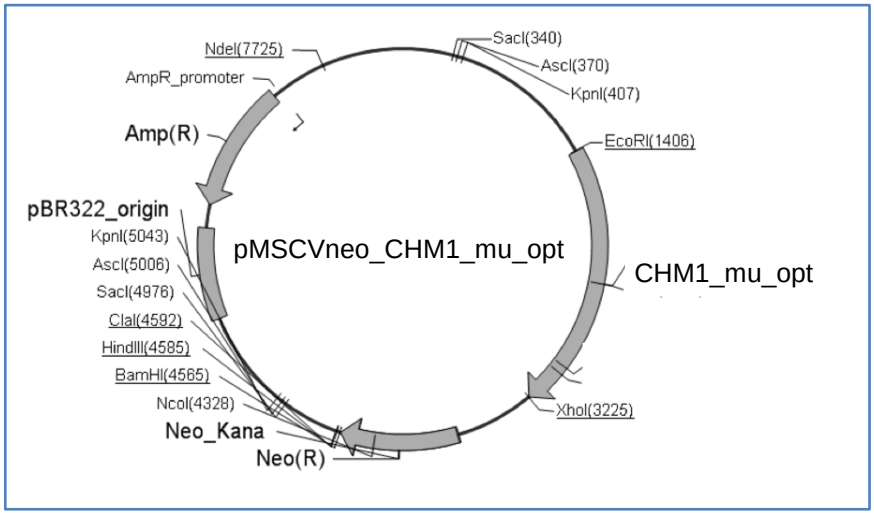

FIGURE 5 Vector map of pMSCVneo_CHM1_mu_opt.

Restriction sites within the insert not shown.

4.8.2 pMP71-Constructs

The vector pMP71_GFP was a kind gift of Prof. Angela Krackhardt, Medizinische Klinik III, Klinikum Rechts der Isar, Technical University Munich. pMP71_EZH2_mu_opt and pMP71_CHM1_mu_opt were generated with the help of GeneArt, Life Technologies, Regensburg. (Vector maps modified from material provided by GeneArt, Life Technologies, Regensburg).

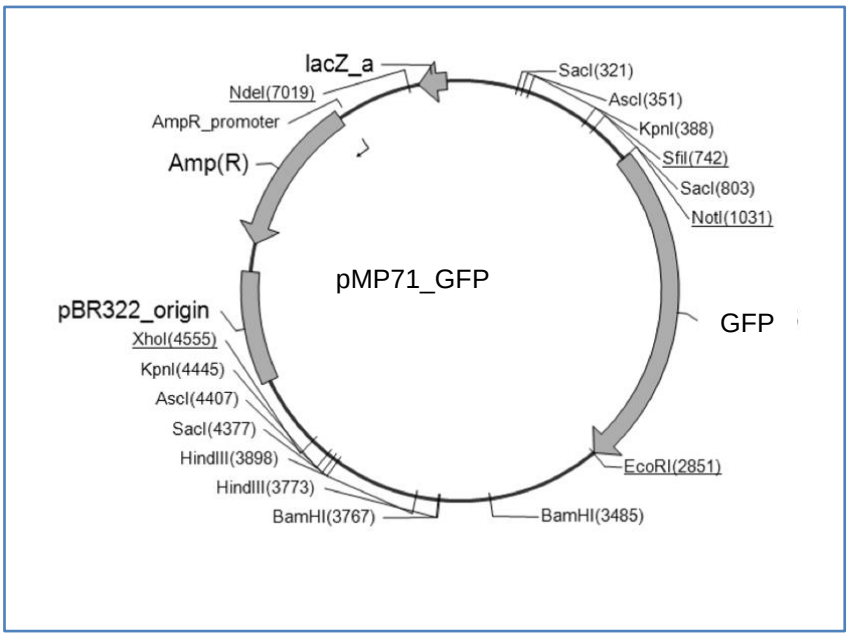

FIGURE 6 Vector map of control vector pMP71_GFP.

Restriction sites within the insert not shown.

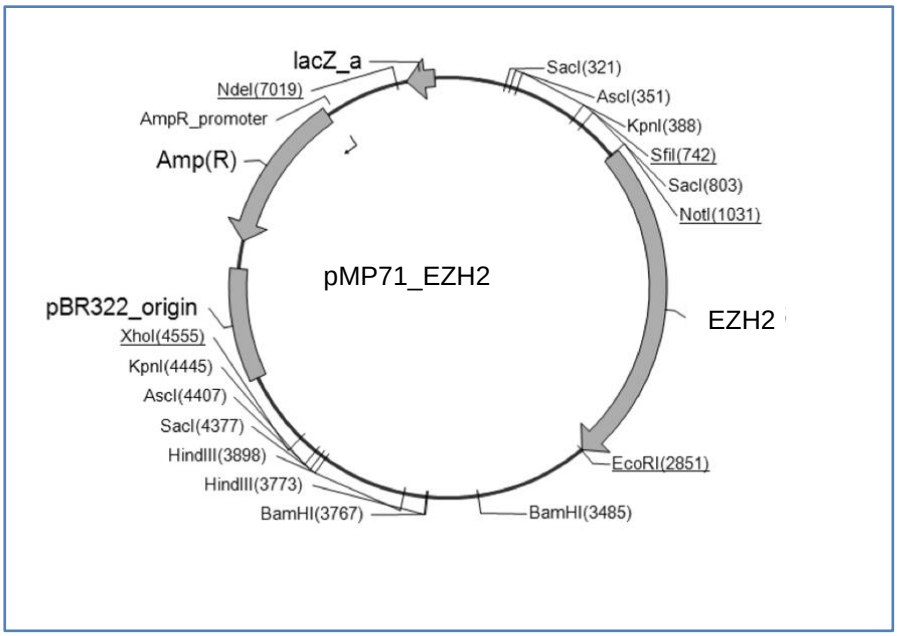

FIGURE 7 Vector map of pMP71_EZH2.

Restriction sites within the insert not shown.

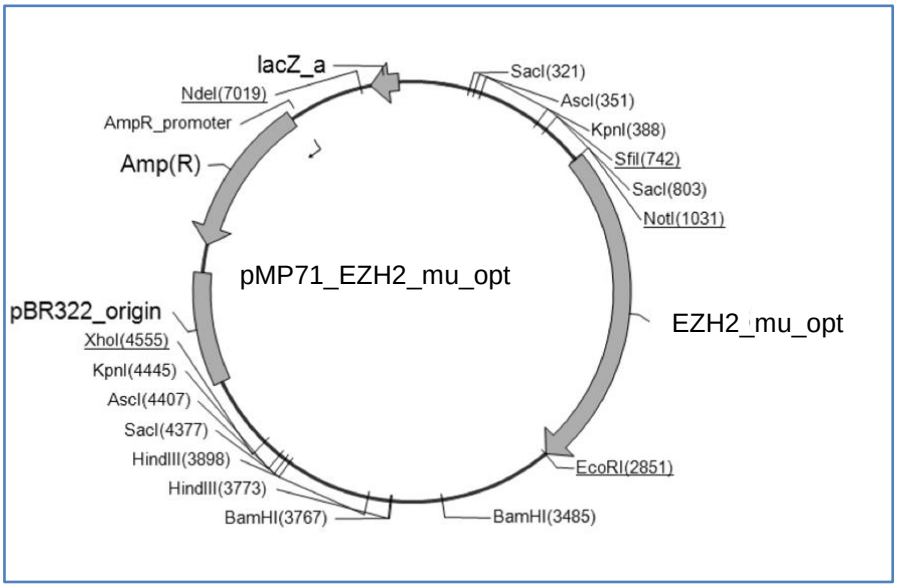

FIGURE 8 Vector map of pMP71_EZH2_mu_opt.

Restriction sites within the insert not shown.

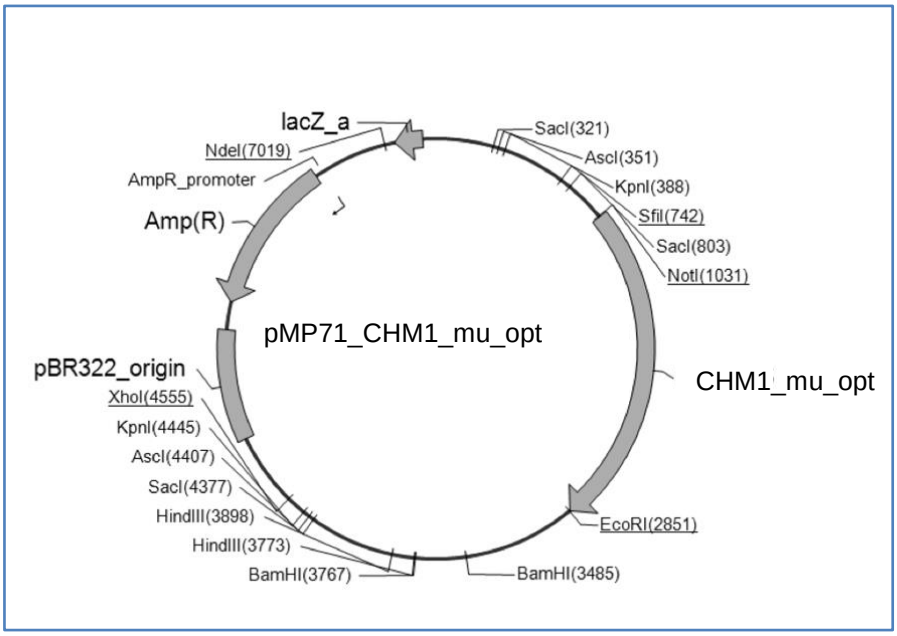

FIGURE 9 Vector map of pMP71_CHM1_mu_opt.

Restriction sites within the insert not shown.

4.8.3 GAG-POL

This vector was a kind gift of Prof. Angela Krackhardt, Medizinische Klinik III, Klinikum Rechts der Isar, Technical University Munich.

4.8.4 ENV

This vector was a kind gift of Prof. Angela Krackhardt, Medizinische Klinik III, Klinikum Rechts der Isar, Technical University Munich.

4.8.5 PPCR-SCRIPT AMP

The vector pPCR-Script Amp was part of the PCR-Script Amp Cloning Kit (Agilent Technologies, Böblingen, Germany). (Vector map taken from PCR-Script Amp Cloning Kit manual.)

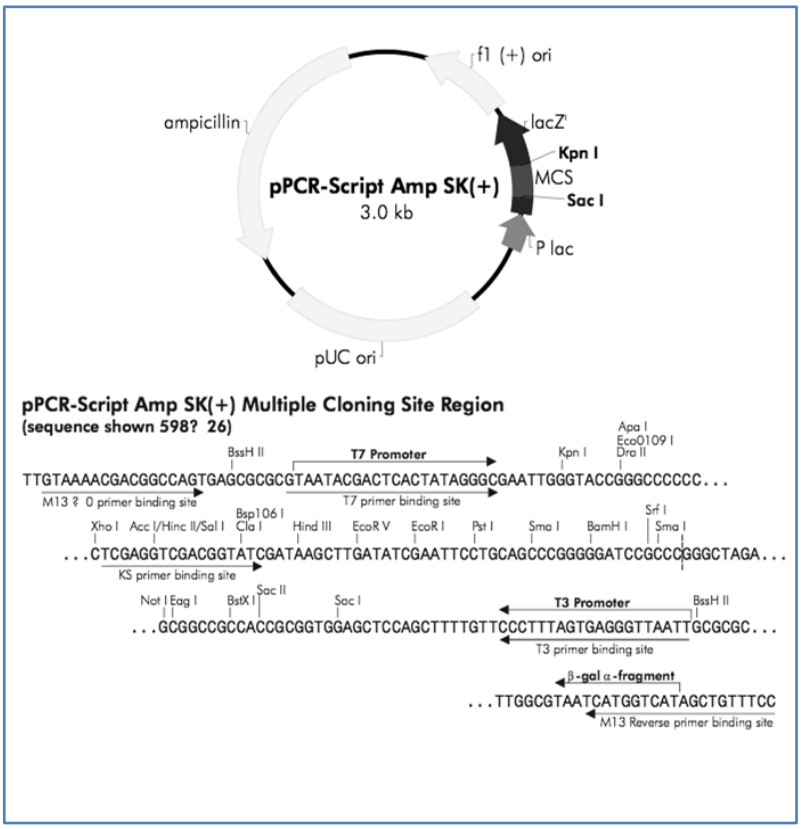

FIGURE 10 Vector map of pPCR-Script Amp.

4.9 Cell culture media and solutions

RPMI (10 % FCS)

- RPMI 1640
- 10 % FCS
- 2 mM L-glutamine
- 100 U/ml Pen Strep

DMEM (10% FCS)

- DMEM
- 10 % FCS
- 2 mM L-glutamine
- 1 mM Sodium pyruvate
- 1 x NEAA
- 100 U/ml Pen Strep

LCL and Jurkat (J67) cell medium

- RPMI 1640
- 10 % FCS
- 2 mM L-glutamine
- 1 mM Sodium pyruvate
- 1 x NEAA
- 100 U/ml Pen Strep

T-cell medium

- AIM V
- 5 % human serum type AB
- 2 mM L-glutamine
- 100 U/ml Pen Strep

DC medium

- X-Vivo 15
- 1 % human serum type AB

Standard freezing medium

- FCS
- 10 % dimethyl sulfoxide (DMSO)

Freezing medium for T cells

- Human serum type AB
- 10 % DMSO

5 METHODS

5.1 CELL CULTURE METHODS

5.1.1 FREEZING AND THAWING OF CELLS

For freezing, cells were centrifuged at 1500 rounds per minute (rpm) for 5 min. T cells were re-suspended in precooled human AB serum with 10 % DMSO, all others in precooled FCS with 10 % DMSO, kept in -80 °C freezer and transferred to liquid nitrogen freezer the next day for long-term storage.

For thawing, cells were rapidly taken into medium, centrifuged once at 1500 rpm for 5 min and re-suspended in the appropriate culture medium.

5.1.2 CULTURING OF CELL LINES

Suspension and adherent cell lines were split every 3 to 4 days according to their individual growth rate. For splitting of suspension cells, half of cell suspension was removed and replaced by fresh medium. Adherent cells were washed with 5 to 10 ml PBS, then incubated with 3 to 5 ml trypsin at 37 °C. After detachment, cells were washed, centrifuged at 1500 rpm for 5 min and re-cultured in flasks.

5.1.3 CELL COUNTING

To determine the cell number, cells were diluted 1:2 with trypan blue. Because trypan blue does only stain defect cells, viable cells can be identified and were counted in four squares of a Neubauer counting chamber. Cell concentrations were determined using the following formula:

$c[\text{cells/ml}] = \text{number of cells counted per square} \times 10^4 \times \text{dilution factor}$

5.2 Isolation of blood cells

5.2.1 Isolation of peripheral blood mononuclear cells

Peripheral blood mononuclear cells (PBMC) were isolated from concentrates provided by the DRK-Blutspendedienst Baden-Wuerttemberg/ Hessen in Ulm using Ficoll density gradient centrifugation. Therefore, the blood-cell concentrate was diluted 1:2 with PBS and carefully layered on top of Ficoll-Paque in a ratio of 2:3. After centrifugation at 2200 rpm for 30 min without brake, the buffy coat was aspirated and transferred to a fresh tube. PBS was added to a final volume of 50 ml and the suspension was centrifuged at 700 rpm for 7 min to remove the platelets. After two additional washing steps, cells were counted and frozen or further purified and cultured.

5.2.2 Isolation of $CD14^+$ cells

After isolation of PBMC (see 5.2.1) from a HLA-A*0201$^+$ healthy blood donor, $CD14^+$ cells were purified using the BD Anti-Human CD14 Magnetic Particles kit and the BD IMagnet^{TM} according to the manufacturer's instructions. Afterwards, $CD14^+$ cells were used to generate dendritic cells (see 5.3).

5.2.3 Isolation of $CD8^+$ T cells

To isolate $CD8^+$ T cells, either the $CD8^+$ T Cell isolation kit (negative selection) or CD8 microbeads (positive selection) were used according to the manufacturer's instructions.

5.2.4 CD34 separation

$CD34^+$ stem cells were isolated from fresh HLA-A*0201$^-$ cord blood using ficoll density centrifugation (see 5.2.1). If necessary, erythrocytes were lysed after centrifugation by incubating the pellet with 13 ml erythrocyte lysis buffer for 4 min at room temperature. Afterwards, $CD34^+$ cells were purified with the help of the $CD34^+$ Progenitor Cell Isolation Kit according to the manufacturer's instruction. The purity of $CD34^+$ cells was tested by flow cytometry (staining for

CD3/CD34/CD38). The purified $CD34^+$ cells were used for transplantation of $Rag2^{-/-}\gamma_c^{-/-}$ mice (Chicha, Tussiwand et al. 2005) (see 5.19), whereas the remaining PBMC could be used for the production of transgenic T cells (see 5.15).

5.3 Generation of dendritic cells

After isolation from PBMC (day 0) (see 5.2.1), $CD14^+$ cells were cultured in X-Vivo15 medium containing 1 % human serum type AB, 1000 IU/ml IL-4 and 800 IU/ml granulocyte macrophage colony-stimulating factor (GM-CSF) in a concentration of 3×10^5 cells/ml. On day 3, cytokines were renewed and on day 6 a cytokine cocktail was added consisting of 10 ng/ml TNF-α, 10 ng/ml IL-1β, 1000 IU/ml IL-6 and 1 µg/ml PGE_2. On day 8 or 9, a flow cytometry staining was performed. When positive for CD86, CD83 and HLA-DR, DC were considered mature and used for the priming of T cells (see 5.4).

5.4 *In vitro* priming of $CD8^+$ T cells

HLA-$A*0201^+$ mature DC were pulsed with the appropriate peptide in a concentration of 30 to 50 µM for four hours at 37 °C in the presence of 20 µg/ml β2-Microglobuline. Afterwards, the pulsed DC were co-cultured with HLA-$A*0201^-$ $CD8^+$ T cells in 96-well-plates containing T-cell medium. The stimulator to responser rate was 1 : 20 (5×10^3 DC per well : 10^5 $CD8^+$ T cells per well). 10 ng/ml IL-12 and 1000 U/ml IL-6 were added. After one week, the T cells were stimulated again with the same number of loaded DC in the presence of 5 ng/ml IL-7 and 100 U/ml IL-2.

5.5 Multimer staining

To evaluate the specificity of primed $CD8^+$ T cells or transgenic T cells, a flow cytometry staining was performed. Unlabeled Pro5 MHC class I pentamers were labeled with Pro5 Fluorotag R-PE and used according to the manufacturer's instructions. Optionally, specific multimers were generated by

the working group of Prof. Dirk Busch, Institute for Medical Microbiology, Immunology and Hygiene, Technical University Munich, and used according to their protocols.

5.6 FACS

For FACS, cells were stained as described in 5.8. If an increased number of cells was required, an appropriate higher amount of antibody or peptide-specific multimer was added. To exclude dead cells from sorting, propidium iodide was added to the samples (working concentration 1 µg/ml). Primed $CD8^+$ T cells with endogenous TCR or transgenic T cells with effector phenotype were sorted for CD8-FITC and multimer-PE. Transgenic T cells with central memory phenotype were sorted for CD62L-APC and multimer-PE. Sorting was performed on a FACS Aria in the laboratory of Prof. Dirk Busch, Institute for Medical Microbiology, Immunology and Hygiene, Technical University Munich.

5.7 Limiting dilution

Whenever a single cell cloning was needed (e.g. after multimer-mediated FACS of primed T cells), limiting dilution was performed. Therefore, 1 T cell per well of a 96-well plate was co-cultured with anti-CD3 (30 ng/ml), irradiated LCL (100 Gy; 1 x 10^5 cells per well) and irradiated PBMC (30 Gy; 5 x 10^4 cells per well) pooled form three different healthy donors (see 5.2.1). 100 U/ml IL-2 and 2 ng/ml IL-15 were added. After one week, cytokines and half of the medium were replaced.

5.8 Flow cytometry

Per sample, 2 to 5 x 10^5 cells were washed in staining buffer. If necessary, present F_c-receptors were blocked by adding 1 µg human Immunoglobulin G (IgG) and incubating the suspension at 4 °C for 10 min. After again washing the cells in staining buffer, 3 µl of each required antibody was added and the suspension was incubated for another 30 min at 4 °C, shielded from light. Two

additional washing steps were performed before samples were taken into 300 µl PBS to start the measurements. If samples had to be stored for more than two hours before analysis, they were instead fixed in 300 µl PBS containing 1 % paraformaldehyde (PFA).

5.9 Vβ analysis

For the Vβ analysis of a TCR repertoire, the IOTest Beta Mark Kit was used according to the manufacturer's instruction.

5.10 ELISpot assay

On day 1, 50 µl of capture antibody solution (antibodies and their concentrations see 4.5) were transferred to each well of the ELISpot plates and the plates were incubated at 4 °C over night.

On day 2, the ELISpot plates were washed four times with PBS at 4 °C. Afterwards, PBS was replaced by T cell medium (150 µl/well) for 60 min at 37 °C to block unspecific binding. If T2 cells were used, they were pulsed with peptide for 2 hours and were mixed every 15 minutes. Afterwards, peptide-loaded T2 cells were washed three times. If ES cell lines were required as target cells, they were incubated with 100 IU/ml IFNγ 48 h before use.

After blocking of the plate, 50 µl T cell medium containing 1000 T cells (IFNγ or IL-2 ELISpot) or 50 µl of a twofold serial dilution (200,000 to 3,125 T cells per well; Granzyme B ELISpot) were pipetted into each well and incubated for at least 30 min at 37 °C. 20,000 target cells in 50 µl T-cell medium were carefully layered over the T cell suspension in each well and the plates were incubated at 37 °C for 20 hours.

On day 3, ELISpot plates were washed six times with PBS containing 0.05 % Tween and incubated with 100 µl of detection antibody per well. After incubation at 37 °C for 2 hours, plates were washed again und 100 µl Streptavidin-Horse Radish Peroxidase were pipetted into each well. Plates were incubated at room temperature for 1 hour shielded from light and then were washed three times

with PBS Tween and three times with normal PBS. 100 µl of development solution was allocated per well and reaction was stopped after 5 to 10 min by washing the plates. After drying, ELISpot plates were analyzed using the ELISpot reader.

5.11 Expansion of cytotoxic T lymphocytes with endogenous TCR

Cytotoxic T lymphocytes (CTL) with endogenous TCR were expanded after passing the first ELISpot screen to create higher cell numbers for more extensive screens or for isolation of RNA.

In detail, 5 x 10^4 to 1 x 10^5 T cells were expanded in 25 ml T cell medium together with 5 x 10^6 irradiated LCL (100 Gray (Gy)) and 2.5 x 10^7 irradiated PBMC (30 Gy) pooled from three different healthy donors (see 5.2.1). 30 ng/ml anti-CD3 were added. The next day and then every other day 100 IU/ml IL-2 and 2 ng/ml IL-15 were pipetted into the suspension. Part of the medium was replaced whenever necessary.

5.12 Basic methods of molecularbiology

5.12.1 RNA isolation

RNA isolation was performed using TriReagent according to the manufacturer's instructions. After re-suspension in DEPC-treated water, RNA was stored at –80 °C.

5.12.2 cDNA synthesis

To transcribe RNA into cDNA, High Capacity Reverse Transcription Kit was used according to the manufacturer's instructions.

5.12.3 MINIPREPARATION OF PLASMID DNA

Minipreparation of plasmid DNA was performed using the NucleoSpin Plasmid Kit according to the supplier's information. DNA was eluted with 50 µl AE and stored at -20 °C. Successful cloning was checked by restriction analysis and – if blunt end cloning was performed – by sequencing (Sequiserve, Vaterstetten).

5.12.4 MAXIPREPARATION OF PLASMID DNA

Maxipreparation of plasmid DNA was performed using the EndoFree Plasmid Purification Kit according to the manufacturer's instructions. Purified DNA was re-suspended in 200 to 500 µl of endotoxin-free buffer TE and stored at –20 °C. Success of cloning was checked (see 5.12.3).

5.12.5 RESTRICTION ANALYSIS

For restriction analysis, purified plasmids were digested with the corresponding restriction enzymes and an appropriate buffer according to the manufacturer's instructions. After digestion, the mix was loaded onto an agarose gel to prove the presence of expected fragments.

5.12.6 DNA/ RNA MEASUREMENT

All nucleic acid measurements were executed with a Nanophotometer Pearl according to manufacturer's information.

5.12.7 AGAROSE GEL ELECTROPHORESIS AND GEL EXTRACTION

The separation of Vαβ-Repertoire analysis fragments was performed in 2 % agarose – separations for other purposes in 1 % agarose. 0.02 µl/ml ethidium bromide was added before casting the gel. After adding the 6 x loading dye, DNA solutions were loaded into the gel slots next to a 1 kb plus ladder. After electrophoresis at a voltage of 5 to 10 V/cm, the desired fragments could be

extracted from the gel using Strataprep DNA gel extraction kit according to the manufacturer's instructions.

5.13 VAB-REPERTOIRE ANALYSIS

For analysis of Vα- and Vβ-repertoire, the AccuPrime Taq DNA Polymerase System was used.

RNA was isolated from T cell clones (see 5.12.1) and transcribed into cDNA (see 5.12.2), which constituted the template for the PCR reactions. Different variable primers (Vαx respectively Vβx) were used coding for the 5'-end of different variable chains of TCR. The primers named 3'TCα respectively 3'CβII constituted the corresponding 3'-primers located in the constant region, near the variable chain. The Primers P5'-αST and P3'-αST were used as internal controls for α-chain PCR as they are binding in regions of constant α-chain. In analogy, primers P5'-βST and P3'-βST were used as controls for β-chain PCR (see Figure 11). All primer sequences are shown in 11.1.

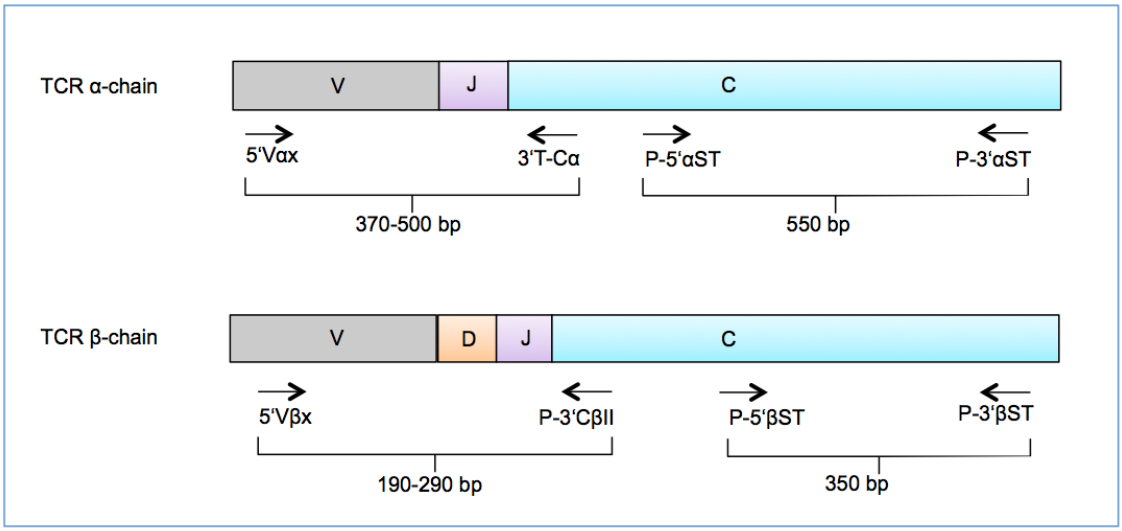

FIGURE 11 Schematic representation: Annealing sites of Vαβ-repertoire primers in the TCR genes. In the upper panel RNA regions of a TCR-α-, in the lower panel of a TCR-β-chain are shown together with the primers for Vαβ-repertoire analyses. Expected length of the PCR products is illustrated. Bp = base pairs, V = variable segment, J = joining segment, C = constant segment, D = diversity segment. Figure modified from the dissertation of Ingrid Schuster from Medizinische Klinik III, Klinikum Rechts der Isar, Technical University Munich (Schuster 2008).

PCR mix:
2.5 µl 10 x Buffer I
18.5 µl H_2O
0.5 µl primer P-5'αST / P-5'βST
0.5 µl primer P-3'βST/ P-3'βST
1 µl primer 3'TCα/ P-3'CβII
1.5 µl primer Vαx/ Vβx
0.5 µl AccuPrimeR Taq DNA Polymerase

PCR program:

94 °C	6 min	
94 °C	1 min	40 cycles
54 °C	1 min	
68 °C	1 min	
68 °C	7 min	
4 °C	for storage	

Protocol kindly provided by Prof. Angela Krackhardt, Medizinische Klinik III, Klinikum Rechts der Isar, Technical University Munich.

5.14 Cloning of TCR sequences into pMP71 and pMSCVneo

Cloning of TCR sequences into the vectors pMP71 or pMSCVneo included several steps: First, α- and β-chains were cloned separately into pPCRScript. After ligation of both chains and insertion of a P2A fragment, the complete TCR chains were finally cloned into pMP71 and pMSCVneo.

5.14.1 Amplification of TCR with restriction site synthesis

After identification of the endogenous TCR chains of several T-cell clones, primers were designed to clone the α- and β-chain separately into pPCRScript. The 3'-primer contained the 3'-restriction site (EcoRI for pMP71 constructs, XhoI for pMSCVneo constructs), the 5'-primer the 5'-restriction site (NotI for

pMP71 constructs, EcoRI for pMSCVneo constructs) plus a Kozak sequence. All primer sequences are listed in 11.1. For PCR reaction, Pfu native DNA polymerase was used with the appropriate buffer:

PCR mix:
- 5 µl 10 x native plus buffer
- 1 µl dNTP mix
- 1 µl cDNA
- 1 µl 3'-primer
- 1 µl 5'-primer
- 1 µl Pfu native polymerase
- 40 µl H_20

PCR program:

94 °C	2 min	
94 °C	30 sec	5 cycles
54 °C (α-chain)/ 56 °C (β-chain)	30 sec	
72 °C	2 min	
94 °C	30 sec	45 cycles
62 °C	30 sec	
72 °C	2 min	
72 °C	7 min	
4 °C	for storage	

If the subsequent agarose gel showed bands at expected heights, these bands were extracted from the gel (see 5.12.7). The purified DNA was used for blunt end ligation with pPCRScript. Protocol kindly provided by Prof. Angela Krackhardt, Medizinische Klinik III, Klinikum Rechts der Isar, Technical University Munich.

5.14.2 Ligation of pPCRScript with PCR products encoding for A- or B-chain

PCR products (see 5.14.1) were ligated with pPCRScript according to the instructions of PCR-Script Amp Cloning Kit.

5.14.3 Transformation of pPCRScript constructs into E. coli

Transformation was performed using XL10Gold bacteria as described in the PCR-Script Amp Cloning kit. To distinguish between positive and negative bacterial colonies, the color screening method was used.

Apparently positive clones were picked from LB-Amp agar plate, plasmid DNA was purified in a plasmid minipreparation (see 5.12.3) and correct assembly of insert and vector was tested by restriction analysis and sequencing (sequencing primers T3 and T7). All primer sequences are shown in 11.1. If correct assembly was confirmed, a maxipreparation (see 5.12.4) was accomplished to generate higher amounts of plasmid DNA.

5.14.4 Preparative digestion of pPCRScript

To excise the insert out of pPCRScript, appropriate restriction enzymes were used according to the restriction sites. Digestion was performed at 37 °C for 90 min:

Digestion mix:
- 10 µl 10 x Buffer O
- 10 µg plasmid DNA
- 2.5 µl restriction enzyme 1 (NotI for MP71 construct, EcoRI for pMSCVneo construct)
- 2.5 µl restriction enzyme 2 (EcoRI for MP71 construct, XhoI for pMSCVneo construct)
- fill up with H_2O to a final volume of 100 µl

Success of digestion was tested by agarose gel electorphoresis. Appropriate bands (representing the insert) were extracted from the gel.

5.14.5 Attachment of a- and b-chain via PCR

To create the insert for pMP71 or pMSCVneo containing both – the α- and the β-chain – two PCR were performed.

In a first PCR, a P2A fragment was attached to the 5'-end of the β-chain and the 3'-end of the α-chain. For the α-chain, EZH2_alpha_rev_EcoRI or -_XhoI were used as 3'-primers and the P2A-containing primer EZH2_alpha_P2A_forw represented the 5'-primer. For β-chain, P2A-Primer EZH2_beta_P2A_rev was designed to bind at the 3'-end and primers EZH2_beta_forw_NotI or -_EcoRI were used as 5'-primer. Protocol kindly provided by Prof. Angela Krackhardt, Medizinische Klinik III, Klinikum Rechts der Isar, Technical University Munich.

PCR Mix:	5 µl	10 x Pfu-buffer
	1 µl	dNTP mix
	1 µl	native Pfu polymerase
	10 ng	DNA (α-chain or β-chain extracted from the gel)
	1 µl	3'-primer
	1 µl	5'-primer
	fill up with H_2O to a final volume of 50 µl	

PCR program:	94 °C	2 min	
	94 °C	30 sec	5 cycles
	60 °C	30 sec	
	72 °C	4 min	
	94 °C	30 sec	40 cycles
	65 °C	30 sec	
	72 °C	4 min	
	72 °C	5 min	
	4 °C	for storage	

PCR products were loaded onto an agarose gel, desired bands were cut and extracted from the gel.

The alignment of α- and β-chain via the P2A linker took place in a second PCR using now only the restriction-site containing primers. The first part of the PCR was performed without primers and with only a small amount of Pfu native polymerase:

PCR Mix:

5 µl 10 x Pfu Buffer
1 µl dNTP mix
1 µl Pfu native polymerase
50 ng Insert 1 (α-chain with P2A linker)
50 ng Insert 2 (β-chain with P2A linker)
fill up with H_2O to a final volume of 50 µl

PCR program:

95 °C	3 min	
ramp to 40 °C with a rate of 0.2 °C/ sec		4 cycles
40 °C	30 sec	
72 °C	2 min	
72 °C	2 min	

Within the second 72°C-step, 1 µl Pfu native polymerase, 1.5 µl 3'-primer and 1.5 µl 5'-primer were added and the second step of the PCR program was performed:

95 °C	1 min	
55 °C	1 min	35 cycles
72 °C	4 min	
72 °C	5 min	
4 °C	for storage	

PCR products were loaded onto an agarose gel, desired bands were extracted and represented the complete inserts for ligation with pPCRScript and transformation into E. coli as mentioned above (see 5.14.2). Minipreparation was performed and success of cloning was checked by gel electrophoresis and sequencing. If correct assembly was confirmed, a maxipreparation was accomplished to generate higher amounts of plasmid DNA.

This plasmid DNA was digested with the appropriate restriction enzymes (NotI and EcoRI for pMP71 constructs, EcoRI and XhoI for pMSCVneo constructs) and loaded onto an agarose gel. The bands representing the insert were cut

and DNA was extracted. The same procedure was performed with pMP71 or pMSCVneo to extract the vector.

5.14.6 Ligation of digested complete TCR insert with digested pMP71/ pMSCVneo

To ligate the insert with the target vectors pMP71 or pMSCVneo, T4-Ligase was used with the appropriate buffer. The following mix was incubated at 16 °C overnight:

Ligation mix:
- 3 µl digested pMP71/ pMSCVneo
- 1 µl digested insert
- 1 µl 10 x T4 buffer
- 1 µl T4-Ligase
- 4 µl H_2O

5.14.7 Transformation of pMP71/ pMSCVneo constructs into E. coli

For transformation of the TCR-pMP71/ -pMSCVneo constructs, One Shot TOP10 Chemically Competent Cells were used according to the supplier's information. Colonies were picked from LB-Amp agar plates and – after minipreparation of the plasmid DNA – were digested and evaluated by agarose gel electrophoresis. If appropriate bands showed up, maxipreparations of the pMP71 and pMSCVneo constructs were performed and the plasmid DNA was used for infection of T cells.

(Because of high recombination frequency of pMP71 constructs, no glycerol stocks were used for maxipreparation. Instead, re-transformation was performed.)

5.14.8 Construction of murinized and optimized pMP71 constructs

Murinized and optimized pMP71 constructs were manufactured by GeneART, Life Technologies, Regensburg.

5.14.9 Retransformation of murinized and optimized pMP71 and pMSCVneo constructs

Murinized and optimized constructs were retransformed into stbl2 bacteria according to the manufacturer's information. Colonies were picked and plasmid DNA was isolated by maxipreparation. Correct assembly was again confirmed by gel electrophoresis and plasmids were used for transduction of T cells.

5.15 Infection of PBMC/ T cells/ J67 cells with TCR constructs

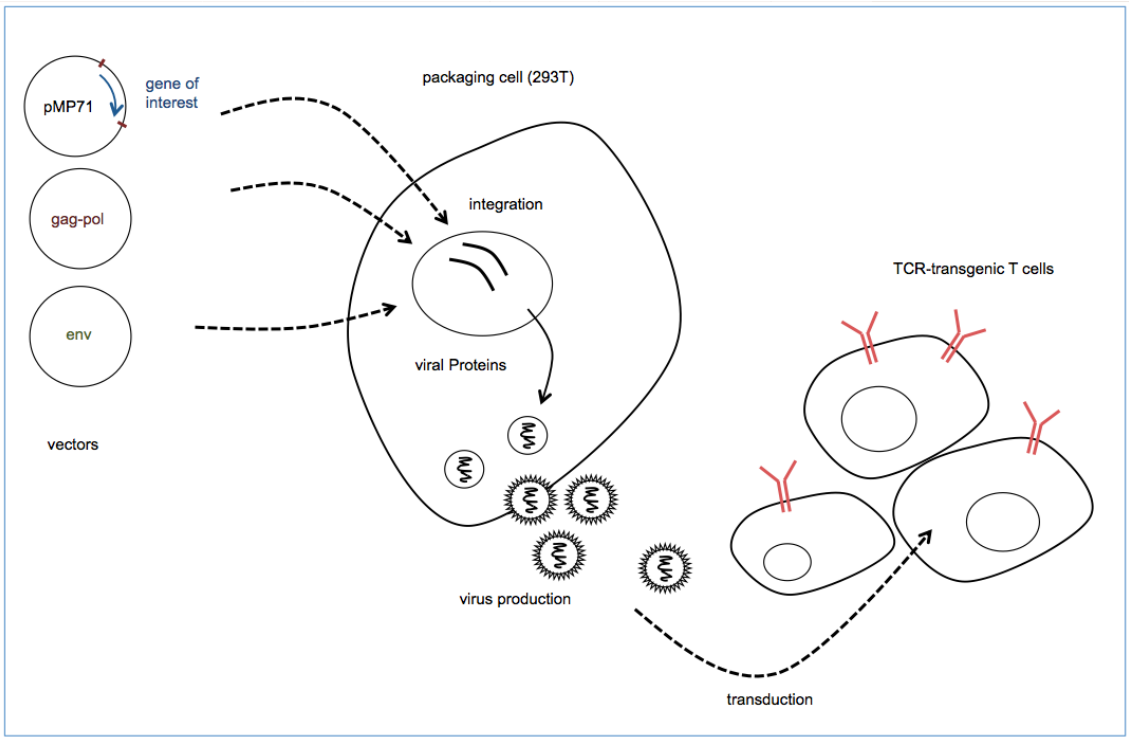

Figure 12 Principle of retroviral gentransfer. The vector (here: pMP71) containing the gene of interest is co-transfected with the vectors gag-pol and env into the packaging cell line 293T. After integration into the genome, the packaging cell line produces virus wich is ready to transduce the TCR sequences into T cells. T cells expressing a transduced TCR on their surface are called TCR-transgenic T cells.

On day 1, 293T cells, which were used as packaging cell line for retroviral transduction, were transferred to 6-well plates (2 x 10^5 cells/well) (see Figure 12).

On day 2, 9 µl TransIT solution and 200 µl serum-free DMEM for each approach were warmed to room temperature, mixed and incubated at room temperature. After 20 min, plasmids were added (1 µg env, 1 µg gag-pol and 1 µg of the plasmid containing the gene of interest) and the solution was incubated for another 30 min at room temperature before it was pipetted into one well of the 6-well plate. PBMC/ T cells were isolated the same day and stimulated with anti-CD3 (50 ng/ml) and required cytokines (100 U/ml IL-2 and 2 ng/ml IL-15).

On day 4, RetroNectin-coated 24-well plates were used for the transduction of PBMC/ T cells or J67 cells. (J67 cells were a kind gift of Prof. Angela Krackhardt, Medizinische Klinik III, Klinikum Rechts der Isar, Technical University Munich.) (RetroNectin coating was performed by an over-night incubation with 5 µg RetroNectin per well and a washing step with 2 ml HBSS per well containing 2.5 % HEPES.) Virus-containing supernatant of 293T cells was collected, centrifuged at 1300 rpm for 5 min and filtered through a 45 µm filter to exclude cells. If necessary, virus supernatant was stored at -80 °C. 1 x 10^6 PBMC/ T cells or 1 x10^5 J67 cells in 1 ml T cell medium were plated into each well of the 24-well plate and co-cultured with 1 ml virus supernatant and 4 µg protamine sulfate. PBMC and T cells additionally required 1 % HEPES and the appropriate cytokines (100 U/ml IL-2 or 30 ng/ml IL-21 and 2 ng/ml IL-15). Plates were centrifuged at 2000 rpm for 90 min at 32 °C and then incubated at 37 °C for 24 hours.

On day 5, transduced cells were split 1 : 1 and the procedure of day 4 was repeated.

On day 7, plates were washed and cytokines were renewed.

On day 10, transduction rates were checked by flow cytometry and – if necessary - selection via G418 (pMSCVneo-constructs), FACS or magnetic bead separation (see 5.17) were performed.

Protocol kindly provided by Prof. Angela Krackhardt, Medizinische Klinik III, Klinikum Rechts der Isar, Technical University Munich.

5.16 Expansion of TCR-transgenic T cells

After selection by FACS or magnetic bead separation on day 10 of infection, 1 x 10^5 to 1 x 10^6 T Cells were directly co-cultured with 6000 U/ml IL-2 in one well of a 24-well plate.

On day 12, the T cells and a hundredfold higher number of irradiated PBMC (pooled from three healthy donors) were transferred to a big cell culture flask containing 75 ml T cell medium and 75 ml RPMI (+ 10 % FCS), as well as 3000 U/ml IL-2 and 30 ng Anti-CD3.

Starting from day 17 to 20, the T cells were tested in flow cytometry and ELISpot.

5.17 Cell sorting with anti-PE microbeads

Optionally to FACS, transgenic T cells could be sorted using anti-PE microbeads. In a first step, multimer staining was performed as described in 5.5. Afterwards, anti-PE microbeads were bound to the multimer-PE complex and multimer positive cells could be separated with MACS columns according to the manufacturer's instruction.

5.18 Detection of murinized T-cell receptors by PCR

To proof the presence of transgenic murinized and optimized T-cell receptor genes, RNA was isolated from transgenic T cells and transcribed into cDNA. Afterwards, a PCR was performed using a 3'-primer binding in the murinized constant region and a 5'-primer that was specific for the relevant variable TCR chain. (Primer sequences are shown in 11.1.) For PCR, Taq DNA polymerase and the appropriate buffer were used:

PCR mix:

5 µl 10 x Buffer – $MgCl_2$
1.5 µl $MgCl_2$
1 µl dNTP mix
0.3 µl Taq DNA polymerase
40.2 µl H_2O
1 µl cDNA
0.5 µl 3'-primer
0.5 µl 5'-primer

PCR program:

95 °C	2 min	
95 °C	30 sec	30 cycles
54 °C	30 sec	
72 °C	50 sec	
4 °C	for storage	

PCR products were loaded onto agarose gel and appropriate bands were extracted. After gel extraction, the presence of specific TCR genes was verified by sequencing (performed by Sequiserve, Vaterstetten).

5.19 Humanized Rag2$^{-/-}$$G_C^{-/-}$ mouse model for primary disease

The day of birth, mice were irradiated with 3.5 Gy and 1.2 x 10^5 HLA-A*0201-$CD34^+$ stem cells derived from human cord blood (see 5.2.4) were injected into the liver of Rag2$^{-/-}$$\gamma_c^{-/-}$ mice as previously described (Traggiai, Chicha et al. 2004). Reconstitution takes about three months and was checked by flow cytometry-based cell staining of spleen biopsies (CD19/ CD45).

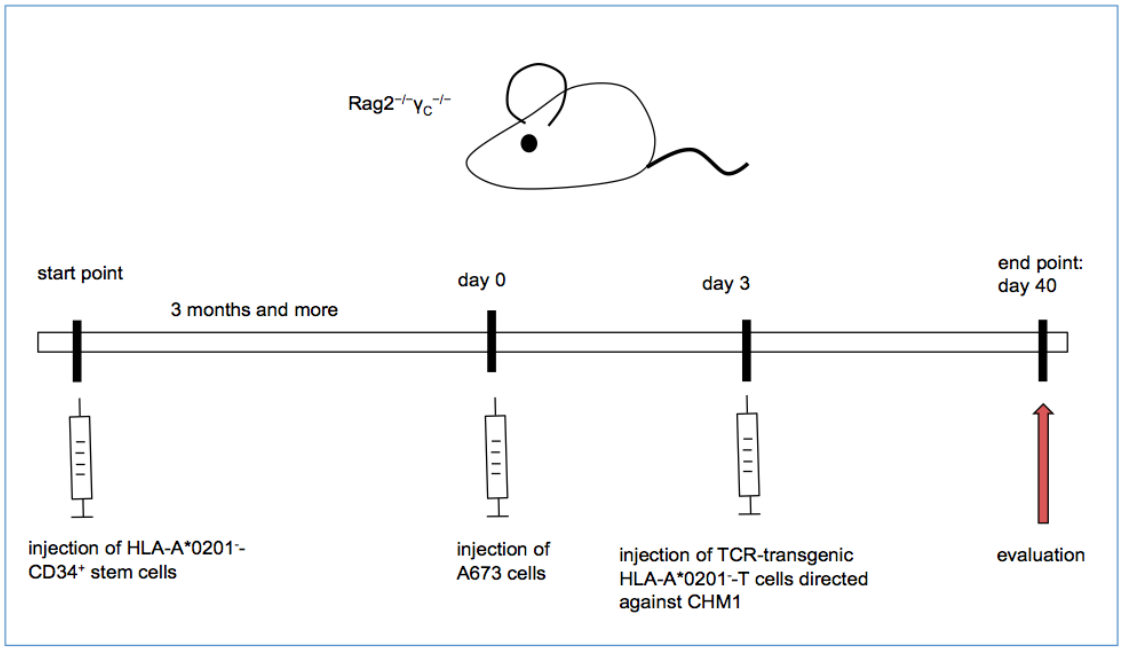

FIGURE 13 Experiment design: humanized Rag2$^{-/-}\gamma_c^{-/-}$ mouse model for primary disease. The experiment started with injection of HLA-A*0201$^-$-CD34$^+$ stem cells into the liver. 3 months later, after reconstitution of a human immune system, A673 ES cells were injected s.c. into the groin on day 0. Three days later, CHM1-specific TCR-transgenic T cells were injected i.v.. Mice were evaluated on day 40.

On day 0 of the experiment 1 x 10^6 A673 cells were injected s.c. (subcutaneously) into the groin. Three days later, T cells (+/- DC) were injected according to the group: Group 1 received no T cells, group 2 received unspecific 5 x 10^6 CD8$^+$ T cells. For mice of group 3 and 4, 5 x 10^6 CD8$^+$ TCR-transgenic CHM1-specific effector T cells were injected without (group 3) or with DC primed with CHM1 (group 4, 2 x 10^6 DC). CD62L$^+$-subpopulation of T cells used for groups 3 and 4 was lower than 5 %. Group 5 and 6 received 5 x 10^6 CD8$^+$ TCR transgenic CHM1-specific central memory T cells (CD62L$^+$-subpopulation higher than 70 %) without (group 5) or with DC primed with CHM1 (group 6, 2 x 10^6 DC). All T cells were HLA-A*0201$^-$ T cells belonging to the same donor of previously injected CD34$^+$ stem cells. T cells were given i.v. (intraveneously).

Mice were killed on day 40, their tumors were weighed and their blood, the spleen and lymph nodes checked for human and CHM1-specific T cells by flow cytometry-based antibody or multimer staining (see Figure 13).

All immune deficient Rag2$^{-/-}\gamma_c^{-/-}$ mice on a BALB/c background were obtained from the Central Institute for Experimental Animals (Kawasaki, Japan) and

maintained in our animal facility under pathogen-free conditions in accordance with the institutional guidelines and approval to Guenther Richter from our laboratory by the local authorities (Regierung von Oberbayern, reference number 55.2-1-54-2531-42-10). We keep our mice under SOPF-conditions within the Zentrum für Praeklinische Forschung (ZPF) of the Klinikum Rechts der Isar, Technical University Munich.

5.20 Statistical Analysis

Error bars of all ELISpot analyses indicate standard deviation of triplicate or sixfold experiments as indicated under the according figure. Two-tailed T test was used for statistical analyses of ELISpot results. $0.01 <= p < 0.05$ was regarded as statistical significant (*), $0.001 <= p < 0.01$ was regarded as statistical very significant (**), $p < 0.001$ was regarded as statistical highly significant (***).

6 Results

6.1 Preliminary work: generation of allo-restricted peptide-specific T-cell clones directed against ES antigens

6.1.1 EZH2 and CHM1 represent target antigens for ES immunotherapy

To identify ES-specific antigens, microarray analyses were performed as published by our group (Staege, Hutter et al. 2004), demonstrating strong up-regulation of Enhancer of Zeste, Drosophila, Homolog 2 (EZH2, OMIM: *601573) and Chondromodulin 1 (CHM1, OMIM: *605147). As a member of PcG (Polycomb) family, EZH2 is involved in transcriptional gene repression and is critical for maintenance of stemness (Richter, Plehm et al. 2009) (Burdach, Plehm et al. 2009). CHM1 is a glycoprotein of cartilage, stimulating the chondrocyte growth. Both candidate antigens were further characterized in a previous publication of our group (Thiel, Pirson et al. 2011): As shown in Figure 14, panel A, EZH2 and CHM1 are highly overexpressed in ES tissue. While EZH2 expression reveals ubiquitously at low levels in normal tissue, CHM1 is not expressed in any of the tested normal tissues, indicating EZH2 being a ES-associated and CHM1 being a ES-specific antigen. Results were confirmed by Realtime-PCR (RT-PCR) as previously published (Figure 14, panel B) (Thiel, Pirson et al. 2011).

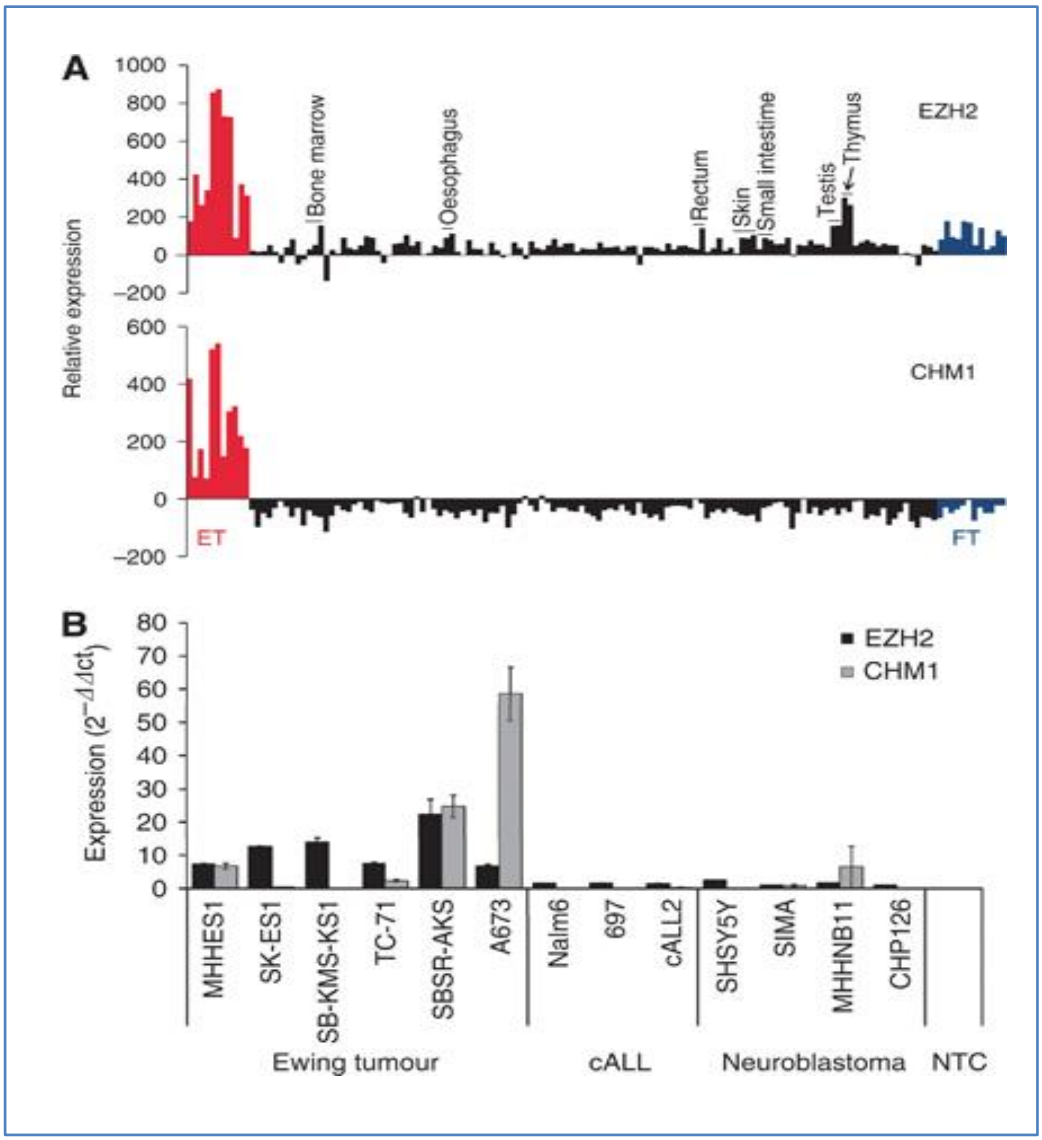

FIGURE 14 EZH2 and CHM1 are overexpressed in ES. (A) Overexpression of Enhancer of Zeste, Drosophila, Homolog 2 (EZH2) and Chondromodulin 1 (CHM1) in Ewing tumors (ET, red bars) compared to normal (grey bars) and foetal tissue (FT, blue bars), detected by microarray analysis. (B) RT-PCR identified EZH2 and CHM1 as highly overexpressed in several ES cell lines compared to common ALL and neuorobastoma cell lines. Error bars represent standard deviation of triplicate experiments. NTC = non-template control. Figure taken from Thiel et al, BJC, 2011.

6.1.2 Generation of EZH2^{666}- and CHM1^{319}-specific allo-restricted T-cell clones

Using BIMAS (http://www-bimas.cit.nih.gov/molbio/hla_bind/) and SYFPEITHI (http://www.syfpeithi.de/), peptides consisting of nine amino acids were identified for both antigens (Pirson 2009). In the present work we focused on the peptides EZH2^{666} (YMCSFLFNL) and CHM1^{319} (VIMPCSWWV). For each peptide, several CD8^{+} HLA-A*0201-restricted clones were generated. In this thesis EZH2 clone 15 (EZH2-15, previously published (Thiel, Pirson et al. 2011) and CHM1 clone 4B4 (CHM1-4B4, manuscript in preparation) were used. Both clones were produced by priming of CD8^{+} T cells with peptide-pulsed mature DC (Leisegang, Engels et al.). CD8^{+}/multimer-HLA-A*0201^{+} cells were sorted via FACS and further expanded using limiting dilution. Exemplarily, FACS for a CHM1-specific clone is shown in Figure 15, panel A. After another expansion, IFNγ-ELISpot analyses and flow cytometry-based multimer staining proved that EZH2-15 and CHM1-4B4 are able to specifically recognize the appropriate antigen in an HLA-A*0201-restricted manner. Figure 15, panel B to D include the ELISpot assay and multimer-(pentamer-)staining results for EZH2-15. In ELISpot screens, the recognition of EZH2-peptide pulsed T2 cells was detected and checked against a negative control (influenza-peptide (FLU) pulsed T2 cells). Additionally, several cell lines and in some cases also the specificity for peptide-HLA-A*0201-transfected COS cells was proved and compared to the recognition of COS cells transfected with HLA-A*0201 and an irrelevant peptide. For multimer staining, binding of the EZH2-multimer was matched against the binding of an irrelevant peptide-multimer.

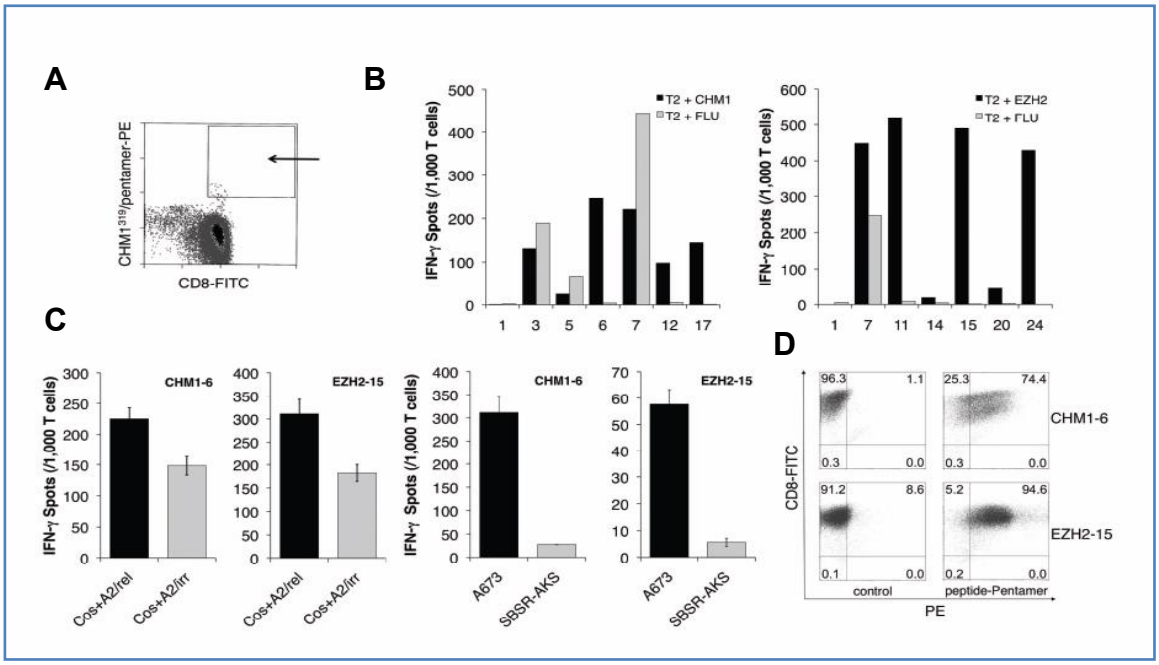

FIGURE 15 FACS and specificity analyses for EZH2- and CHM1-specific T-cell clones. Peptide-HLA-A*0201-multimer$^+$/ CD8$^+$T cells were sorted by flow cytometry directed cell sorting (A). Sorted T cells were tested for peptide specificity and HLA-A*0201 restriction in IFNγ ELISpot assays (A673: HLA-A*0201$^+$ ES, SBSR-AKS = SB-KMS-KS: HLA-A*0201$^-$ ES) (B, C). Flow cytometric determination of peptide specificity with specific EZH2-/ CHM1-HLA-A*0201-multimers shows a complete shift of CD8$^+$ T cell population (D). Effector/Target (E/T) ratio for ELISpot: 1:4. Error bars represent standard deviation of triplicate experiments. Figure taken from Thiel et al, BJC, 2011.

In analogy, ELISpot and pentamer staining results for CHM1-4B4 are shown in Figure 15.

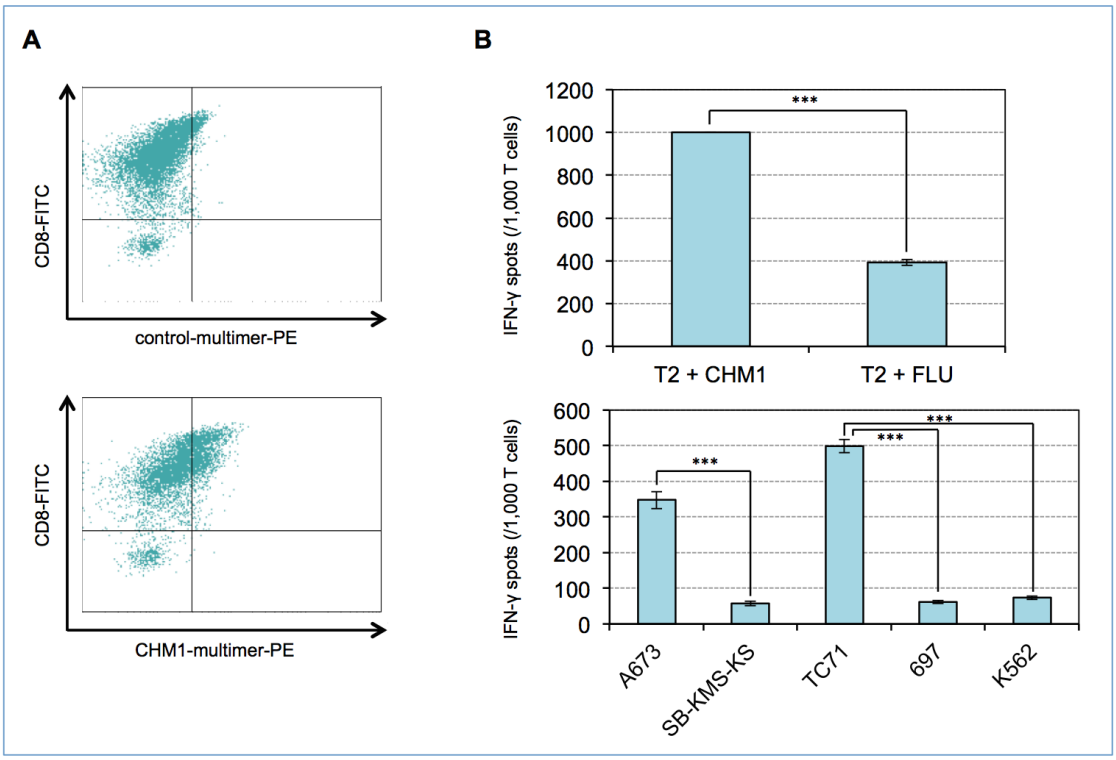

FIGURE 16 FACS and specificity analyses for clone CHM1-4B4. Flow cytometric determination of peptide specificity with specific CHM1-HLA-A*0201-multimers shows a complete shift of $CD8^+$ T cell population (A). An unspecific HLA-A*0201-multimer served as control. In IFNγ ELISpot analyses (B), clone CHM1-4B4 shows peptide specificity and HLA-A*0201 restriction. A673 and TC71: HLA-A*0201^+ ES, SB-KMS-KS: HLA-A*0201^- ES, 697: HLA-A*0201^+ pediatric cALL, K562: MHC^- NK cell control. E/T ratio for ELISpot: 1:4. Error bars represent standard deviation of triplicate experiments, *** means $p < 0.001$. (Data generated by Uwe Thiel, manuscript in preparation.)

6.2 MONOCLONALITY PROOF OF EZH2-15 AND CHM1-4B4 AND IDENTIFICATION OF TCR CHAINS

To identify the variable TCR chains of EZH2-15 and CHM1-4B4, a specific PCR analysis was performed (Figure 17 and Figure 18). Upper bands (550 basepairs (bp) for α-repertoire, 350 bp for β-repertoire) represent the PCR products flanked by the constant primers (3'αST and 5'αST, respectively 3'βST and 5'βST). Although these bands should refer as an inner control, they in some cases disappeared when questionable specific bands emerged – hinting at some competing event between control and specific primers. Specific bands came up at a height of 370 to 500 bp for the α-chain and 190 to 290 bp for the

β-chain and were formed by binding of primers for the detection of variable TCR chains (3'TCα and Vαx respectively 3'CβII and Vβx). The debatable specific bands for the variable chain were all cut from the gel and sent for sequencing. Detectable sequences were analyzed and EZH2-15 was found to be positive for variable TCR chains TRAV12-3*01 and TRBV6-5*01. CHM1-4B4 carries TRAV13-1*02 and TRBV13*01. As EZH2-15 and CHM1-4B4 both showed only one TCR, they were declared monoclonal. Complete DNA sequences for the TCR of both clones were composed in co-operation with Prof. Angela Krackhardt, Medizinische Klinik III, Klinikum Rechts der Isar, Technical University Munich. TCR sequences are shown in 11.2. All primer sequences for TCR repertoire analyses kindly provided by Prof. Angela Krackhardt, Medizinische Klinik III, Klinikum Rechts der Isar, Technical University Munich.

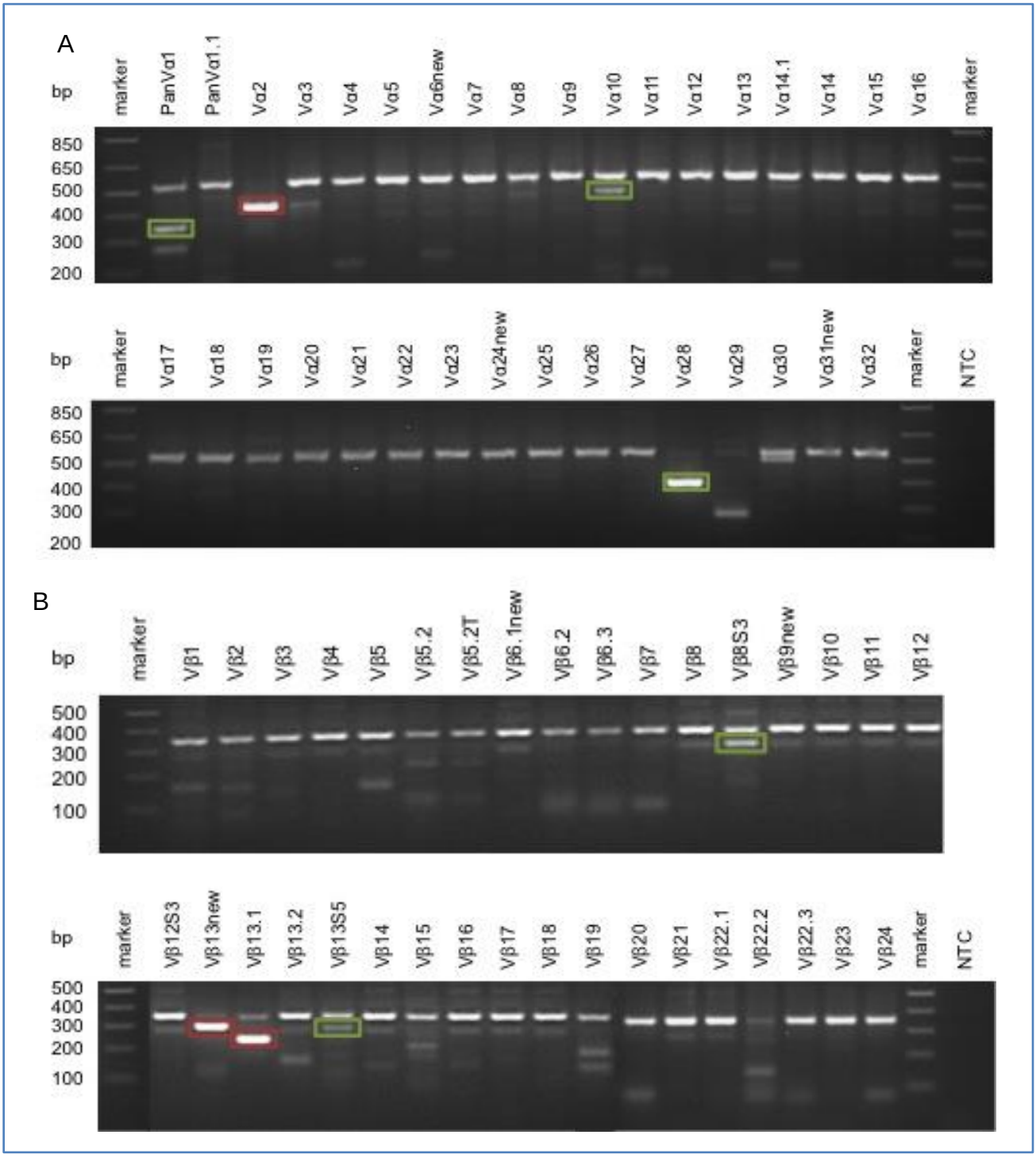

FIGURE 17 TCR Vαβ-repertoire of EZH2-15. Variable α-chains were detected via PCR (A). Upper bands (550 bp) represent the PCR product flanked by the constant primers 3'αST and 5'αST (inner control). Questionnable positive variable α-chains (framed bands, possibly flanked by primer 3'TCα and the Vαx primer) were sequenced. EZH2-15 was found to be positive only for the variable α-chain TRAV12-3*01, detected by primer Vα2 (red border). All other sequenced PCR products were unspecific or showed no open-reading-frame (green border). Variable β-chains were identified in a similar way (B). Inner control bands flanked by primers 3'βST and 5'βST showed up at 350 bp. Debatable positive variable β-chains (framed bands, possibly flanked by primer 3'CβII and the Vβx primer) were sequenced. EZH2-15 was identified to be positive only for the variable β-chain TRBV6-5*01, detected by primers Vβ13new and Vβ13.1 (red border). (Primers Vβ13new and Vβ13.1 were constructed to identify the same TCR chain.) All other sequenced PCR products were unspecific or showed no open-reading-frame (green border). NTC= non-template control.

6.2. Monoclonality proof of EZH2-15 and CHM1-4B4 and identification of TCR chains

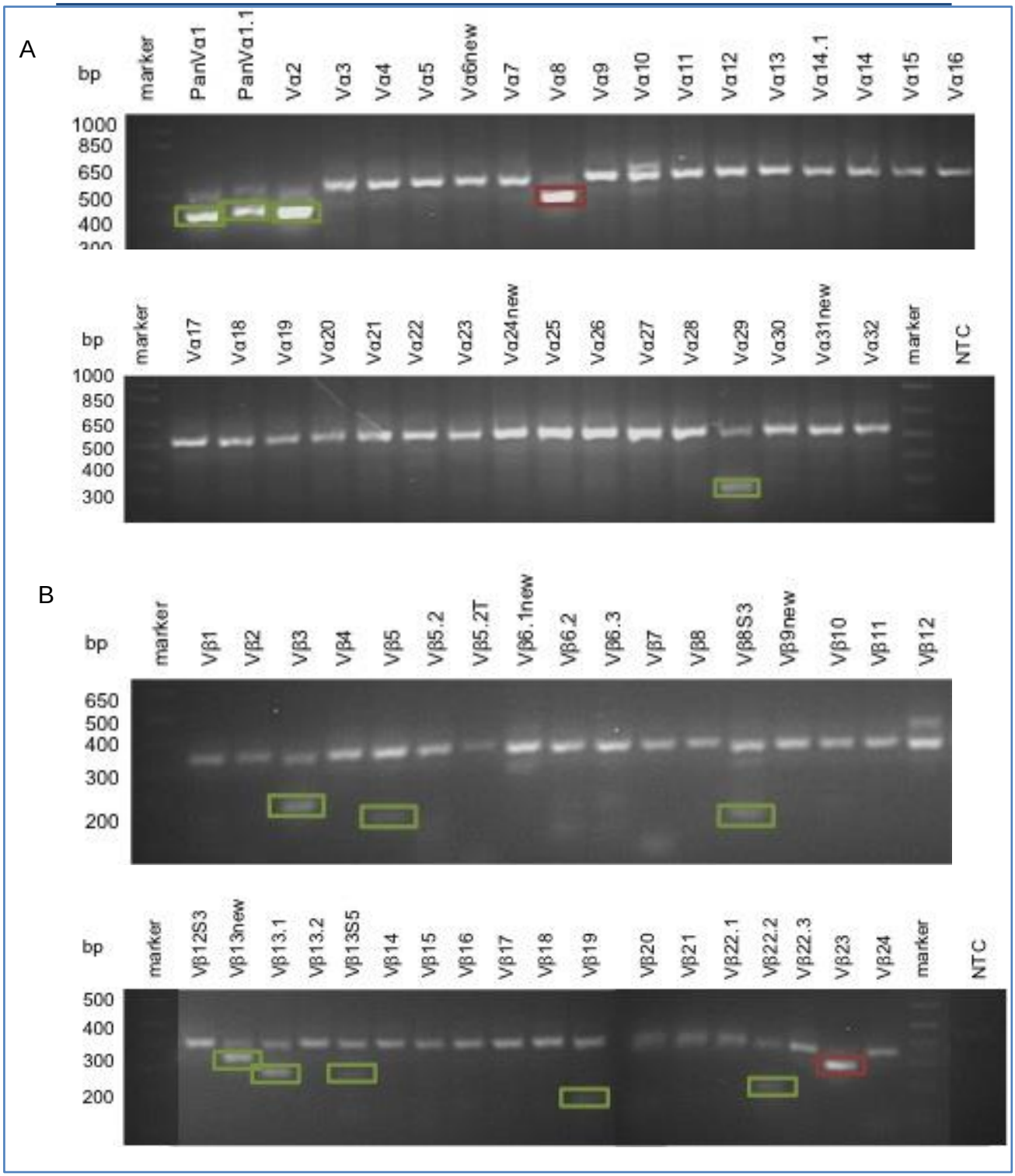

FIGURE 18 **TCR Vαβ-repertoire of CHM1-4B4.** Variable α-chains were detected via PCR (A). Upper bands (550 bp) represent the PCR product flanked by the constant primers 3'αST and 5'αST (inner control). Questionnable positive variable α-chains (framed bands, possibly flanked by primer 3'TCα and the Vαx primer) were sequenced. CHM1 clone 4B4 was found to be positive only for the variable α-chain TRAV13-1*02, detected by primer Vα8 (red border). All other sequenced PCR products were unspecific or showed no open-reading-frame (green border). Variable β-chains were identified in a similar way (B). Inner control bands flanked by primers 3'βST and 5'βST showed up at 350 bp. Debatable positive variable β-chains (framed bands, possibly flanked by primer 3'CβII and the Vβx primer) were sequenced. CHM1-4B4 was identified to be positive only for the variable β-chain TRBV13*01, detected by the primer Vβ23 (red border). All other sequenced PCR products were unspecific or showed no open-reading-frame (green border). NTC= non-template control.

6.3 Cloning of TCR

To investigate the ideal cloning and transduction strategy, the following vectors were constructed (see 4.8):q

Name of construct	Construction strategy
pMP71_GFP (control vector)	Kindly provided by Prof. Angela Krackhardt, Medizinische Klinik III, Klinikum Rechts der Isar, Technical University Munich
pMP71_EZH2	Unoptimized and unmurinized EZH2-specific TCR sequence in pMP71 via EcoRI and NotI
pMP71_EZH2_mu_opt	Codon-optimized and murinized EZH2-specific TCR sequence in pMP71 via EcoRI and NotI (with the help of GeneArt, Life Technologies, Regensburg)
pMP71_CHM1_mu_opt	Codon-optimized and murinized CHM1-specific TCR sequence in pMP71 via EcoRI and NotI (with the help of GeneArt, Life Technologies, Regensburg)
pMSCVneo_EZH2	Unoptimized and unmurinized EZH2-specific TCR sequence in pMSCVneo via EcoRI and XhoI
pMSCVneo_EZH2_mu_opt	Codon-optimized and murinized EZH2-specific TCR sequence in pMSCVneo via EcoRI and XhoI (with the help of GeneArt, Life Technologies, Regensburg)

pMSCVneo_CHM1_mu_opt	Codon-optimized and murinized CHM1-specific TCR sequence in pMSCVneo via EcoRI and XhoI (with the help of GeneArt, Life Technologies, Regensburg)

For additional information see 4.8.

In each case, the TCR β-chain was linked to the α-chain to ensure equimolar expression of both chains (see Figure 19). A P2A linker was introduced between the chains, resulting in a ribosomal skip to generate separate proteins (Leisegang et al, 2008; Szymczak et al, 2004). Codon-optimization was performed to enhance expression rates. The complete murinization of the constant chains is a known method to increase CD3 stability and to decrease the rate of mispairing between transgenic TCR chains and the endogenous TCR chains of the target cells (Cohen 2006). Codon-optimization and murinization were performed with the help of Dr. Matthias Leisegang, Prof. Wolfgang Uckert (both Max-Delbrueck-Center for Molecular Medicine, Berlin) and GeneART, Life Technologies, Regensburg.

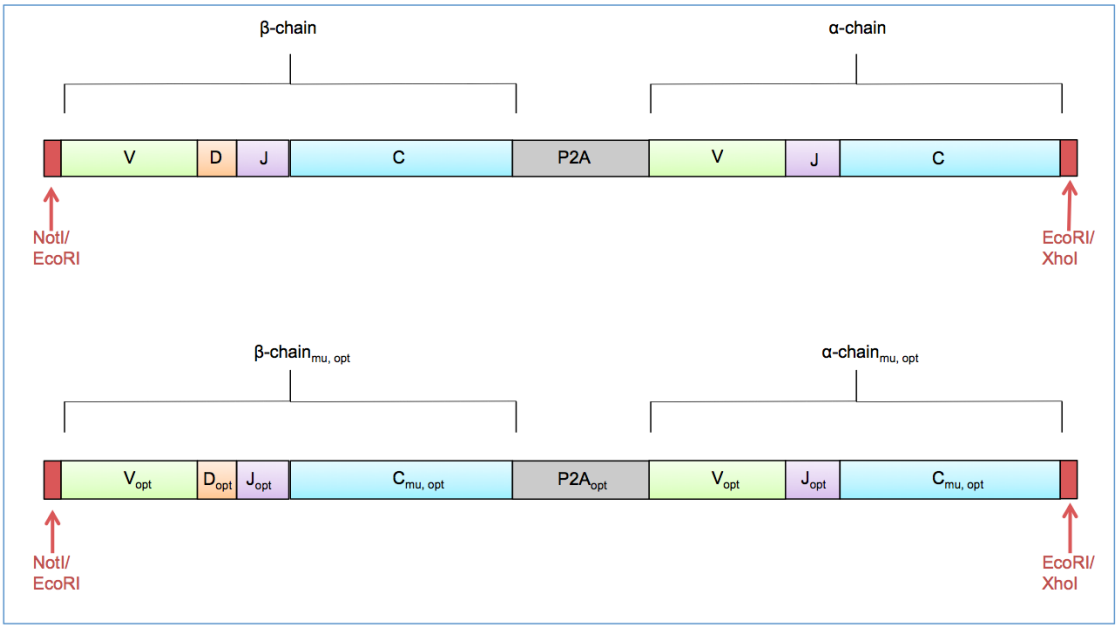

FIGURE 19 Retroviral transduction of TCR: Schematic representation of insert construction and optimization. The upper panel shows the unoptimized TCR insert. β- and α-chain are linked via a P2A linker and connected to the restriction sites. The optimized insert is shown in the lower panel: Constant human chains are exchanged with the murine counterpart. All parts of the TCR are codon-optimized. β- and α-chain are linked via a codon-optimized P2A linker and connected to the restriction sites. V = variable segment, J = joining segment, C = constant segment, D = diversity segment, mu = murinized, opt = codon-optimized.

As mispairing of TCR chains is known to be critical for severe complications in mice (van Loenen, de Boer et al. 2010), unmurinized constructs were only used for several preliminary tests:

6.4 TRANSDUCTION RATES WITH CONTROL VECTOR PMP71_GFP

To establish the transduction of target cells with the retroviral vector pMP71 in our laboratory, $CD8^+$ J67 cells, PBMC and $CD8^+$-preselected PBMC were transduced with the GFP-containing control vector pMP71_GFP. Transduction efficacy was checked by fluorescence microscopy and confirmed by flow cytometry (GFP is found in the FITC channel) (see Figure 20). J67 cells were transduced with the highest rate (61.0 %), most probably because they do not bear an endogenous TCR and therefore competition between endogenous and

transgenic TCR chains do not take place. PBMC reached a transduction rate of 50.0 %. As expected, the rate of transduced $CD8^+$-pre-selected cells was lower (28.3 %), supposedly due to absent co-stimulation of other mononuclear blood cells.

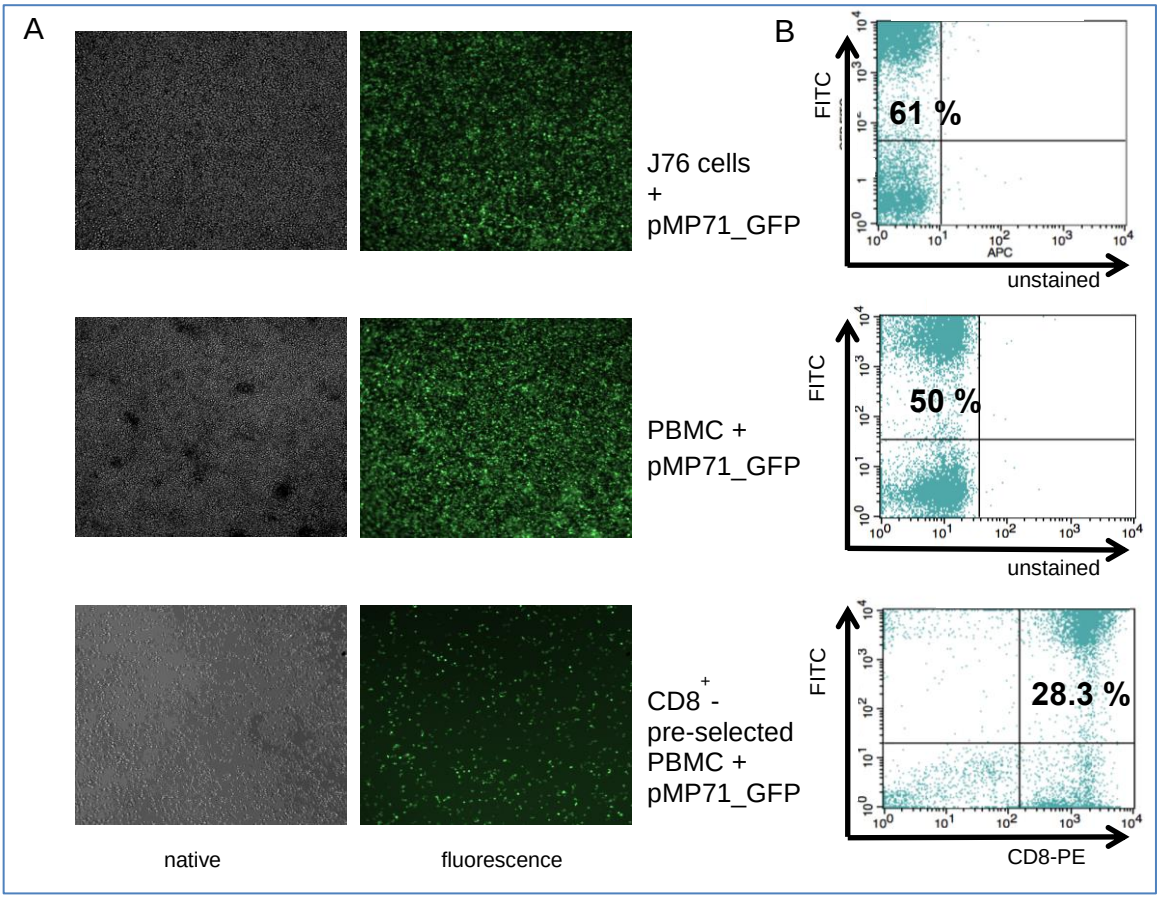

FIGURE 20 Transduction rates of J76 cells compared to PBMC and $CD8^+$-pre-selected PBMC. For transduction, control vector pMP71_GFP was used. On day six after first transduction, fluorescence microscopy (A) and flow cytometry (B) were performed. GFP^+ cells are found in the FITC cannel. $CD8^+$-pre-selected PBMC were counterstained with CD8-PE antibody, all others were left unstained.

6.5 CODON-OPTIMIZATION AND MURINIZATION INCREASE THE EXPRESSION OF TRANSGENIC TCR

PBMC were transduced with the unoptimized and unmurinized retroviral vector pMP71_EZH2 and transduction rates were checked by flow cytometry (Figure 21, top panel). For this purpose, a PE-labeled control-multimer and a PE-labeled HLA-A*0201-EZH2 multimer (kindly provided by Prof. Dirk Busch, Institute for Medical Microbiology, Immunology and Hygiene, Technical University Munich) were used. Due to the very low transduction rates (0.9 %) and the high risk of mispairing of transgenic TCR chains with endogenous TCR chains, transduction was repeated using the codon-optimized and murinized vector MP71_EZH2_mu_opt. With this vector, expression rates of up to 21 % were achieved (Figure 21, bottom panel) confirming the fact that optimization and murinization of the TCR insert results in increased expression of the transgenic product.

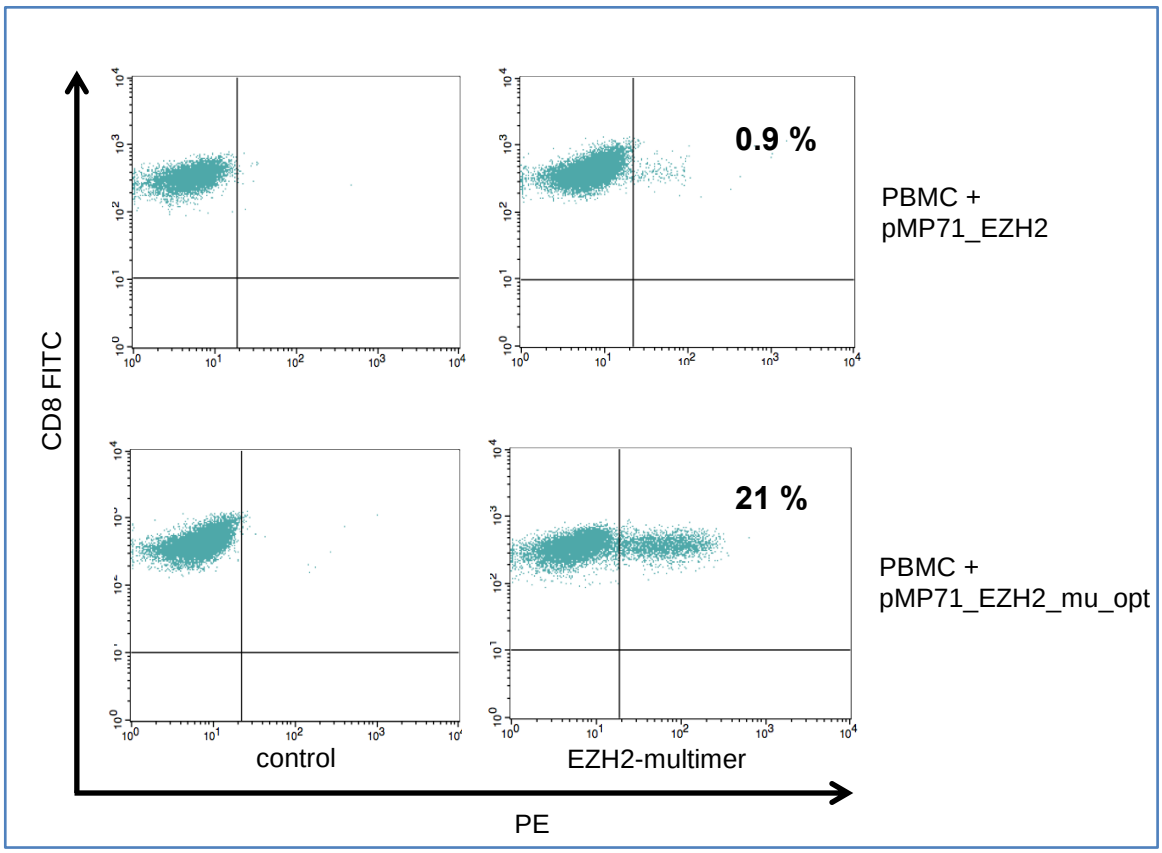

FIGURE 21 Comparison of transduction rates of unmodified with murinized/ codon-optimized pMP71 vector. PBMC were transduced with either pMP71_EZH2 (top panel) or pMP71_EZH2_mu_opt (bottom panel). Transduced PBMC were stained with EZH2-HLA-A*0201-multimer, irrelevant peptide-HLA-A*0201-multimers served as control. Cells were counterstained with CD8-FITC and gated for CD8 positivity.

6.6 Detection of correct transgenic TCR chains by PCR

In order to detect the presence of the precise transgenic TCR chains, RNA was isolated from transgenic EZH2- and CHM1-specific T cells. After cDNA synthesis, PCR was performed with primers shown in 11.1.1 (see Figure 22). Due to the fact that the 3'-primers bound in the constant murine chains, a certain detection of transgenic TCR was guaranteed.

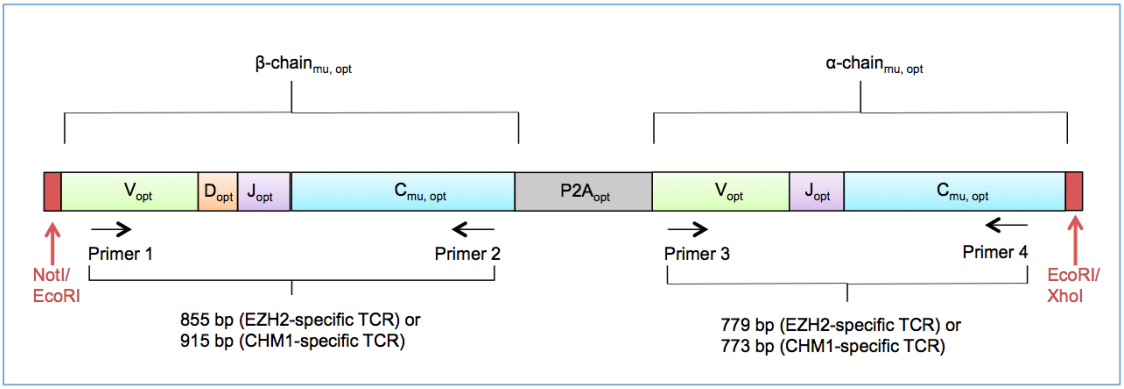

Figure 22 Schematic representation: Primer design for detection of transgenic TCR chains. The optimized and murinized TCR insert is shown with binding sites of detection primers. Primers 1 and 2 detect the murinized and optimized β-chain and result in a PCR product with a length of 855 bp for the EZH2-specific TCR and a length of 915 bp for the CHM1-specific TCR. Primers 3 and 4 result in a PCR product with a length of 779 bp for EZH2-specific TCR and 773 bp for CHM1-specific TCR and detect the α-chain. Primer 1 = EZH2/CHM1_beta_murine_forw, primer 2 = EZH2/CHM1_beta_murine_rev, primer 3 = EZH2/CHM1_alpha_murine_forw, primer 4 = EZH2/CHM1_alpha_murine_rev. V = variable segment, J = joining segment, C = constant segment, D = diversity segment, mu = murinized, opt = codon-optimized.

In subsequent electrophoresis, clear bands emerged at the expected height (see Figure 23). Sequencing confirmed correctness of optimized and murinized TCR DNA sequences.

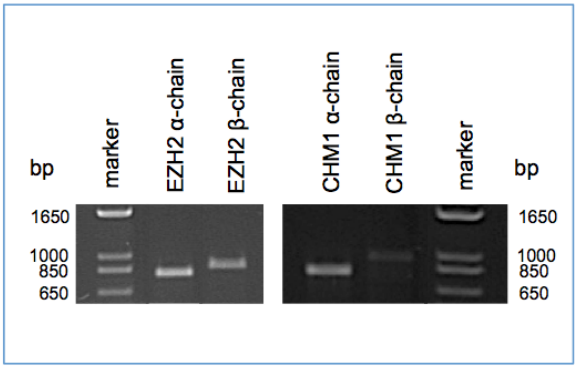

FIGURE 23 Detection of transgenic TCR chains by PCR. After amplification, PCR products were loaded onto agarose gel. Expected bands are shown for EZH2-specific α- and β-chains of the transgenic TCR (779 bp and 855 bp) and for CHM1-specific α- and β-chains of the transgenic TCR (773 bp and 915 bp).

6.7 USE OF PMSCVNEO VECTOR SYSTEM OFFERS ADDITIONAL STRATEGIES

In a parallel approach, PBMC were transduced with the unoptimized and unmurinized vector pMSCVneo_EZH2. Unfortunately, in a subsequent staining with EZH2-HLA-A*0201-multimer, no transduction of the target cells was found (data not shown). To overcome this frontier, the optimized and murinized vectors pMSCVneo_EZH2_mu_opt or pMSCVneo_CHM1_mu_opt were used instead. Transduction rates after selection with G418 were detected by flow cytometry. While transduction with pMSCVneo_CHM1_mu_opt was not successful (data not shown), transduction with pMSCVneo_EZH2_mu_opt yielded to 3.2 % HLA-A*0201-EZH2-multimer$^+$ CD8$^+$ T cells. Staining with an unspecific HLA-A*0201-multimer as negative control showed a relatively high background (0.8 %) (see Figure 24).

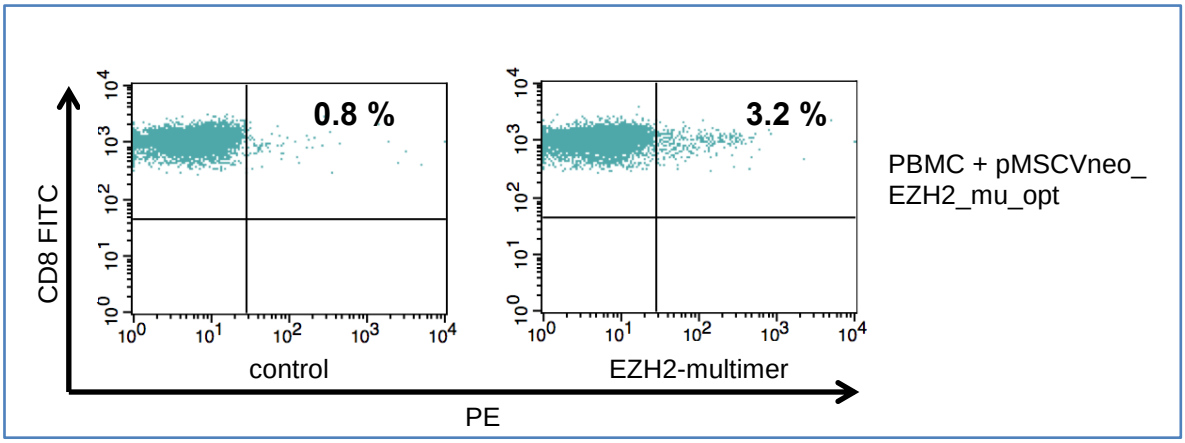

FIGURE 24 Transduction rates with vector pMSCVneo_EZH2_mu_opt. Transduced and selected PBMC were stained for CD8-FITC and EZH2-HLA-A*0201-multimer or control-HLA-A*0201-multimer and analyzed by flow cytometry.

Since an increase of transduction rates after subsequent selection steps could not be reached, the pMSCVneo vector system was not further investigated for the retroviral transfer of transgenic TCR in this thesis. Nevertheless, this vector system might serve as an attractive alternative to pMP71-vectors in the future.

6.8 Transduction of cord blood or peripheral blood yields high transduction rates of immature T cells

In analogy to adult peripheral blood and in preparation for humanized mouse models, PBMC derived from cord blood were transduced with the vector pMP71_CHM1_mu_opt. On day 12 after first transduction, flow cytometry staining showed a high percentage of $CD62L^+/CD8^+/CD45RO^+$ T cells. The presence of CD45RO confirmed that these T cells were not naïve, whereas the positivity for CD62L indicated a central memory phenotype of the cells (see Figure 25, panel A). 23 days later, the cells had become $CD62L^-$ - hinting at the process of maturation to effector phenotype (Figure 25, panel B). Similar results were reached after transduction of peripheral blood.

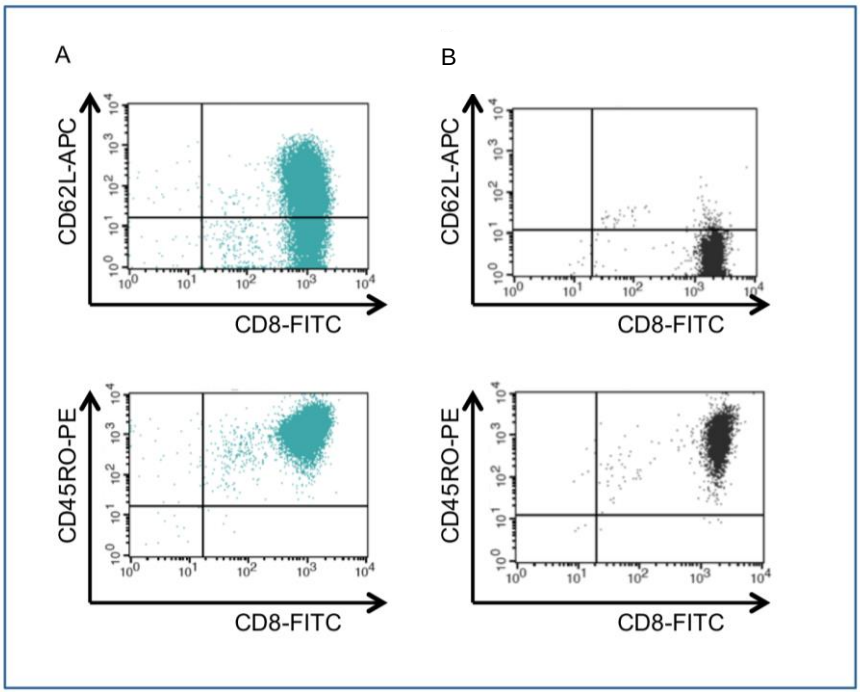

Figure 25 **Phenotype of TCR-transgenic T cells.** Several days after transduction of cord blood with the vector pMP71_CHM1_mu_opt, phenotypic markers of T cells were checked by flow cytometry. Panel A shows the staining results 12 days after first transduction, panel B the results 35 days after first transduction.

6.9 Magnetic bead selection yields to pure populations of multimer-specific transgenic T cells

In order to guarantee a GMP-accredited way of engineering TCR-transgenic T cells, peptide-specific T cells were selected with the help of magnetic beads. Therefore, transduced PBMC derived from cord blood or adult peripheral blood were stained with the appropriate PE-labeled HLA-A*0201-peptide-multimer. PE was then linked to anti-PE microbeads and positive cells were sorted via separation columns. After subsequent expansion, flow cytometric analyses showed an extremely high multimer-positivity of up to 98.3 % for EZH2 and up to 92.7 % for CHM1 (see Figure 26).

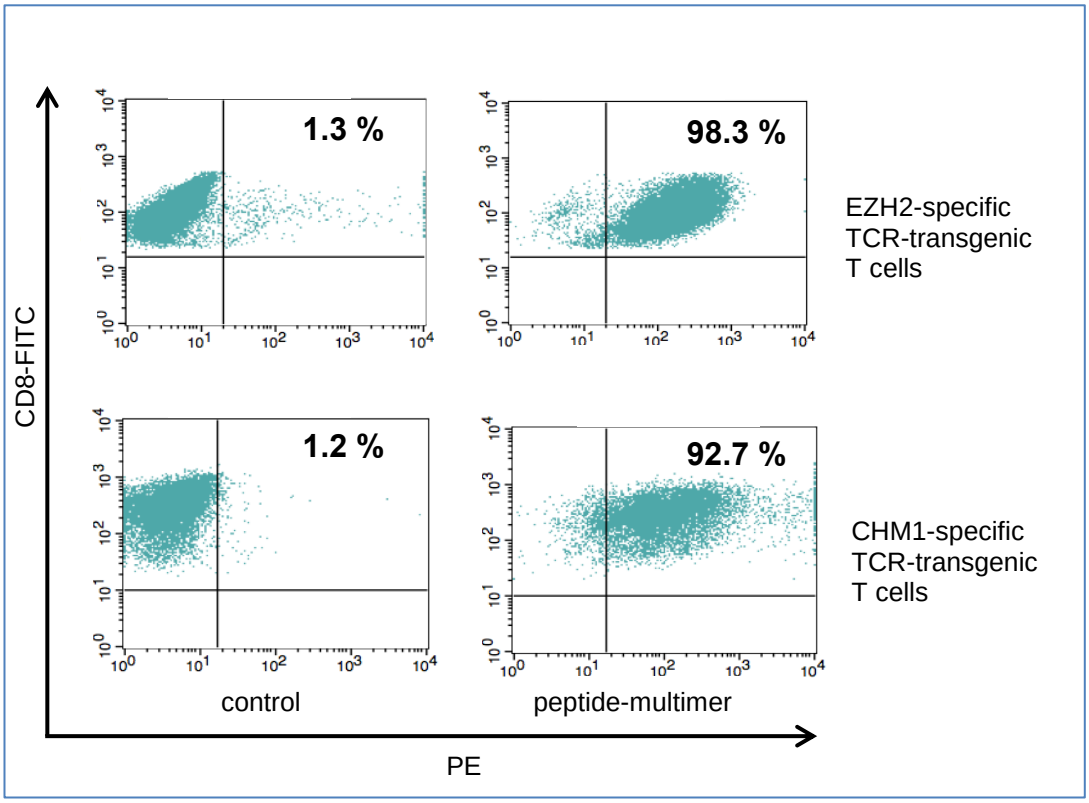

Figure 26 Transduction rates after magnetic bead selection and subsequent expansion. Sorted and expanded TCR-transgenic T cells were stained with the appropriate HLA-A*0201-peptide-multimer. An irrelevant HLA-A*0201-peptide-multimer served as control. EZH2-specific $CD8^+$ T cells are shown in the top panel, CHM1-specific cells in the bottom panel. Cells were gated for CD8-positivity.

6.10 CHM1-SPECIFIC TCR-TRANSGENIC T CELLS SHOW PEPTIDE SPECIFICITY AND HLA-A*0201-RESTRICTION *IN VITRO*

TCR-transgenic T cells were tested in ELISpot assays two to five weeks after transduction. When presented on TAP-deficient T2 cells, EZH2-specific T cells recognized the appropriate antigen specifically and released IFNγ (Figure 27). Unfortunately, EZH2-specific transgenic T cells were not able to detect any of the tumor cell lines presented in the IFNγ-ELISpot assay (data not shown). Therefore, we also tested the ability of EZH2-specific transgenic T cells to release Granzyme B and IL-2. Again, they were able to recognize T2 cells (see Figure 27) but did not react against ES cell lines (data not shown, see 7.7).

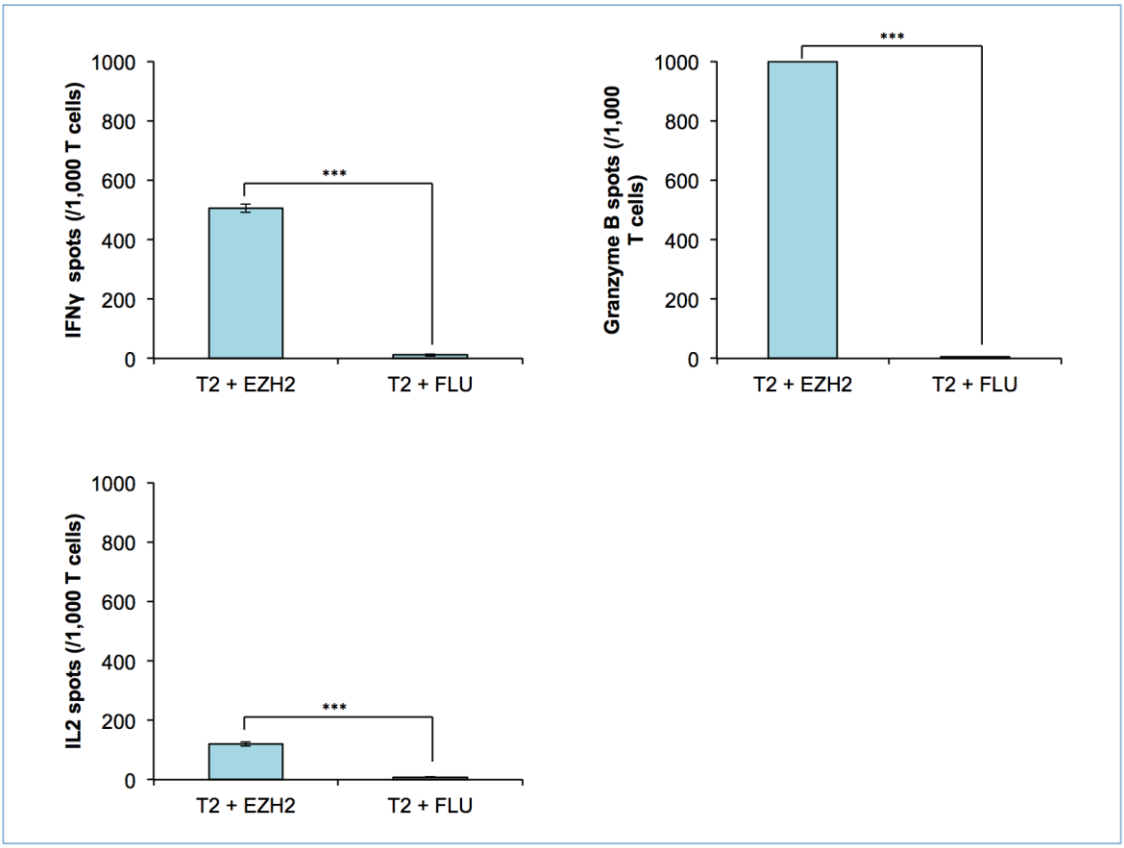

FIGURE 27 Peptide specificity of EZH2-specific TCR-transgenic T cells in IFNγ, Granzyme B and IL2-ELISpot assays. T2 cells were either pulsed with EZH2-peptide or with control-peptide (FLU). E/T-Ratio: 1:4. Error bars represent standard deviation of triplicate experiments, *** means $p < 0.001$.

Although we tested several expansion conditions (IL-21±IL-7±IL-15±IL-2) and the impact of the phenotype (T_{CM} versus T_{Eff}), we were not able to observe a specificity of EZH2-specific TCR-transgenic T cells against ES cell lines in any of these experiments. In consequence, we focused on CHM1-specific TCR-transgenic T cells:

CHM1-specific TCR-transgenic T cells were not only able to react against peptide-pulsed T2 cells, but also showed a good reactivity against ES cell lines and restriction for HLA-A*0201 in IFNγ-ELISpot analyses. In Granzyme-B-ELISpot analyses they were able to specifically lyse the HLA-A*0201^{+} ES cell line A673 in a dose-dependent manner (see Figure 28). The specificity of CHM1-specific transgenic T cells was not dependent on expansion conditions or phenotype.

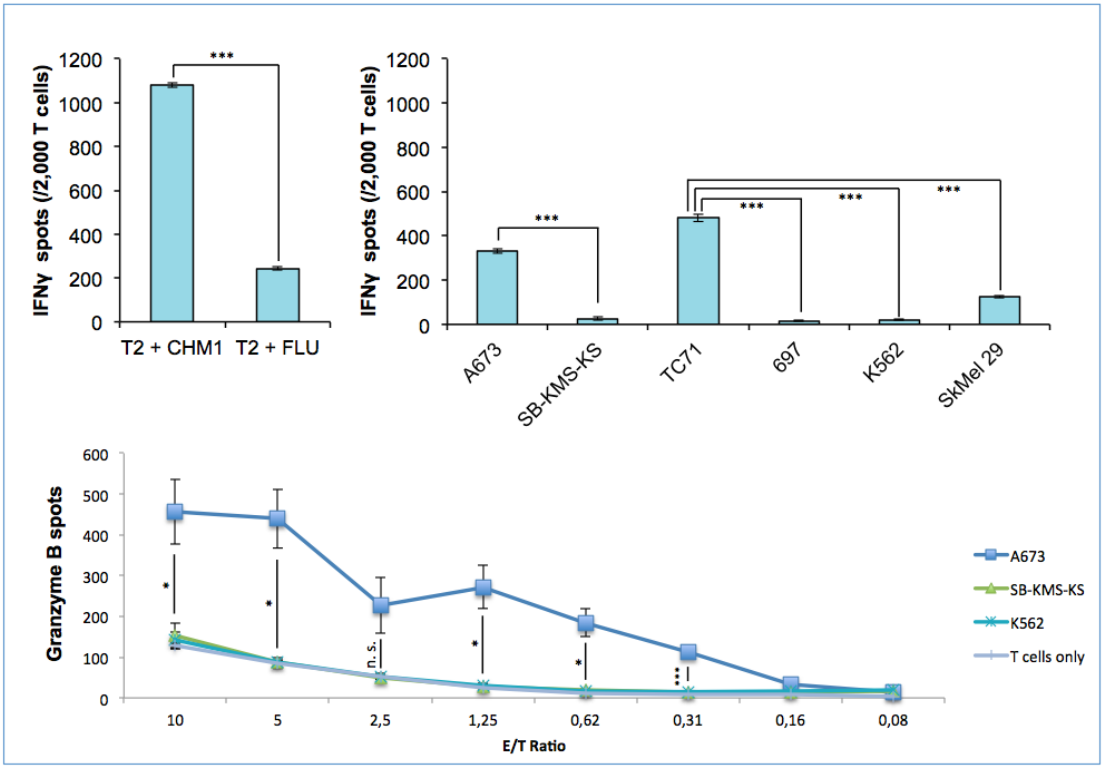

FIGURE 28 Peptide specificity and HLA-A*0201-restriction of CHM1-specific TCR-transgenic T cells. Specific reactivity against peptide-loaded T2 cells and several tumor cell lines was verified in IFNγ- and Granzyme-B-ELISpot analyses (A673 and TC71: HLA-A*0201^{+} ES, SB-KMS-KS: HLA-A*0201^{-} ES, 697: HLA-A*0201^{+} pediatric cALL, K562: MHC^{-} NK cell control, SK-Mel-29: HLA-A*0201^{+} melanoma). E/T ratio for IFNγ-ELISpots is 1:4. Error bars represent standard deviation of sixfold (for IFNγ) or triplicate (for Granzyme B) experiments. * means 0.01 <= p < 0.5, *** means p < 0.001, n.s. means not significant.

6.11 Specificity of CHM1-specific TCR-transgenic T cells *in vivo*

In a first approach, we investigated the effect of CHM1-specific TCR-transgenic T cells on primary tumor growth in reconstituted $Rag2^{-/-}\gamma c^{-/-}$ mice. Three months after injection of $CD34^+$ stem cells into the liver, establishment of an HLA-A*0201$^-$ human immune system was checked by flow cytometry-based cell staining of spleen biopsies (CD19/ CD45). After reconstitution, all mice received an injection of A673 ES cells (HLA-A*0201$^+$) into the groin. Three days later, we injected HLA-A*0201$^-$ CHM1-specific TCR-transgenic T cells i.v. according to six different groups. To imitate the situation after allo-SCT, these T cells were derived from the same cord blood sample as the $CD34^+$ stem cells. Group 1 served as a control group and received no T cells. Group 2 – as second control group – was only treated with unspecific $CD8^+$ T cells. Groups 3 to 6 received CHM1-specific TCR-transgenic T cells either holding a central memory or an effector phenotype and with or without additional injection of CHM1-pulsed DC. Mice were sacrificed 40 days after tumor injection. Unfortunately, we could not detect a delay of tumor growth caused by CHM1-specific TCR-transgenic T cells in any of the study groups (see Figure 29). Additionally, no transgenic T cells were detectable in any of the mice – either in the tumors, in the lymph nodes (if present) or in the blood or spleen (see Figure 31). Two mice of group 3, one mouse of group 5 and one mouse of group 6 had to be sacrificied before reaching the endpoint of the experiment possibly due to tumor progression.

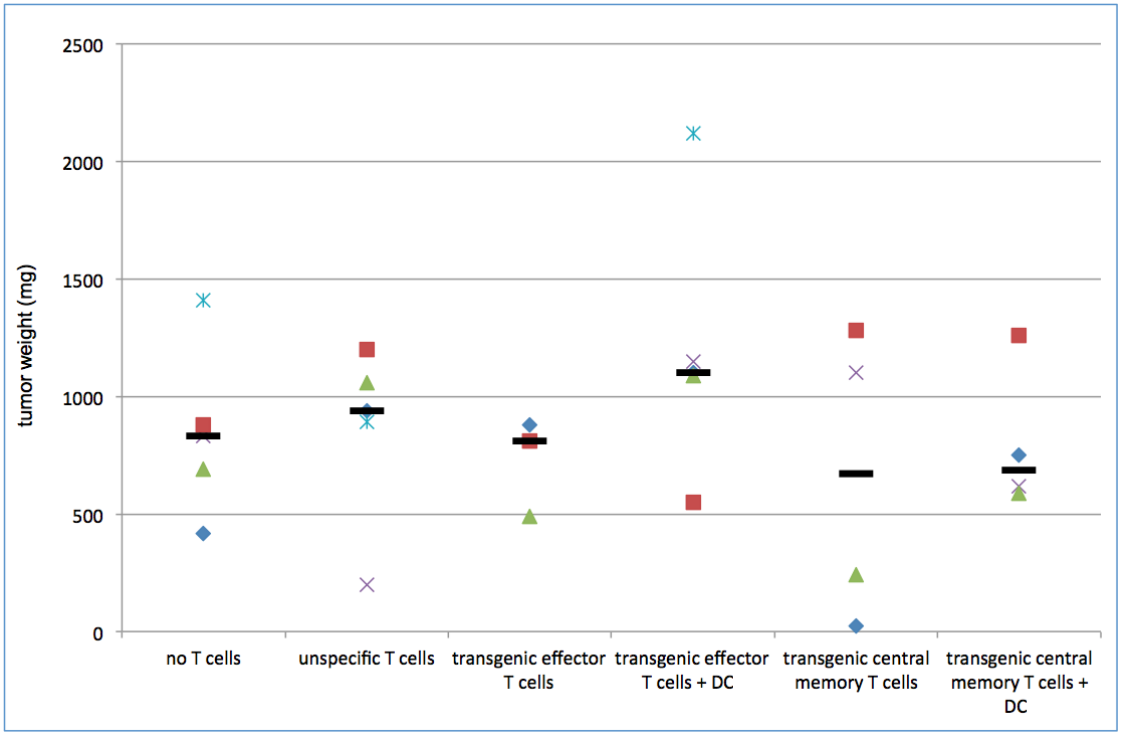

FIGURE 29 ***In vivo* experiment: CHM1-specific TCR-transgenic T cells show no regression of tumor growth in humanized Rag2$^{-/-}$γc$^{-/-}$ mice.** Rag2$^{-/-}$γc$^{-/-}$ mice were reconstituted with human CD34^{+} stem cells. After injection of an A673 ES into the groin, six groups were defined: Group 1 received no T cells, group 2 unspecific CD8^{+} T cells, group 3 CHM1-specific TCR-transgenic T cells with effector phenotype (CD62L^{+} cell fraction less than 5 %). Group 4 was treated like group 3 but received CHM1-pulsed DC additionally. Into group 5, CHM1-specific TCR-transgenic T cells were injected having a central memory phenotype (CD62L^{+} cell fraction higher than 70 %), group 6 was additionally treated with CHM1-pulsed DC. This figure shows the tumor weight in the groin 40 days after injection of the tumor cells. Each symbol represents one mouse of the appropriate group, bars represent the median.

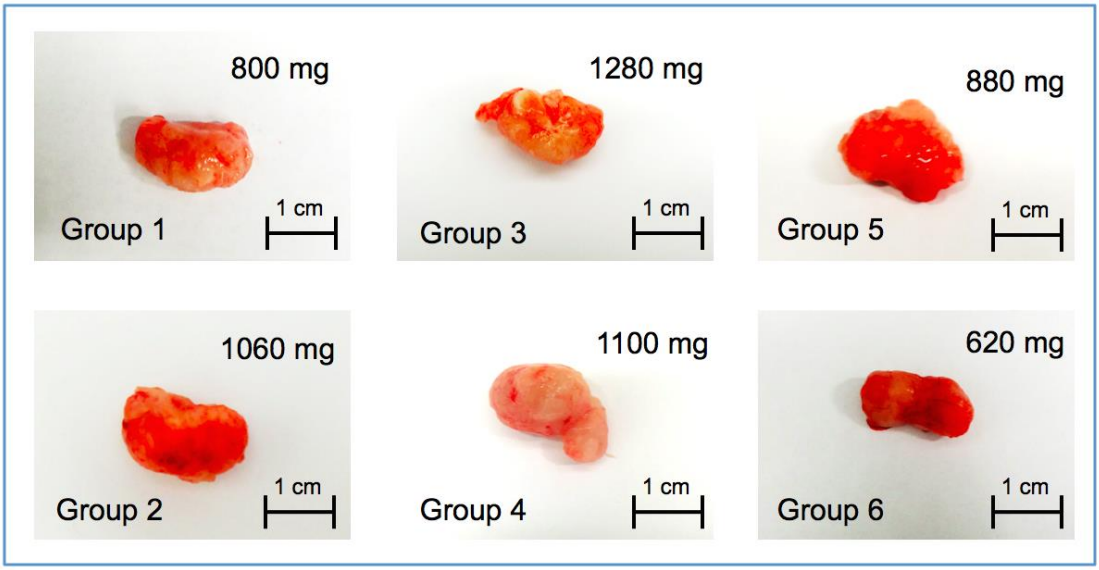

FIGURE 30 ***In vivo* experiment: Exemplary tumor size and weight of reconstituted Rag2$^{-/-}$γc$^{-/-}$ mice.** Rag2$^{-/-}$γc$^{-/-}$ mice were reconstituted with human CD34^{+} stem cells. After injection of an A673 ES into the groin, six groups were defined: Group 1 received no T cells, group 2 unspecific CD8^{+} T cells, group 3 CHM1-specific TCR-transgenic T cells with effector phenotype (CD62L^{+} cell fraction less than 5 %). Group 4 was treated like group 3 but received CHM1-pulsed DC additionally. Into group 5, CHM1-specific TCR-transgenic T cells were injected having a central memory phenotype (CD62L^{+} cell fraction higher than 70 %), group 6 was additionally treated with CHM1-pulsed DC. This figure shows exemplary tumor size and weight of reseptively one mouse of each group 40 days after injection of the tumor.

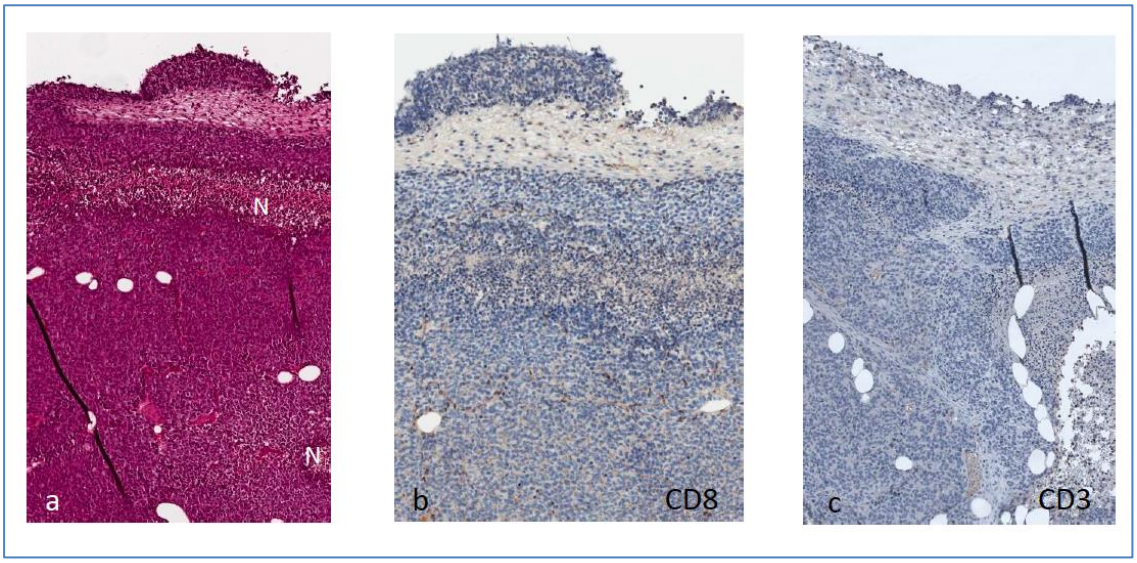

FIGURE 31 ***In vivo* experiment: Pathological evaluation of the tumors** Exemplarily pathological evaluation of a tumor extracted from a CHM1-specific TCR-transgenic T-cell treated mouse (group 4) 40 days after injection of the tumor. Hematoxylin and eosin staining show a solid-diffuse growing tumor with numberous necrotic areals (indicated as “N”) (panel a). Immunhistochemical staining against CD8 (panel b) or CD3 (panel c) indicate no infiltration of T cells. All pictures show 100-fold magnification and were kindly provided by Katja Steiger, Institute of Pathology of the Technical University Munich.

7 DISCUSSION

7.1 SELECTION OF ANTIGENS FOR ES IMMUNOTHERAPY

In a first step, success of ES immunotherapy with cytotoxic T cells is dependent on antigen presentation of the tumor. The ideal target antigen would i) be expressed only on ES and not on any other tissue, ii) be expressed stable and on the majority of ES and iii) be essential for the survival of the tumor. Regarding the last point, peptides taken from the region of the fusion protein EWS-FLI1 would represent ideal targets as the fusion protein is pathognomonic for 85 % of ES. Unfortunately, our work group could not find any good HLA-A*0201-binders within this region in previous work.

In this work, we focused on the proteins EZH2 and CHM1. EZH2 is a histone methyl-transferase and determines oncogenicity and the stem cell phenotype in ES. EWS-FLI1 was found to bind to EZH2. Previous work of our laboratory also showed that down-regulation of EZH2 results in inhibition of ES growth in immunodeficient $Rag2^{-/-}\gamma_C{}^{-/-}$ mice (Richter, Plehm et al. 2009). EZH2 is known as a ES-associated antigen. It is expressed not only in ES but – even though in small amounts – also in several other tissues of the body, especially thymus, testis and bone marrow. Consequently, EZH2-specific immunotherapy might include the risk of side effects affecting these organs (except for the testis which does not express HLA).

In contrast, until now only little is known about the cartilage-specific glycoprotein CHM1. CHM1 is a ES-specific antigen, which is overexpressed in ES and does not show any expression in normal body tissue. It was found to stimulate proliferation and differentiation of chrondrocytes as well as to inhibit the angiogenesis *in vitro* and *in vivo* (Suzuki 1996) (Hiraki, Kono et al. 1997). The latter appears surprising as a characteristic of a tumor-specific antigen. Nevertheless, it might play a role in the formation of hypoxic tumor cells within the ES mass. Inhibition of angiogenesis could also be seen as part of a tumor escape mechanism as it prevents therapeutic substances from getting into the

inside of a tumor mass. Taken together, targeting CHM1 might not only implicate the chance of producing no or only very limited side effects, but may also implicate a higher vulnerability of the tumor mass towards other treatments.

For immunotherapy of other tumor entities, the use of cancer testis antigens (CTA) such as NY-ESO-1 or MAGE already revealed great success. These antigens are only expressed on the cancer itself, as well as on germ cells and sometimes on trophoblast tissue. As the testis does not express HLA, it seems to be safe from TCR-mediated immunotherapy. Nevertheless, T cells directed against cancer testis antigen MAGE were already able to show anti-tumor reactivity in patients with myeloma and melanoma but did also implicate the risk of severe myocardial damage and death caused by a cross-reactivity of the MAGE-specific TCR against Titin, a striated muscle-specific protein (Cameron, Gerry et al. 2013) (Linette, Stadtmauer et al. 2013). Additionally, severe neurotoxicity (such as comas, Parkinson-like symptoms and changes of mental status) occurred in patients treated with autologous MAGE-specific T cells. In order to explain these findings, the Rosenberg group performed quantitative RT-PCR, nano string quantitation and deep-sequencing and detected MAGE-expression in the brain probably resulting in an unintended TCR-mediated inflammatory process and neuronal cell destruction (Morgan, Chinnasamy et al. 2013). However, one promising CTA for ES immunotherapy might be lipase I (LIPI, membrane-associated phospholipase A1-β) which is highly overexpressed in ES tissues. LIPI-specific T cells with endogenous TCR were already able to react against ES cell lines *in vitro* as previously published by Mahlendorf and Staege (Mahlendorf and Staege 2013). For this work, we also tried to identify a LIPI-specific T cell clone with a TCR which would be suitable for genetic transfer. Unfortunately, we did not succeed but would like to re-start this project in the future.

Taken together, searching for an ideal target antigen seems to play a crucial role for a successful ES immunotherapy. In the future, more effort will be spend on finding the perfect antigen or targeting a variety of antigens at the same time, for example by introducing two TCR into primary T cells or using a mixture of two or three specific T-cell populations. Apart from that - as the experience with MAGE-specific T cells taught us – special focus must be placed on safety

aspects not only concerning side-expressions of antigens but also cross-reactivity.

7.2 Allogeneic approaches for ES immunotherapy

Prior to this work, our working group already generated wildtype EZH2- and CHM1-specific T cells in an autologous setting as well as in an allogeneic setting. In the autologous setting, T cells were primed with DC derived from the same donor – whereas in the allogeneic approach, DC donor and T-cell donor were not identical (Thiel, Pirson et al. 2011).

Whenever working with adoptively transferred T cells, safety on one hand - and effectiveness on the other has to be taken into account:

Regarding safety, allogeneic approaches include the risk of severe graft-versus-host disease. GvHD is caused by cytotoxic T-lymphocytes of the donor reacting against normal body tissue of the host (Ferrara, Levy et al. 1999). This reaction mainly affects the liver, bowel and skin and requires therapy with immunosuppressive drugs depending on the grade and severity of GvHD. Three of our T-cell treated mice died possibly due to tumor progression - but also the risk of GvHD has to be taken into account. As we saw no clinical evidence for death caused by GvHD, we did not perform a pathological/ immunohistochemical screening for GvHD. Nethertheless, this might be inevitable in the future to proof safety of TCR-transgenic allogeneic T cells.

In contrast, in the autologous setting, transferred T cells are derived from the patient himself and therefore do not hold the risk of GvHD. Nevertheless, side effects in adoptively treated melanoma patients occurred but were not based on the T cells themselves but rather due to the IL-2-conditioning the patients received as supplementary treatment (Ellebaek, Iversen et al. 2012).

In comparison to GvHD, graft-versus-leukemia (GvL) respectively graft-versus-tumor (GvT) effect represents the other side of the coin and plays a major role in effectiveness of adoptively transferred T cells. GvT effect means the elimination of tumor cells by allo-reactive T cells derived from the donor

(Bleakley and Riddell 2004). It is mainly based on HLA-incompatibility and is therefore often seen in allogeneic approaches. In patients with leukemia (such as acute lymphoblastic leukemia) allo-SCT is an important element of therapeutic protocols for high risk or relapsed patients. It was shown (mainly for chronic myeloid leukemia, CML) that even when relapsed after allo-SCT, patients may profit from DLI as they are able to induce durable remissions (Dazzi, Szydlo et al. 2000). In contrast, in the autologous setting, evidence occurred that mutated gene products are the main targets of melanoma-infiltrating T lymphocytes. Melanoma is known to show high numbers of mutational events (Davies and Samuels 2010). Some of these mutations seem to result in neo-epitopes which are recognized by tumor-specific autologous T cells (Robbins, Lu et al. 2013).

Whether the allogeneic or the autologous setting is used for treatment still depends on the tumor entity and different therapeutic protocols.

For patients with ALL, haplo-SCT has already made its way into current therapeutic protocols (such as the AIEOP registry). When treated with haplo-SCT at time-point of first remission – either from matched family or unrelated donors – high-risk patients show a 10-year overall survival rate of more than 60 % (Fagioli, Quarello et al. 2013).

Although, to date, patients with advanced ES are still mostly transplanted autologously, allo-SCT for these patients and possible GvT effects on ES as well as other sarcomas such as rhabdomyosarcomas became a matter of debate (Bregni, Bernardi et al. 2004) (Kido, Amano et al. 2010) (Burdach, van Kaick et al. 2000) (Thiel, Koscielniak et al. 2013). In this context, one question seems to be indispensable: How to prevent GvHD without losing the GvT effect? How in detail GvHD is linked to GvT effect is a subject to research until now. Some studies indicated lowest relapse rates in patients who suffered from severe GvHD after allo-SCT hinting to the point that GvT effect is somehow dependent on GvHD (Weiden, Flournoy et al. 1979) (Weiden, Sullivan et al. 1981). On the other hand, it is reported that allogeneic T cells hold a GvT effect independent from GvHD (Horowitz, Gale et al. 1990).

For allo-SCT, already several approaches were established to decrease graft-related toxicity respectively GvHD without compromising engraftment or losing

possible GvL/ GvT effects. In many transplant centers, $CD34^+$-selection of the graft is performed in order to prevent severe GvHD by reduction of T cells (Handgretinger, Klingebiel et al. 2001). This approach already showed convincing results concerning engraftment and survival rates in several patient groups but revealed poor outcome in patients with ALL who are transplanted with active disease (Klingebiel, Cornish et al. 2010) (Lang, Greil et al. 2004). On the other hand, $CD34^+$-selection implicates losing other immune cells such as natural killer (NK) cells or DC. To overcome this frontier, instead of $CD34^+$-selection, for example CD3/CD19-depletion of allo-grafts were performed allowing to selectively deplete T and B cells without affecting other immune components (Lang, Teltschik et al. 2014). Depletion of B cells plays a major role in preventing the patient from B-cell derived infectious diseases such as Epstein-Barr-virus infections (EBV). In the meanwhile, effort was spent to even more specifically deplete T and B cells by TCRαβ/ CD19 depletion (Ghosh, Schuster et al. 2014) (Schumm, Lang et al. 2013) (Bertaina, Merli et al. 2014).

The aim of this thesis is the production of high numbers of highly specific and less toxic T cells for DLI after allo-SCT. Therefore, we decided to continue our work on the allogeneic T cells generated by Stefan Pirson and Uwe Thiel from our work group (Thiel, Pirson et al. 2011) (Pirson 2009), who already infused wildtype EZH2-/ CHM1-specific T cells into one patient with AES after allo-SCT. They did neither see a tumor regression nor side effects such as GvHD (manuscript in preparation). As this approach was limited due to low cell numbers and fading specificity, we decided to identify the TCR of EZH2-/ CHM1-specific allo-restricted T cells for gene transfer into primary T cells:

7.3 Identification of the TCR sequence and monoclonality proof of allogeneic T cells

The TCR repertoire of the two allogeneic T-cell lines CHM1-4B4 and EZH2-15 was characterized by a specific PCR first published by Steinle et al in 1995 (Steinle, Reinhardt et al. 1995). One of the problems concerning this method

was the observation that in many cases the control band vanished as soon as a specific band emerged. The most possible reason for this is a competing event between the control and the specific primers. In most cases this will not result in a wrong TCR repertoire – on the other hand, in rare cases, it might happen that the control primer dominates the competition against the specific primer and a specific band is not detected.

Apart from that, another specificity problem concerning the primers appeared: After performing the PCR, questionable positive bands were sent for sequencing and in some cases we identified the primers as not specific enough for the appropriate variable region, instead coding for example for the IL-2 receptor.

In any case, we have to work on improvements of this method or consider repeating the PCR for questionable clones without control primers. Before using this PCR for TCR repertoires and proof of monoclonality, the IOtest beta kit was used for flow cytometry-based identification of TCR β-chains. Despite high costs, it covers only about 70 % of all possible human β-chains, whereas the PCR identifies already 90 % of all α- and β-chains. Nevertheless, even if using the PCR for monoclonality proof of T-cell “clones”, the risk of searching one of the not-covered chains has to be taken into account. When working on other cell lines, we often saw two α-chains and a β-chain or even two α-chains and two β-chains after multiple steps of limiting dilution. It is known that T cells may have an additional α-chain not showing peptide specificity when combined to the β-chain. Especially immature T cells can still carry a second α-chain until positive selection occurs and the second α-chain is down-regulated by posttranslational mechanisms (Niederberger, Holmberg et al. 2003) (Malissen, Trucy et al. 1992).

As the CHM1-specific TCR showed its specificity even in the transgenic context, we can be sure that we found the CHM1-specific α- and β-chain of clone CHM1-4B4. For clone EZH2-15 doubts occurred since the wildtype clone was able to recognize ES cell lines in ELISpot assays and showed only one α- and one β-chain in the PCR, but lost the ability to recognize tumor cells in the transgenic setting. The presence of an additional α-chain not identifiable by the

PCR nevertheless remains little probable since the transgenic clone reacted against peptide-loaded T2 cells and therefore showed peptide specificity.

For several other clones, we could not prove monoclonality – even after multiple limiting dilution steps as they still showed multiple α- and/ or β-chains. An easy way to identify the peptide-specific β-chain is the use of flow cytometry counterstaining with a peptide-MHC-multimer and antibodies against the questionable positive β-chains. Unfortunately, these antibodies do not exist for every possible α-chain yet, meaning that in most cases the right α-chain can only be detected in the transgenic setting, when both TCR are cloned and their specificity is compared in TCR-transgenic T cells.

Having a look into TCR-repertoire analysis in the future, sequencing strategies such as exome sequencing could play a major role – not only to identify and predict immunogenic tumor mutations but also ensuring the correct DNA sequence of a peptide-specific TCR (Yadav, Jhunjhunwala et al. 2014). The working group around Dziubianau already generated a next-generation-sequencing based platform for identification of correct TCR sequences and a safer proof of monoclonality (Dziubianau, Hecht et al. 2013).

7.4 Cloning strategies for transgenic TCR

In this work, we used the retroviral vector systems pMP71 and pMSCVneo for cloning of TCR (Engels, Cam et al. 2003). pMP71 is one of the standard vectors used for TCR transfer and was now established in our lab, whereas pMSCVneo was not used for this purpose until now. Working with pMP71 uncovers its high recombination rate meaning that it is not possible to work with glycerol stocks and subcloning might only be successful with recombinase-negative Stbl2 bacteria.

Because of its high stability and the neomycin resistance we tried out pMSCVneo. After frustrating approaches using conventional electroporation protocols, we performed the same infection protocol as used for pMP71 and reached transduction of T cells – although with very small rates. Apart from that, we were not able to successfully select the transduced from not-transduced

primary T cells by treatment with neomycin. As we quickly found good selection methods (using FACS or magnetic beads) even for pMP71-transduced T cells we left the pMSCVneo approach and continued to work on pMP71.

Regarding the inserts of either pMSCVneo or pMP71, we compared the conventional unmodified insert (β- and α-chain of the TCR linked via P2A) with an optimized insert (Leisegang, Engels et al. 2008). The unmodified insert was taken from the original sequence of the TCR and was only modified by insertion of a Kozak sequence, the restriction sites and a P2A linker. P2A linkers are known to cause a ribosomal skip resulting in two individual proteins – the α- and the β-chain (Szymczak, Workman et al. 2004). The Kozak sequence indicates the start point of translation for the ribosome (Kozak 1984).

Optimized inserts were designed *in silico* and based on the sequence of the conventional insert: The constant part of the α- and the β-chain was completely substituted by the murine counterpart. As this was the first approach in our lab, we performed a so-called complete murinization. In the meantime, evidence occurred that a minimal murinization (substitution of only nine amino acids) leads to comparably good transduction results and reveals a better functionality of the transgenic TCR (Sommermeyer and Uckert 2010). The rationale for performing a murinization is an increase of transduction rates. Apart from that, murinization of transgenic TCR chains minimizes their mispairing with endogenous TCR chains as the human constant chains should not pair with the murine (or partly murine) counterparts (Cohen, Zhao et al. 2006). A publication of van Loenen et al underlined the possible threat of mispairing. They showed that mispairing of unmodified transgenic with endogenous TCR chains led to death by neoreactivity in mice (van Loenen, de Boer et al. 2010). Of course, murinization means the introduction of murine DNA material into human T cells which might include the risk of rejection or intolerance reactions. For this reason, effort should be spent on minimizing the murinization and inserting safety aspects such as suicide genes (Marin, Cribioli et al. 2012).

To increase the rate of correctly paired TCR chains, it is possible to insert an additional disulfide bond between the constant parts of the chain (Kuball, Dossett et al. 2007) (Cohen, Li et al. 2007). As we were able to already achieve

high transduction rates and peptide specificity, we refrained from this insertion but might re-evaluate its use in the future.

In a last step, the *in silico* designed construct was sent to GeneArt, Life Technologies, Regensburg, who generated the insert and performed a codon-optimization to increase the expression rates of the insert (Scholten, Kramer et al. 2006). During codon-optimization, codons which are not often translated are exchanged for codons which are more often translated (but are encoding for the same amino acid).

In this work, we were able to confirm an increased transduction rate caused by codon-optizimization and murinization for ES-specific TCR-transgenic T cells. To date, a murinization and codon-optimization of TCR sequences for transgenic approaches seems to be inevitable to not only increase the expression rates but also minimize the risk of mispairing and neoreactivity.

7.5 Problems of transgenic T cells concerning the recognition of cell lines

As shown in 6.10, EZH2-specific TCR-transgenic T cells were only able to recognize peptide-loaded T2 cells in ELISpot assays, but didn't show any reactivity against ES cell lines. Neither did they release IFNγ nor Granzyme B or IL-2 – neither as central-memory T cells nor as effector T cells. In contrast, we measured a highly significant IFNγ, Granzyme B and IL-2 release after presentation of EZH2-loaded T2 cells. T2 cells are TAP-deficient cells not being able to express endogenously processed peptides on their surface. Instead, they are known to take up externally existing peptides and present them on MHC class I complexes. Only little is known about the molecular process of T cells recognizing T2 cells in detail. It may be possible that a recognition of T2 cells is not that complex as a recognition of tumor cell lines – not only because of a probably different molecular mechanism but also because of the higher peptide density on T2 cells. It remains confusing that the EZH2-specific TCR was able to identify ES cell lines before being genetically transferred. The optimized and murinized TCR as well as the unoptimized TCR would have lost

their specificity for ES cell lines just by genetic transfer! As DNA mutations could be excluded by sequencing the original not-transgenic T cell clone, we presume an avidity loss or down-regulation of the EZH2-specific TCR after cloning.

Other members of our working group observed the phenomenon that TCR-transgenic T cells which didn't react against ES cell lines in a first approach, did so in a second or third attempt although culturing or transduction conditions were the same. We presume that – in contrast to T2 recognition – the ES cell line recognition seems to be an unstable reaction depending on the grade of T-cell activation and maturity or other variables. Our work group will keep on trying to solve this problem. Nevertheless, it remains interesting that the CHM1-specific TCR used for this thesis reacted against ES cell lines in every experiment performed, whereas the EZH2-specific TCR did not do so in any of the experiments and reactivity was not improved by several different culturing conditions or maturity grades.

Concerning avidity of TCR, it is known that high-avidity T cells show superior antitumor activity compared to medium- or low-avidity T cells (Dutoit, Rubio-Godoy et al. 2001). On the other hand, evidence occurred concerning an avidity-threshold: Starting from this threshold, higher TCR avidity does not lead to increased antitumor responses. Moreover, even the existence of down-regulation mechanisms affecting super-high-avidity T cells is discussed, as the immune system has to prevent the normal body tissue from self-damage by these T cells (Zhong, Malecek et al. 2013). Taken together, there might be not only a minimum limit but also a maximum limit concerning avidity of TCR used for genetic transfer. In the future, it might be inevitable or at least very helpful to check the avidity of endogenous TCR before transferring them into the transgenic context or clinical settings (Nauerth, Weissbrich et al. 2013).

Furthermore, the possibility of transducing allogeneic TCR into autologous T cells needs to be discussed and could build the bridge between allogeneic and autologous approaches. As autologous TCR recognize peptides of self-proteins presented by self-MHC molecules, they often show low functional avidity because of tolerance mechanisms (Burdach and Kolb 2013). In contrast, high-avidity TCR are found in the allogeneic context. These allo-restricted high-

avidity TCR could be used for genetic transfer into autologous T cells. On the other handside, experiences made by Prof. Schendel and Prof. Uckert and their working group has to be taken into consideration (Leisegang, Wilde et al. 2010): They generated transgenic T cells which are HLA-A*0201-restricted and specifically recognize a peptide of the tumor antigen survivin. When transduced into HLA-A*0201$^-$ T cells (allogeneic setting), these transgenic T cells reacted against peptide-loaded T2 cells as well as against tumor cells expressing survivin. In contrast, when transducing the HLA-A*0201-restricted TCR into HLA-A*0201$^+$ T cells (autologous setting) they observed high rates of apoptosis among the transgenic T cells – the so-called fractricide. During expansion, the T cells themselves produce high amounts of survivin which is presented by the T cells by HLA-A*0201 and therefore marking each T cell of the population as a target for the others. These observation would mean that introduction of allogeneic HLA-A*0201-restricted TCR into T cells can only be efficient when transduced into T cells of an HLA-A*0201$^-$ patient (allogeneic setting). This effect is not limited to survivin but could occur with every self-antigen which is presented on the T-cell surface during T-cell expansion or maturation.

7.6 Phenotype of TCR-transgenic T cells

For this thesis, we used the marker CD62L to distinguish between T_{CM} and T_{Eff} cells and the marker CD45RO to exclude the presence of naïve T cells (Klebanoff, Gattinoni et al. 2006) (Hinrichs, Borman et al. 2009). In peripheral human blood, the frequency of T_{CM} is known to vary between 13 and 35 % of CD8$^+$ T cells (Wu, Zhang et al. 2013). When we transduced human cord blood or human peripheral blood with TCR genes and expanded them for two weeks, we saw a population of T_{CM} constituting 70 to 80 % of CD8$^+$ T cells. After another two weeks of expansion, the population of CD62L$^+$ T cells decreased to less than 5 % of CD8$^+$ T cells. These cells were determined as differentiated effector T cells. As a better effectiveness of central-memory T cells was already proven by other groups *in vitro (Wu, Zhang et al. 2013),* we tried to compare the effectiveness of the transgenic central-memory T cells with transgenic effector T cells *in vivo*. We therefore re-constituted Rag2$^{-/-}\gamma_C{}^{-/-}$ mice, injected 1 x 10^6

A673 cells s.c. on day 0 and 5 x 10^6 thawed TCR-transgenic central-memory or effector T cells with or without peptide-pulsed DC i.v. on day 3. Unluckily, we were neither able to show tumor regression on day 40 nor to find the transduced T cells in the blood, the spleen or the lymph nodes of the mice (see 6.11). For these reasons, we of course could not compare the functionality of transgenic T_{CM} with T_{Eff} cells *in vivo*.

In the meantime, evidence occurred that naïve T cells might constitute an even better cell group for TCR transduction as they show high transduction rates, good expansion and resistance to terminal differentiation (Hinrichs, Borman et al. 2011).

Summarized, there will be an urgent need to either repeat the T-cell infusions and/ or create a central memory by single or co-infusion of T_{CM} cells or even naïve T cells. In the future, several efforts need to be spent on gaining knowledge concerning survival and kinetics of ES-specific transgenic T cells *in vivo* to generate more suitable *in vivo* models.

7.7 Challenges in the *in vivo* recognition of solid tumors by adoptively transferred T cells

As described above, CHM1-specific TCR-transgenic T cells were able to recognize not only peptide-loaded T2 cells but also distinguished between several tumor cell lines *in vitro*. They demonstrated peptide specificity and HLA-A*0201-restriction as they reacted against CHM1-expressing HLA-A*0201$^+$ cell lines (A673, TC71) but not against HLA-A*0201$^-$ cell lines (SB-KMS-KS, 697) – even if CHM1 was overexpressed as well. The MHC$^-$ cell line K562 was used as negative control and excluded the presence of NK cells. Interestingly, CHM1-specific TCR-transgenic T cells showed a low activity against the melanoma cell line Sk-Mel 29 although this cell line is HLA-A*0201$^-$ and does not express CHM1. We observed this phenomenon in many of our experiments either with transgenic or not-transgenic T cells and not depending on the antigen they are directed against. The reason for this increased reactivity against Sk-Mel 29 might be founded by a generally higher immunogenicity of melanoma cell lines.

Despite these convincing results *in vitro*, CHM1-specific TCR-transgenic T cells were not able to prohibit or at least decelerate tumor growth after injection of A673 cells in our first experiment with re-constituted $Rag2^{-/-}\gamma_C^{-/-}$ mice.

In order to find strategies to overcome these limitations, tumor evasion mechanisms as well as tolerance induction (Mapara and Sykes 2004) (Topfer, Kempe et al. 2011) and problems regarding the setting of the experiment and the quality of the cells has to be taken into account:

i) As tumors arise from normal body tissue, they mainly express self-antigens. Induced either by central or peripheral tolerance mechanisms, T cells normally do not react against these antigens. Since CHM1 is not expressed in any healthy body tissue, tolerance mechanisms should not elude these T cells just because of their antigen specificity – either in the mouse or in the human body. Nevertheless, evidence occurred that T cells with a high avidity to their antigen in some cases become anergic or at least suffer from down-regulation mechanisms by the immune system to prevent auto-reactivity (Zhong, Malecek et al. 2013). Taken together, one reason for the failure of the *in vivo* experiment might be an extremely high avidity of our CHM1-specific transgenic TCR.

ii) Many tumors, such as prostate carcinoma (Sanda, Restifo et al. 1995), lung cancer (Korkolopoulou, Kaklamanis et al. 1996) and others, are capable of manipulating their antigen presentation machinery. Known mechanisms are down-regulation or complete loss of MHC class I molecules, mutations of β2-microglobulin or changing levels of transcription factors as well as epigenetic alterations concerning the MHC expression. When ES were investigated, no or a relatively low constitutive expression of MHC class I genes and induction of MHC class I gene expression by IFNγ were reported by Berghuis et al (Berghuis, de Hooge et al. 2009), hinting at a similar tumor evasion mechanism in ES. Forcing the tumor to up-regulate its MHC complexes could constitute a strategy to support the transgenic T-cell attack in future mouse models. On the other hand, MHC-independent approaches should be considered such as the use of CAR for ES immunotherapy. These hybrid receptors connected to the T cell surface were already generated for a variety of antigens (such as CD19 and ERBB2) and showed convincing results in the treatment of B cell leukemia and lymphoma (Brentjens, Latouche et al. 2003) (Xu, Zhao et al. 2013). Lacking the

possibility of antigen presentation can not be the only mechanism of inducing T-cell tolerance: B-cell lymphomas derived from antigen-presenting cells (APC) - and therefore normally equipped with everything needed for a good antigen presentation – are also capable of inducing tolerance in T cells. Sotomayor et al, who observed this effect, concluded that even in other tumor entities, tolerance and anergy of T cells could be induced by cross-presentation of tumor antigens by bone-marrow-derived APC (Sotomayor, Borrello et al. 2001).

Apart from these mechanisms, extravasation of lymphocytes to the tumor site can be inhibited and cause problems in T cells getting to the tumor. This inhibition seems to be caused by defects in adhesion on blood vessels in tumor entities such as human squamous cell carcinoma (Clark, Huang et al. 2008), melanoma (Piali, Fichtel et al. 1995) and breast cancer (Madhavan, Srinivas et al. 2002).

iii) Patients with malignancies such as lung cancer (Wolf, Wolf et al. 2003) (Yannelli, Tucker et al. 2009), breast cancer (Perez, Karamouzis et al. 2007) and liver cancer (Ormandy, Hillemann et al. 2005) were already known to show high numbers of $CD4^+$ $CD25^{high}$ regulatory T cells (Treg) in their circulation or in the tumor itself. The finding of Treg often correlates with a poor prognosis in these patients (Viguier, Lemaitre et al. 2004) (Kobayashi, Hiraoka et al. 2007) (Curiel, Coukos et al. 2004). Also in ES, Treg were found to be increased in the bone marrow of patients with metastatic disease (Brinkrolf, Landmeier et al. 2009), supporting the presumption that the increase of Treg might function as a tumor evasion mechanism in ES as well. Treg are moreover characterized by the expression of FoxP3 and GITR and are able to suppress responses of not only $CD4^+$ T cells but also $CD8^+$ T cells (Sakaguchi, Yamaguchi et al. 2008).

It is known that many tumors create an immunosuppressive environment for example by high levels of transforming growth factor-beta (TGF-β). Additionally to a variety of other interactions, TGF-β again leads to anergy of T cells but could also mediate transformation of tumor-infiltrating T cells to Treg - which in turn are able to suppress other T cells (Moo-Young, Larson et al. 2009). Regarding this, it could be helpful to measure the frequency of Treg in the ES of mouse models. Regarding the use of transgenic T cells in the clinic, the presence of Treg in ES underlines the importance of chemotherapeutic

lymphodepletion protocols prior to adoptive T cell therapy in patients (Wrzesinski, Paulos et al. 2010) (Rosenberg and Dudley 2009).

iv) The transgenic CHM1-specific T cells used for this *in vivo* model were sorted with the help of magnetic beads, expanded in the presence of irradiated PBMC in a high-dose IL-2 protocol and frozen on day 12 and day 35 after first transduction. We chose this protocol because it was GMP conform and ensured high numbers of transgenic T cells. Nevertheless, the high-dose IL-2 treatment might have caused an over-stimulation of the T cells that could have resulted in anergy when brought into the mouse. Apart from that, T cells were frozen and thawed again, whereas tumor cells were given directly from a fresh culture. Thawing might have damaged the majority of the transgenic T cells. In contrast, we excluded a negative effect of the magnetic bead sorting on the functionality of the cells, as they showed peptide specificity and HLA-A*0201 restriction *in vitro*. Regarding the *in vivo* protocol, numbers of given cells could be optimized and a repeat of T cell injections should be considered. Additional DC vaccination with co-injection of CHM1-loaded DC was already tested and showed no significant effect on the tumor growth.

v) In this *in vivo* model, we worked on immune-deficient Rag2$^{-/-}\gamma_C{}^{-/-}$ mice. After injection of CD34^{+} HLA-A*0201^{-} human stem cells into the liver, these mice develop a human immune system with lymph nodes and a human-like cytokine environment (Traggiai, Chicha et al. 2004) (Chicha, Tussiwand et al. 2005). As this approaches the immune status of a patient after allo-SCT, it seemed to be an ideal model for *in vivo* tests of TCR-transgenic T cells for AES patients. Nevertheless, it is a challenging model and a complicated procedure. Recently, Richard Klar et al were able to show reactivity of acute myeloid leukemia specific TCR-transgenic T cells in BRG mice (Klar, Schober et al. 2014). Taken together, still effort needs to be spent on finding the perfect mouse model for targeting solid tumors, and especially ES, with adoptively transferred TCR-transgenic T cells.

7.8 Current clinical treatment of AES and perspective

In our clinic, the MetaEICESS (Meta European Intergroup Cooperative Ewing Sarcoma Study Group) protocol is used for suitable patients suffering from AES (see Figure 32). These studies (CESS/ EICESS/ MetaEICESS) were constantly advanced during the past decades. In 1993, studies revealed that myeloablative radiochemotherapy with subsequent SCT can improve prognosis of patients with AES (Burdach, Jurgens et al. 1993). Regarding lymphodepletion, no improvement of survival could be shown with reduced- versus high-intensity conditioning (Thiel, Wawer et al. 2011). Nevertheless, conditioning is inevitable for subsequent allo-SCT, which is known to induce regression in patients with AES (Lucas, Schwartz et al. 2008) (Koscielniak, Gross-Wieltsch et al. 2005). In 2000, allo- and auto-SCT for patients with AES were compared (Burdach, van Kaick et al. 2000). Although it was not possible to increase the event-free survival of these patients by allo-SCT, allo-SCT was included into the MetaEICESS protocol. It does not only exclude the risk of contamination with autologous tumor cells (Rill, Santana et al. 1994) but also holds the possibility of causing a GvT effect which is bought with the risk of causing severe GvHD. In 2010, the MetaEICESS Study Group published that the combination of MRI-governed involved-compartment irradiation with high-dose chemotherapy increases the long-term survival of patients with AES (Burdach, Thiel et al. 2010).

The current MetaEICESS protocol includes several therapeutic blocks (see Figure 32): After staging examinations such as (positron emission tomography) magnetic resonance imaging ((PET-) MRI), blood / bone-marrow withdrawal and obligatory biopsy for expression profiling, therapy is started with induction blocks which are – if necessary - interrupted/ followed by autologous stem-cell apharesis and harvest. Induction blocks normally consist of Vincristine, Ifosfamide, Doxorubicin and Etoposide (Wexler, DeLaney et al. 1996) (Paulussen, Ahrens et al. 2001). Cyclophosphamide could also be used instead of Ifosfamide but shows higher toxicity rates. Etoposide seems to add a benefit especially to high-risk patients (Paulussen, Craft et al. 2008). During the subsequent local intensification blocks consisting of Vincristine, Ifosfamide and Etoposide, involved-lesion irradiation is performed followed by systemic

intensification. Systemic intensification blocks contain Melphalan, Etoposide, Topotecan and Treosulfan as it was shown that high-dose chemotherapy may improve prognosis in early relapsed ES. On the other handside, additional high-dose therapy has no impact on prognosis (Rasper, Jabar et al. 2014). Subsequent to systemic intensification, SCT (in our clinic mostly haplo-identical) is performed. One question remains: If further intensification of chemotherapy does not improve the outcome of high-risk patients and instead holds the risk of increased toxic side effects, how can the treatment of patients with AES be improved?

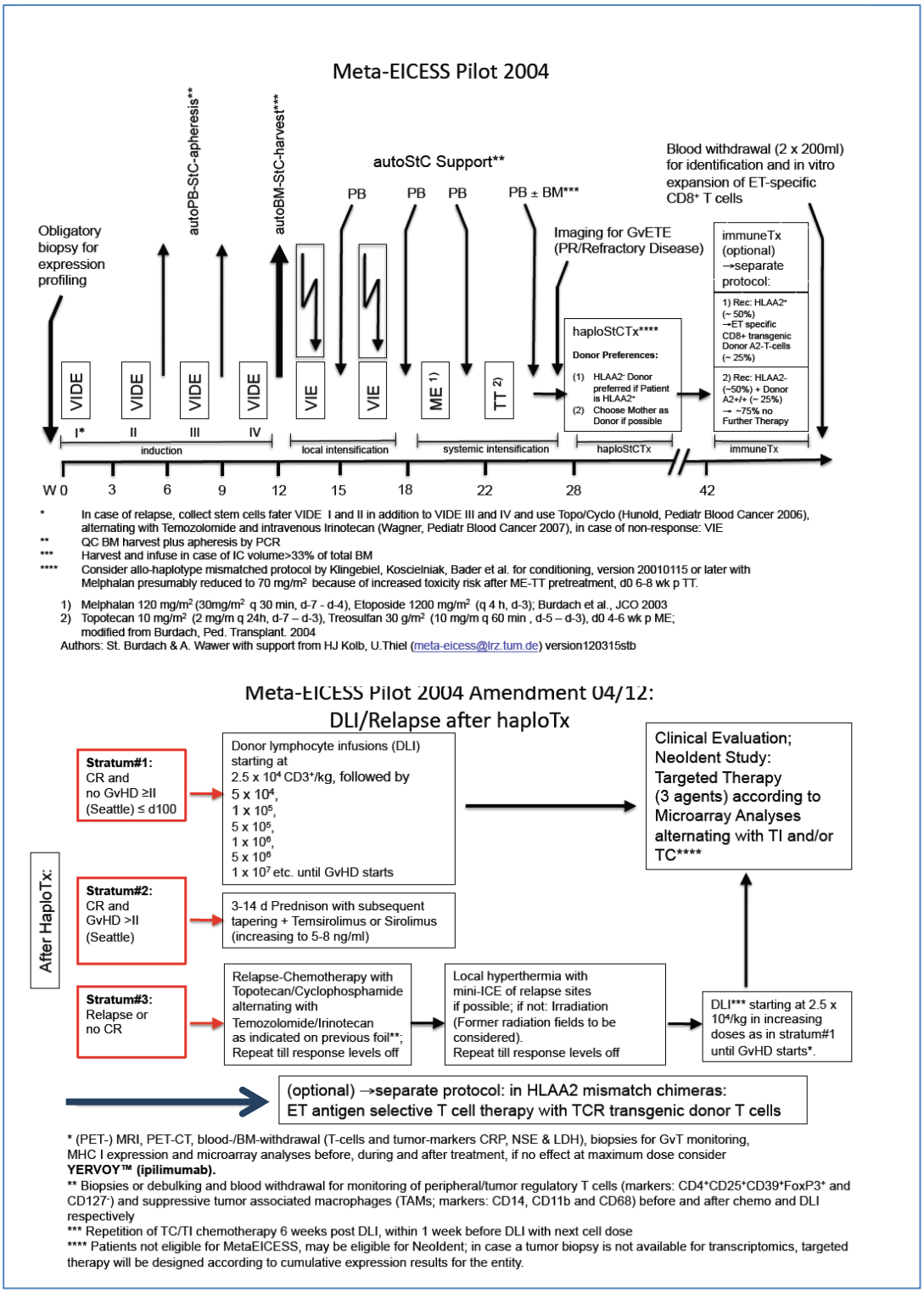

FIGURE 32 Inclusion of TCR-transgenic T cells into the Meta-EICESS Pilot 2004 protocol. After induction therapy, local and systemic intensification and haploidentical SCT, TCR-transgenic donor T cells can be infused instead of normal DLI (blue arrow). VIDE = Vincristine, Ifosfamide, Doxorubicin and Etoposide, W = week, VIE = Vincristine, Ifosfamide and Etopside, ME = Melphalan and Etoposide, TT = Topotecan and Treosulfan, autoPB-StC = autologous peripheral blood stem cell, autoBM-StC = autologous bone marrow stem cell, PB = peripheral blood, BM = bone marrow, GvETE = graft versus Ewing tumor effect, ET = Ewing tumor, PR = partial remission, haploStCTx = haploidentical stem cell transplantation, Rec = recipient, CR = complete remission, ICE = Ifosfamide, Carboplatin, Etoposide, TC = Docetaxel and Cyclophosphamide, TI = Docetaxel and Ifosfamide. Figure by Stefan Burdach and Angela Wawer.

During the past years, specific effort was spent on identifying new target structures and according drugs for ES therapy. ET-743, Ecteinascidin 743, which is a natural chemotherapeutic agent, is known to have a particular activity against translocation-positive sarcomas (such as ES) and interferes with the activity of EWS-FLI1 at the promoter (Grohar, Griffin et al. 2011). Unfortunately, the phase II trial did not show convincing effectiveness of ET-743 in ES. Within the years, the role of insulin-like growth factor (IGF) -pathway in ES became a matter of debate. It was shown that IGF mediates the EWS-FLI1 driven malignant transformation (Kim, Toretsky et al. 2009). Several agents targeting the IGF-pathway or downstream molecules such as mTOR (mechanistic target of Rapamycin) are still under investigation. Within the last years, epigenetic targeting gained an important stage as it is known that the chromatin structure is dysregulated in ES (Lawlor and Thiele 2012). As published by our group, EWS-FLI1 directly regulates the methyl-transferase EZH2 which maintains stemness of ES and might represent a good target – not only for immunotherapy but also for approaches of targeted therapy (Richter, Plehm et al. 2009).

Concerning the usage and development of new therapeutic approaches, it seems to be inevitable or at least very helpful to establish an expression profile (for example microarray analysis) prior to therapy for every single patient – not only to predict the effectiveness of individual drugs but also to identify new target structures.

The rationale for the research performed for this thesis, was the aim to render current therapeutic protocols (such as the Meta-EICESS protocol) after haplo-identical SCT more effective and less toxic. To date, after allo-SCT, the grade of remission/ relapse is evaluated and relapse chemotherapy or new therapeutic approaches (such as targeted therapy or specific immunotherapy) are considered depending on expression profiles and HLA types. When patients are in (complete) remission (either directly after haplo-SCT or after relapse treatment), in most cases DLI are performed. Until now, these DLI are unspecific and again implicate the risk of GvHD. In order to minimize this risk

and increase the specificity of DLI, we will exchange the conventional DLI for an infusion of antigen-specific TCR-transgenic T cells in the future.

In this thesis, we were successful in generating TCR-transgenic T cells directed against ES-specific or –associated peptides in the context of a translational research approach. We proofed a good functionality of CHM1-specific HLA-A*0201-restricted TCR-transgenic T cells *in vitro*. Still effort needs to be spent to confirm this functionality *in vivo* by usage of other expansion/ culturing conditions or mouse models.

To this point, introduction into the clinic could only be accomplished in the context of an individual therapeutic approach and is limited due to the fact that the patient does not only need to have an CHM1-expressing HLA-A*0201^{+} tumor but also has to be transplanted from an HLA-A*0201^{-} donor.

In the future, we would like to confirm the functionality of ES-specific TCR-transgenic T cells *in vivo*, introduce a completely GMP-accredited protocol for the generation of transgenic T cells und extend the approaches towards other antigens and HLA alleles. This work, stating the first successful production of ES-specific TCR-transgenic T cells with a high functionality *in vitro*, constitutes the first step in reaching our aim of improving the outcome of children with advanced ES with the help of TCR-transgenic T cells.

8 SUMMARY

Advanced Ewing's sarcomas (AES) are defined by primary bone or bone marrow metastases and early, multiple or multifocal relapse and are associated with poor prognosis. Despite multimodal therapeutic approaches including surgery, irradiation, (high-dose-) chemotherapy (with or without allogeneic stem cell transplantation; allo-SCT), overall-survival is still unsatisfactory. In preliminary work, clonal ES-specific allo-restricted T cells were generated for adoptive transfer to enhance efficacy and to decrease toxicity of donor lymphocyte infusions after allo-SCT. However, inclusion of these cells into current therapy protocols is limited due to high production complexity, low cell numbers and the high differentiation grade of these T cells. In order to overcome these obstacles and to facilitate good manufacturing practice (GMP) accredited off-the-shelf products in the future, we generated HLA-A*0201-restricted T-cell receptor (TCR) transgenic T cells directed against ES-associated antigens $EZH2^{666}$ and $CHM1^{319}$ by retroviral transduction. IL-2 based expansion protocols revealed sufficient TCR-transgenic T cell numbers expressing a $CD62L^{+}/CD45RO^{+}$ central memory phenotype up to 80%. In ELISpot assays, CHM1-specific TCR-transgenic T cells maintain specific recognition and killing of HLA-A*0201^{+} ES cell lines expressing the antigen. Unfortunately, a first pilot approach using $Rag2^{-/-}\gamma_c^{-/-}$ mice was not able to confirm this functionality *in vivo*. In the future, effort needs to be spent on finding a suitable mouse model and according expansion conditions. The infusion of TCR-transgenic donor lymphocytes may serve to render DLI after allo-SCT more efficacious and less toxic.

9 ZUSAMMENFASSUNG

Fortgeschrittene Ewing Sarkome (AES) sind definiert als Ewing Sarkome mit initialen Knochen- oder Knochenmarksmetastasen oder frühem, multiplem oder multifokalem Rezidiv und gehen mit einer schlechten Prognose einher. Trotz multimodaler Therapieansätze, bestehend aus chirurgischer Tumorkontrolle, Bestrahlung und (Hochdosis-) Chemotherapie (mit oder ohne allogener Stammzelltransplantation; allo-SCT), bleibt das Gesamtüberleben in dieser Patientengruppe unbefriedigend. In Vorarbeiten wurden klonale ES-spezifische allorestringierte T-Zellen für den adoptiven Transfer hergestellt, die die Effektivität von Donorlymphozyteninfusionen nach allo-SCT erhöhen und gleichzeitig die Toxizität begrenzen sollen. Dennoch ist der Einsatz dieser Zellen in gängigen Therapieprotokollen bislang nur eingeschränkt möglich - nicht nur wegen der hohen Komplexität der Produktion, sondern auch wegen zu niedriger Zellzahlen und eines zu ausdifferenzierten Phänotyps der T-Zellen. Um diese Schwierigkeiten zu überwinden und eine “good-manufacturing-practice”- (GMP-) gerechte Herstellung von „off-the-shelf“-Produkten anzustreben, haben wir durch retroviralen Gentransfer HLA-A*0201-restringierte T-Zell-Rezeptor (TCR) transgene T-Zellen hergestellt, die gegen die ES-assoziierten Antigene $EZH2^{666}$ und $CHM1^{319}$ gerichtet sind. IL-2-basierte Expansionsprotokolle führten zu ausreichend hohen Zellzahlen, die mit einem Anteil von bis zu 80 % einen $CD62L^{+}/CD45RO^{+}$ Central-memory-Phänotypen exprimierten. In ELISpot-Analysen zeigen CHM1-spezifische TCR-transgene T-Zellen eine spezifische Reaktion gegen HLA-A*0201^{+} ES-Zelllinien, die das entsprechende Antigen auf der Oberfläche präsentieren. Leider konnten wir in einem ersten Pilotversuch mit $Rag2^{-/-}\gamma_c^{-/-}$-Mäusen diese Effektiviät *in vivo* nicht bestätigen. Es werden weitere Versuche nötig sein, um ein passendes Mausmodell und die entsprechenden Expansionsbedingungen zu etablieren. Die Infusion TCR-transgener Donorlymphozyten soll in der Zukunft zu einer Effektivitätssteigerung sowie Toxizitätsminderung der konventionellen DLI nach allo-SCT führen.

10 LITERATURE

Amrolia, P. J., S. D. Reid, L. Gao, B. Schultheis, G. Dotti, M. K. Brenner, J. V. Melo, J. M. Goldman and H. J. Stauss (2003). "Allorestricted cytotoxic T cells specific for human CD45 show potent antileukemic activity." Blood **101**(3): 1007-1014.

Bacci, G., S. Ferrari, A. Longhi, D. Donati, E. Barbieri, C. Forni, F. Bertoni, M. Manfrini, S. Giacomini and P. Bacchini (2004). "Role of surgery in local treatment of Ewing's sarcoma of the extremities in patients undergoing adjuvant and neoadjuvant chemotherapy." Oncology reports **11**(1): 111-120.

Baxevanis, C. N., G. V. Dedoussis, N. G. Papadopoulos, I. Missitzis, G. P. Stathopoulos and M. Papamichail (1994). "Tumor specific cytolysis by tumor infiltrating lymphocytes in breast cancer." Cancer **74**(4): 1275-1282.

Berghuis, D., A. S. de Hooge, S. J. Santos, D. Horst, E. J. Wiertz, M. C. van Eggermond, P. J. van den Elsen, A. H. Taminiau, L. Ottaviano, K. L. Schaefer, U. Dirksen, E. Hooijberg, A. Mulder, C. J. Melief, R. M. Egeler, M. W. Schilham, E. S. Jordanova, P. C. Hogendoorn and A. C. Lankester (2009). "Reduced human leukocyte antigen expression in advanced-stage Ewing sarcoma: implications for immune recognition." The Journal of pathology **218**(2): 222-231.

Berghuis, D., S. J. Santos, H. J. Baelde, A. H. Taminiau, R. M. Egeler, M. W. Schilham, P. C. Hogendoorn and A. C. Lankester (2011). "Pro-inflammatory chemokine-chemokine receptor interactions within the Ewing sarcoma microenvironment determine CD8(+) T-lymphocyte infiltration and affect tumour progression." J Pathol **223**(3): 347-357.

Bernstein, M., H. Kovar, M. Paulussen, R. L. Randall, A. Schuck, L. A. Teot and H. Juergens (2006). "Ewing's sarcoma family of tumors: current management." The oncologist **11**(5): 503-519.

Bernstein, M., H. Kovar, M. Paulussen, R. L. Randall, A. Schuck, L. A. Teot and H. Juergens (2006). "Ewing's sarcoma family of tumors: current management." Oncologist **11**(5): 503-519.

Bertaina, A., P. Merli, S. Rutella, D. Pagliara, M. E. Bernardo, R. Masetti, D. Pende, M. Falco, R. Handgretinger, F. Moretta, B. Lucarelli, L. P. Brescia, G. Li Pira, M. Testi, C. Cancrini, N. Kabbara, R. Carsetti, A. Finocchi, A. Moretta, L.

Moretta and F. Locatelli (2014). "HLA-haploidentical stem cell transplantation after removal of alphabeta+ T and B cells in children with nonmalignant disorders." Blood **124**(5): 822-826.

Bleakley, M. and S. R. Riddell (2004). "Molecules and mechanisms of the graft-versus-leukaemia effect." Nat Rev Cancer **4**(5): 371-380.

Bregni, M., M. Bernardi, F. Ciceri and J. Peccatori (2004). "Allogeneic stem cell transplantation for the treatment of advanced solid tumors." Springer Semin Immunopathol **26**(1-2): 95-108.

Brentjens, R. J., M. L. Davila, I. Riviere, J. Park, X. Wang, L. G. Cowell, S. Bartido, J. Stefanski, C. Taylor, M. Olszewska, O. Borquez-Ojeda, J. Qu, T. Wasielewska, Q. He, Y. Bernal, I. V. Rijo, C. Hedvat, R. Kobos, K. Curran, P. Steinherz, J. Jurcic, T. Rosenblat, P. Maslak, M. Frattini and M. Sadelain (2013). "CD19-targeted T cells rapidly induce molecular remissions in adults with chemotherapy-refractory acute lymphoblastic leukemia." Science translational medicine **5**(177): 177ra138.

Brentjens, R. J., J. B. Latouche, E. Santos, F. Marti, M. C. Gong, C. Lyddane, P. D. King, S. Larson, M. Weiss, I. Riviere and M. Sadelain (2003). "Eradication of systemic B-cell tumors by genetically targeted human T lymphocytes co-stimulated by CD80 and interleukin-15." Nature medicine **9**(3): 279-286.

Brinkrolf, P., S. Landmeier, B. Altvater, C. Chen, S. Pscherer, A. Rosemann, A. Ranft, U. Dirksen, H. Juergens and C. Rossig (2009). "A high proportion of bone marrow T cells with regulatory phenotype (CD4+CD25hiFoxP3+) in Ewing sarcoma patients is associated with metastatic disease." Int J Cancer **125**(4): 879-886.

Burchill, S. A. (2003). "Ewing's sarcoma: diagnostic, prognostic, and therapeutic implications of molecular abnormalities." Journal of clinical pathology **56**(2): 96-102.

Burdach, S. (2004). "Treatment of advanced Ewing tumors by combined radiochemotherapy and engineered cellular transplants." Pediatric transplantation **8 Suppl 5**: 67-82.

Burdach, S. and H. Jurgens (2002). "High-dose chemoradiotherapy (HDC) in the Ewing family of tumors (EFT)." Critical reviews in oncology/hematology **41**(2): 169-189.

Burdach, S., H. Jurgens, C. Peters, W. Nurnberger, C. Mauz-Korholz, D. Korholz, M. Paulussen, H. Pape, D. Dilloo, E. Koscielniak and et al. (1993). "Myeloablative radiochemotherapy and hematopoietic stem-cell rescue in poor-prognosis Ewing's sarcoma." Journal of clinical oncology : official journal of the American Society of Clinical Oncology **11**(8): 1482-1488.

Burdach, S. and H. J. Kolb (2013). "The vigor of defense against non-self: potential superiority of allorestricted T cells in immunotherapy of cancer?" Front Oncol **3**: 100.

Burdach, S., A. Meyer-Bahlburg, H. J. Laws, R. Haase, B. van Kaik, B. Metzner, A. Wawer, R. Finke, U. Gobel, J. Haerting, H. Pape, H. Gadner, J. Dunst and H. Juergens (2003). "High-dose therapy for patients with primary multifocal and early relapsed Ewing's tumors: results of two consecutive regimens assessing the role of total-body irradiation." Journal of clinical oncology : official journal of the American Society of Clinical Oncology **21**(16): 3072-3078.

Burdach, S., S. Plehm, R. Unland, U. Dirksen, A. Borkhardt, M. S. Staege, C. Muller-Tidow and G. H. Richter (2009). "Epigenetic maintenance of stemness and malignancy in peripheral neuroectodermal tumors by EZH2." Cell cycle **8**(13): 1991-1996.

Burdach, S., U. Thiel, M. Schoniger, R. Haase, A. Wawer, M. Nathrath, H. Kabisch, C. Urban, H. J. Laws, U. Dirksen, M. Steinborn, J. Dunst and H. Jurgens (2010). "Total body MRI-governed involved compartment irradiation combined with high-dose chemotherapy and stem cell rescue improves long-term survival in Ewing tumor patients with multiple primary bone metastases." Bone marrow transplantation **45**(3): 483-489.

Burdach, S., B. van Kaick, H. J. Laws, S. Ahrens, R. Haase, D. Korholz, H. Pape, J. Dunst, T. Kahn, R. Willers, B. Engel, U. Dirksen, C. Kramm, W. Nurnberger, A. Heyll, R. Ladenstein, H. Gadner, H. Jurgens and U. Go el (2000). "Allogeneic and autologous stem-cell transplantation in advanced Ewing tumors. An update after long-term follow-up from two centers of the European Intergroup study EICESS. Stem-Cell Transplant Programs at Dusseldorf University Medical Center, Germany and St. Anna Kinderspital, Vienna, Austria." Ann Oncol **11**(11): 1451-1462.

Burdach, S., B. van Kaick, H. J. Laws, S. Ahrens, R. Haase, D. Korholz, H. Pape, J. Dunst, T. Kahn, R. Willers, B. Engel, U. Dirksen, C. Kramm, W.

Nurnberger, A. Heyll, R. Ladenstein, H. Gadner, H. Jurgens and U. Go el (2000). "Allogeneic and autologous stem-cell transplantation in advanced Ewing tumors. An update after long-term follow-up from two centers of the European Intergroup study EICESS. Stem-Cell Transplant Programs at Dusseldorf University Medical Center, Germany and St. Anna Kinderspital, Vienna, Austria." Annals of oncology : official journal of the European Society for Medical Oncology / ESMO **11**(11): 1451-1462.

Burnet, F. M. (1971). "Immunological surveillance in neoplasia." Transplantation reviews **7**: 3-25.

Cameron, B. J., A. B. Gerry, J. Dukes, J. V. Harper, V. Kannan, F. C. Bianchi, F. Grand, J. E. Brewer, M. Gupta, G. Plesa, G. Bossi, A. Vuidepot, A. S. Powlesland, A. Legg, K. J. Adams, A. D. Bennett, N. J. Pumphrey, D. D. Williams, G. Binder-Scholl, I. Kulikovskaya, B. L. Levine, J. L. Riley, A. Varela-Rohena, E. A. Stadtmauer, A. P. Rapoport, G. P. Linette, C. H. June, N. J. Hassan, M. Kalos and B. K. Jakobsen (2013). "Identification of a Titin-derived HLA-A1-presented peptide as a cross-reactive target for engineered MAGE A3-directed T cells." Sci Transl Med **5**(197): 197ra103.

Casucci, M. and A. Bondanza (2011). "Suicide gene therapy to increase the safety of chimeric antigen receptor-redirected T lymphocytes." Journal of Cancer **2**: 378-382.

Cavazzana, A. O., J. S. Miser, J. Jefferson and T. J. Triche (1987). "Experimental evidence for a neural origin of Ewing's sarcoma of bone." Am J Pathol **127**(3): 507-518.

Chaturvedi, A., L. M. Hoffman, A. L. Welm, S. L. Lessnick and M. C. Beckerle (2012). "The EWS/FLI Oncogene Drives Changes in Cellular Morphology, Adhesion, and Migration in Ewing Sarcoma." Genes & cancer **3**(2): 102-116.

Cheadle, E. J., H. Gornall, V. Baldan, V. Hanson, R. E. Hawkins and D. E. Gilham (2014). "CAR T cells: driving the road from the laboratory to the clinic." Immunological reviews **257**(1): 91-106.

Chicha, L., R. Tussiwand, E. Traggiai, L. Mazzucchelli, L. Bronz, J. C. Piffaretti, A. Lanzavecchia and M. G. Manz (2005). "Human adaptive immune system Rag2-/-gamma(c)-/- mice." Annals of the New York Academy of Sciences **1044**: 236-243.

Chmielewski, M., C. Kopecky, A. A. Hombach and H. Abken (2011). "IL-12 release by engineered T cells expressing chimeric antigen receptors can effectively Muster an antigen-independent macrophage response on tumor cells that have shut down tumor antigen expression." Cancer research **71**(17): 5697-5706.

Clark, R. A., S. J. Huang, G. F. Murphy, I. G. Mollet, D. Hijnen, M. Muthukuru, C. F. Schanbacher, V. Edwards, D. M. Miller, J. E. Kim, J. Lambert and T. S. Kupper (2008). "Human squamous cell carcinomas evade the immune response by down-regulation of vascular E-selectin and recruitment of regulatory T cells." The Journal of experimental medicine **205**(10): 2221-2234.

Cohen, C. J., Y. F. Li, M. El-Gamil, P. F. Robbins, S. A. Rosenberg and R. A. Morgan (2007). "Enhanced antitumor activity of T cells engineered to express T-cell receptors with a second disulfide bond." Cancer research **67**(8): 3898-3903.

Cohen, C. J., Y. Zhao, Z. Zheng, S. A. Rosenberg and R. A. Morgan (2006). "Enhanced antitumor activity of murine-human hybrid T-cell receptor (TCR) in human lymphocytes is associated with improved pairing and TCR/CD3 stability." Cancer research **66**(17): 8878-8886.

Cotterill, S. J., S. Ahrens, M. Paulussen, H. F. Jurgens, P. A. Voute, H. Gadner and A. W. Craft (2000). "Prognostic factors in Ewing's tumor of bone: analysis of 975 patients from the European Intergroup Cooperative Ewing's Sarcoma Study Group." Journal of clinical oncology : official journal of the American Society of Clinical Oncology **18**(17): 3108-3114.

Curiel, T. J., G. Coukos, L. Zou, X. Alvarez, P. Cheng, P. Mottram, M. Evdemon-Hogan, J. R. Conejo-Garcia, L. Zhang, M. Burow, Y. Zhu, S. Wei, I. Kryczek, B. Daniel, A. Gordon, L. Myers, A. Lackner, M. L. Disis, K. L. Knutson, L. Chen and W. Zou (2004). "Specific recruitment of regulatory T cells in ovarian carcinoma fosters immune privilege and predicts reduced survival." Nature medicine **10**(9): 942-949.

Davies, M. A. and Y. Samuels (2010). "Analysis of the genome to personalize therapy for melanoma." Oncogene **29**(41): 5545-5555.

Davila, M. L., R. Brentjens, X. Wang, I. Riviere and M. Sadelain (2012). "How do CARs work?: Early insights from recent clinical studies targeting CD19." Oncoimmunology **1**(9): 1577-1583.

Davila, M. L., C. C. Kloss, G. Gunset and M. Sadelain (2013). "CD19 CAR-targeted T cells induce long-term remission and B Cell Aplasia in an immunocompetent mouse model of B cell acute lymphoblastic leukemia." PloS one **8**(4): e61338.

Dazzi, F., R. M. Szydlo, N. C. Cross, C. Craddock, J. Kaeda, E. Kanfer, K. Cwynarski, E. Olavarria, A. Yong, J. F. Apperley and J. M. Goldman (2000). "Durability of responses following donor lymphocyte infusions for patients who relapse after allogeneic stem cell transplantation for chronic myeloid leukemia." Blood **96**(8): 2712-2716.

Delattre, O., J. Zucman, T. Melot, X. S. Garau, J. M. Zucker, G. M. Lenoir, P. F. Ambros, D. Sheer, C. Turc-Carel, T. J. Triche and et al. (1994). "The Ewing family of tumors--a subgroup of small-round-cell tumors defined by specific chimeric transcripts." The New England journal of medicine **331**(5): 294-299.

Delattre, O., J. Zucman, B. Plougastel, C. Desmaze, T. Melot, M. Peter, H. Kovar, I. Joubert, P. de Jong, G. Rouleau and et al. (1992). "Gene fusion with an ETS DNA-binding domain caused by chromosome translocation in human tumours." Nature **359**(6391): 162-165.

Deschoolmeester, V., M. Baay, E. Van Marck, J. Weyler, P. Vermeulen, F. Lardon and J. B. Vermorken (2010). "Tumor infiltrating lymphocytes: an intriguing player in the survival of colorectal cancer patients." BMC immunology **11**: 19.

Donaldson, S. S. (2004). "Ewing sarcoma: radiation dose and target volume." Pediatric blood & cancer **42**(5): 471-476.

Dunst, J. and A. Schuck (2004). "Role of radiotherapy in Ewing tumors." Pediatric blood & cancer **42**(5): 465-470.

Dutoit, V., V. Rubio-Godoy, P. Y. Dietrich, A. L. Quiqueres, V. Schnuriger, D. Rimoldi, D. Lienard, D. Speiser, P. Guillaume, P. Batard, J. C. Cerottini, P. Romero and D. Valmori (2001). "Heterogeneous T-cell response to MAGE-A10(254-262): high avidity-specific cytolytic T lymphocytes show superior antitumor activity." Cancer research **61**(15): 5850-5856.

Dziubianau, M., J. Hecht, L. Kuchenbecker, A. Sattler, U. Stervbo, C. Rodelsperger, P. Nickel, A. U. Neumann, P. N. Robinson, S. Mundlos, H. D. Volk, A. Thiel, P. Reinke and N. Babel (2013). "TCR Repertoire Analysis by Next Generation Sequencing Allows Complex Differential Diagnosis of T Cell-

Related Pathology." American journal of transplantation : official journal of the American Society of Transplantation and the American Society of Transplant Surgeons.

Ellebaek, E., T. Z. Iversen, N. Junker, M. Donia, L. Engell-Noerregaard, O. Met, L. R. Holmich, R. S. Andersen, S. R. Hadrup, M. H. Andersen, P. thor Straten and I. M. Svane (2012). "Adoptive cell therapy with autologous tumor infiltrating lymphocytes and low-dose Interleukin-2 in metastatic melanoma patients." Journal of translational medicine **10**: 169.

Engels, B., H. Cam, T. Schuler, S. Indraccolo, M. Gladow, C. Baum, T. Blankenstein and W. Uckert (2003). "Retroviral vectors for high-level transgene expression in T lymphocytes." Human gene therapy **14**(12): 1155-1168.

Ewing, J. (1972). "Classics in oncology. Diffuse endothelioma of bone. James Ewing. Proceedings of the New York Pathological Society, 1921." CA: a cancer journal for clinicians **22**(2): 95-98.

Fagioli, F., P. Quarello, M. Zecca, E. Lanino, C. Rognoni, A. Balduzzi, C. Messina, C. Favre, R. Foa, M. Ripaldi, S. Rutella, G. Basso, A. Prete and F. Locatelli (2013). "Hematopoietic stem cell transplantation for children with high-risk acute lymphoblastic leukemia in first complete remission: a report from the AIEOP registry." Haematologica **98**(8): 1273-1281.

Ferrara, J. L., R. Levy and N. J. Chao (1999). "Pathophysiologic mechanisms of acute graft-vs.-host disease." Biol Blood Marrow Transplant **5**(6): 347-356.

Ghosh, S., F. R. Schuster, O. Adams, F. Babor, A. Borkhardt, P. Comoli, R. Handgretinger, P. Lang, H. J. Laws, M. Siepermann and R. Meisel (2014). "Haploidentical stem cell transplantation in DOCK8 deficiency - Successful control of pre-existing severe viremia with a TCRass/CD19-depleted graft and antiviral treatment." Clin Immunol **152**(1-2): 111-114.

Gonzalez-Galarza, F. F., S. Christmas, D. Middleton and A. R. Jones (2011). "Allele frequency net: a database and online repository for immune gene frequencies in worldwide populations." Nucleic acids research **39**(Database issue): D913-919.

Grohar, P. J., L. B. Griffin, C. Yeung, Q. R. Chen, Y. Pommier, C. Khanna, J. Khan and L. J. Helman (2011). "Ecteinascidin 743 interferes with the activity of EWS-FLI1 in Ewing sarcoma cells." Neoplasia **13**(2): 145-153.

Grupp, S. A., M. Kalos, D. Barrett, R. Aplenc, D. L. Porter, S. R. Rheingold, D. T. Teachey, A. Chew, B. Hauck, J. F. Wright, M. C. Milone, B. L. Levine and C. H. June (2013). "Chimeric antigen receptor-modified T cells for acute lymphoid leukemia." The New England journal of medicine **368**(16): 1509-1518.

Haanen, J. B., A. Baars, R. Gomez, P. Weder, M. Smits, T. D. de Gruijl, B. M. von Blomberg, E. Bloemena, R. J. Scheper, S. M. van Ham, H. M. Pinedo and A. J. van den Eertwegh (2006). "Melanoma-specific tumor-infiltrating lymphocytes but not circulating melanoma-specific T cells may predict survival in resected advanced-stage melanoma patients." Cancer immunology, immunotherapy : CII **55**(4): 451-458.

Haeusler, J., A. Ranft, T. Boelling, G. Gosheger, G. Braun-Munzinger, V. Vieth, S. Burdach, H. van den Berg, H. Juergens and U. Dirksen (2010). "The value of local treatment in patients with primary, disseminated, multifocal Ewing sarcoma (PDMES)." Cancer **116**(2): 443-450.

Handgretinger, R., T. Klingebiel, P. Lang, M. Schumm, S. Neu, A. Geiselhart, P. Bader, P. G. Schlegel, J. Greil, D. Stachel, R. J. Herzog and D. Niethammer (2001). "Megadose transplantation of purified peripheral blood CD34(+) progenitor cells from HLA-mismatched parental donors in children." Bone Marrow Transplant **27**(8): 777-783.

Hauer, K., J. Calzada-Wack, K. Steiger, T. G. Grunewald, D. Baumhoer, S. Plehm, T. Buch, O. Prazeres da Costa, I. Esposito, S. Burdach and G. H. Richter (2013). "DKK2 mediates osteolysis, invasiveness, and metastatic spread in Ewing sarcoma." Cancer Res **73**(2): 967-977.

Hawkins, D. S., J. Felgenhauer, J. Park, S. Kreissman, B. Thomson, J. Douglas, S. D. Rowley, T. Gooley, J. E. Sanders and T. W. Pendergrass (2002). "Peripheral blood stem cell support reduces the toxicity of intensive chemotherapy for children and adolescents with metastatic sarcomas." Cancer **95**(6): 1354-1365.

Hinrichs, C. S., Z. A. Borman, L. Cassard, L. Gattinoni, R. Spolski, Z. Yu, L. Sanchez-Perez, P. Muranski, S. J. Kern, C. Logun, D. C. Palmer, Y. Ji, R. N. Reger, W. J. Leonard, R. L. Danner, S. A. Rosenberg and N. P. Restifo (2009). "Adoptively transferred effector cells derived from naive rather than central memory CD8+ T cells mediate superior antitumor immunity." Proc Natl Acad Sci U S A **106**(41): 17469-17474.

Hinrichs, C. S., Z. A. Borman, L. Gattinoni, Z. Yu, W. R. Burns, J. Huang, C. A. Klebanoff, L. A. Johnson, S. P. Kerkar, S. Yang, P. Muranski, D. C. Palmer, C. D. Scott, R. A. Morgan, P. F. Robbins, S. A. Rosenberg and N. P. Restifo (2011). "Human effector CD8+ T cells derived from naive rather than memory subsets possess superior traits for adoptive immunotherapy." Blood **117**(3): 808-814.

Hinrichs, C. S. and S. A. Rosenberg (2014). "Exploiting the curative potential of adoptive T-cell therapy for cancer." Immunological reviews **257**(1): 56-71.

Hiraki, Y., T. Kono, M. Sato, C. Shukunami and J. Kondo (1997). "Inhibition of DNA synthesis and tube morphogenesis of cultured vascular endothelial cells by chondromodulin-I." FEBS letters **415**(3): 321-324.

Horowitz, M. M., R. P. Gale, P. M. Sondel, J. M. Goldman, J. Kersey, H. J. Kolb, A. A. Rimm, O. Ringden, C. Rozman, B. Speck and et al. (1990). "Graft-versus-leukemia reactions after bone marrow transplantation." Blood **75**(3): 555-562.

Huang, H. Y., P. B. Illei, Z. Zhao, M. Mazumdar, A. G. Huvos, J. H. Healey, L. H. Wexler, R. Gorlick, P. Meyers and M. Ladanyi (2005). "Ewing sarcomas with p53 mutation or p16/p14ARF homozygous deletion: a highly lethal subset associated with poor chemoresponse." Journal of clinical oncology : official journal of the American Society of Clinical Oncology **23**(3): 548-558.

Husby, G., P. M. Hoagland, R. G. Strickland and R. C. Williams, Jr. (1976). "Tissue T and B cell infiltration of primary and metastatic cancer." The Journal of clinical investigation **57**(6): 1471-1482.

Itzhaki, O., E. Hovav, Y. Ziporen, D. Levy, A. Kubi, D. Zikich, L. Hershkovitz, A. J. Treves, B. Shalmon, D. Zippel, G. Markel, R. Shapira-Frommer, J. Schachter and M. J. Besser (2011). "Establishment and large-scale expansion of minimally cultured "young" tumor infiltrating lymphocytes for adoptive transfer therapy." Journal of immunotherapy **34**(2): 212-220.

Jedlicka, P. (2010). "Ewing Sarcoma, an enigmatic malignancy of likely progenitor cell origin, driven by transcription factor oncogenic fusions." International journal of clinical and experimental pathology **3**(4): 338-347.

Johnson, L. A., R. A. Morgan, M. E. Dudley, L. Cassard, J. C. Yang, M. S. Hughes, U. S. Kammula, R. E. Royal, R. M. Sherry, J. R. Wunderlich, C. C. Lee, N. P. Restifo, S. L. Schwarz, A. P. Cogdill, R. J. Bishop, H. Kim, C. C. Brewer, S. F. Rudy, C. VanWaes, J. L. Davis, A. Mathur, R. T. Ripley, D. A.

Nathan, C. M. Laurencot and S. A. Rosenberg (2009). "Gene therapy with human and mouse T-cell receptors mediates cancer regression and targets normal tissues expressing cognate antigen." Blood **114**(3): 535-546.

Juergens, C., C. Weston, I. Lewis, J. Whelan, M. Paulussen, O. Oberlin, J. Michon, A. Zoubek, H. Juergens and A. Craft (2006). "Safety assessment of intensive induction with vincristine, ifosfamide, doxorubicin, and etoposide (VIDE) in the treatment of Ewing tumors in the EURO-E.W.I.N.G. 99 clinical trial." Pediatric blood & cancer **47**(1): 22-29.

Kalos, M., B. L. Levine, D. L. Porter, S. Katz, S. A. Grupp, A. Bagg and C. H. June (2011). "T cells with chimeric antigen receptors have potent antitumor effects and can establish memory in patients with advanced leukemia." Science translational medicine **3**(95): 95ra73.

Kelleher, F. C. and D. M. Thomas (2012). "Molecular pathogenesis and targeted therapeutics in Ewing sarcoma/primitive neuroectodermal tumours." Clinical sarcoma research **2**(1): 6.

Kenneth Murphy, P. T., Mark Walport (2008). "Janeway's Immunobiology."

Khong, H. T., Q. J. Wang and S. A. Rosenberg (2004). "Identification of multiple antigens recognized by tumor-infiltrating lymphocytes from a single patient: tumor escape by antigen loss and loss of MHC expression." Journal of immunotherapy **27**(3): 184-190.

Kido, A., I. Amano, K. Honoki, H. Tanaka, T. Morii, H. Fujii, K. Yoshitani and Y. Tanaka (2010). "Allogeneic and autologous stem cell transplantation in advanced small round cell sarcomas." J Orthop Sci **15**(5): 690-695.

Kim, S. Y., J. A. Toretsky, D. Scher and L. J. Helman (2009). "The role of IGF-1R in pediatric malignancies." Oncologist **14**(1): 83-91.

Klar, R., S. Schober, M. Rami, S. Mall, J. Merl, S. M. Hauck, M. Ueffing, A. Admon, J. Slotta-Huspenina, M. Schwaiger, S. Stevanovic, R. A. Oostendorp, D. H. Busch, C. Peschel and A. M. Krackhardt (2014). "Therapeutic targeting of naturally presented myeloperoxidase-derived HLA peptide ligands in myeloid leukemia cells by TCR-transgenic T cells." Leukemia.

Klebanoff, C. A., L. Gattinoni and N. P. Restifo (2006). "CD8+ T-cell memory in tumor immunology and immunotherapy." Immunological reviews **211**: 214-224.

Klingebiel, T., J. Cornish, M. Labopin, F. Locatelli, P. Darbyshire, R. Handgretinger, A. Balduzzi, J. Owoc-Lempach, F. Fagioli, R. Or, C. Peters, F.

Aversa, E. Polge, G. Dini, V. Rocha, D. Pediatric, B. Acute Leukemia Working Parties of the European Group for and T. Marrow (2010). "Results and factors influencing outcome after fully haploidentical hematopoietic stem cell transplantation in children with very high-risk acute lymphoblastic leukemia: impact of center size: an analysis on behalf of the Acute Leukemia and Pediatric Disease Working Parties of the European Blood and Marrow Transplant group." Blood **115**(17): 3437-3446.

Kobayashi, N., N. Hiraoka, W. Yamagami, H. Ojima, Y. Kanai, T. Kosuge, A. Nakajima and S. Hirohashi (2007). "FOXP3+ regulatory T cells affect the development and progression of hepatocarcinogenesis." Clinical cancer research : an official journal of the American Association for Cancer Research **13**(3): 902-911.

Kochenderfer, J. N., M. E. Dudley, S. A. Feldman, W. H. Wilson, D. E. Spaner, I. Maric, M. Stetler-Stevenson, G. Q. Phan, M. S. Hughes, R. M. Sherry, J. C. Yang, U. S. Kammula, L. Devillier, R. Carpenter, D. A. Nathan, R. A. Morgan, C. Laurencot and S. A. Rosenberg (2012). "B-cell depletion and remissions of malignancy along with cytokine-associated toxicity in a clinical trial of anti-CD19 chimeric-antigen-receptor-transduced T cells." Blood **119**(12): 2709-2720.

Kochenderfer, J. N., W. H. Wilson, J. E. Janik, M. E. Dudley, M. Stetler-Stevenson, S. A. Feldman, I. Maric, M. Raffeld, D. A. Nathan, B. J. Lanier, R. A. Morgan and S. A. Rosenberg (2010). "Eradication of B-lineage cells and regression of lymphoma in a patient treated with autologous T cells genetically engineered to recognize CD19." Blood **116**(20): 4099-4102.

Kohn, D. B., M. S. Hershfield, D. Carbonaro, A. Shigeoka, J. Brooks, E. M. Smogorzewska, L. W. Barsky, R. Chan, F. Burotto, G. Annett, J. A. Nolta, G. Crooks, N. Kapoor, M. Elder, D. Wara, T. Bowen, E. Madsen, F. F. Snyder, J. Bastian, L. Muul, R. M. Blaese, K. Weinberg and R. Parkman (1998). "T lymphocytes with a normal ADA gene accumulate after transplantation of transduced autologous umbilical cord blood CD34+ cells in ADA-deficient SCID neonates." Nature medicine **4**(7): 775-780.

Kolb, H. J., A. Schattenberg, J. M. Goldman, B. Hertenstein, N. Jacobsen, W. Arcese, P. Ljungman, A. Ferrant, L. Verdonck, D. Niederwieser, F. van Rhee, J. Mittermueller, T. de Witte, E. Holler, H. Ansari, B. European Group for and L. Marrow Transplantation Working Party Chronic (1995). "Graft-versus-leukemia

effect of donor lymphocyte transfusions in marrow grafted patients." Blood **86**(5): 2041-2050.

Korkolopoulou, P., L. Kaklamanis, F. Pezzella, A. L. Harris and K. C. Gatter (1996). "Loss of antigen-presenting molecules (MHC class I and TAP-1) in lung cancer." British journal of cancer **73**(2): 148-153.

Koscielniak, E., U. Gross-Wieltsch, J. Treuner, P. Winkler, T. Klingebiel, P. Lang, P. Bader, D. Niethammer and R. Handgretinger (2005). "Graft-versus-Ewing sarcoma effect and long-term remission induced by haploidentical stem-cell transplantation in a patient with relapse of metastatic disease." Journal of clinical oncology : official journal of the American Society of Clinical Oncology **23**(1): 242-244.

Kovar, H., J. Alonso, P. Aman, D. N. Aryee, J. Ban, S. A. Burchill, S. Burdach, E. De Alava, O. Delattre, U. Dirksen, A. Fourtouna, S. Fulda, L. J. Helman, D. Herrero-Martin, P. C. Hogendoorn, U. Kontny, E. R. Lawlor, S. L. Lessnick, A. Llombart-Bosch, M. Metzler, R. Moriggl, S. Niedan, J. Potratz, F. Redini, G. H. Richter, L. T. Riedmann, C. Rossig, B. W. Schafer, R. Schwentner, K. Scotlandi, P. H. Sorensen, M. S. Staege, F. Tirode, J. Toretsky, S. Ventura, A. Eggert and R. Ladenstein (2012). "The first European interdisciplinary ewing sarcoma research summit." Frontiers in oncology **2**: 54.

Kozak, M. (1984). "Point mutations close to the AUG initiator codon affect the efficiency of translation of rat preproinsulin in vivo." Nature **308**(5956): 241-246.

Kuball, J., M. L. Dossett, M. Wolfl, W. Y. Ho, R. H. Voss, C. Fowler and P. D. Greenberg (2007). "Facilitating matched pairing and expression of TCR chains introduced into human T cells." Blood **109**(6): 2331-2338.

Ladenstein, R., U. Potschger, M. C. Le Deley, J. Whelan, M. Paulussen, O. Oberlin, H. van den Berg, U. Dirksen, L. Hjorth, J. Michon, I. Lewis, A. Craft and H. Jurgens (2010). "Primary disseminated multifocal Ewing sarcoma: results of the Euro-EWING 99 trial." Journal of clinical oncology : official journal of the American Society of Clinical Oncology **28**(20): 3284-3291.

Lang, P., J. Greil, P. Bader, R. Handgretinger, T. Klingebiel, M. Schumm, P. G. Schlegel, T. Feuchtinger, M. Pfeiffer, H. Scheel-Walter, M. Fuhrer, D. Martin and D. Niethammer (2004). "Long-term outcome after haploidentical stem cell transplantation in children." Blood Cells Mol Dis **33**(3): 281-287.

Lang, P., H. M. Teltschik, T. Feuchtinger, I. Muller, M. Pfeiffer, M. Schumm, M. Ebinger, C. P. Schwarze, B. Gruhn, A. Schrauder, M. H. Albert, J. Greil, C. Urban and R. Handgretinger (2014). "Transplantation of CD3/CD19 depleted allografts from haploidentical family donors in paediatric leukaemia." Br J Haematol **165**(5): 688-698.

Larkin, J., C. D. Lao, W. J. Urba, D. F. McDermott, C. Horak, J. Jiang and J. D. Wolchok (2015). "Efficacy and Safety of Nivolumab in Patients With BRAF V600 Mutant and BRAF Wild-Type Advanced Melanoma: A Pooled Analysis of 4 Clinical Trials." JAMA Oncol **1**(4): 433-440.

Lawlor, E. R. and C. J. Thiele (2012). "Epigenetic changes in pediatric solid tumors: promising new targets." Clin Cancer Res **18**(10): 2768-2779.

Leisegang, M., B. Engels, P. Meyerhuber, E. Kieback, D. Sommermeyer, S. A. Xue, S. Reuss, H. Stauss and W. Uckert (2008). "Enhanced functionality of T cell receptor-redirected T cells is defined by the transgene cassette." Journal of molecular medicine **86**(5): 573-583.

Leisegang, M., S. Wilde, S. Spranger, S. Milosevic, B. Frankenberger, W. Uckert and D. J. Schendel (2010). "MHC-restricted fratricide of human lymphocytes expressing survivin-specific transgenic T cell receptors." J Clin Invest **120**(11): 3869-3877.

Lessnick, S. L., C. S. Dacwag and T. R. Golub (2002). "The Ewing's sarcoma oncoprotein EWS/FLI induces a p53-dependent growth arrest in primary human fibroblasts." Cancer cell **1**(4): 393-401.

Linette, G. P., E. A. Stadtmauer, M. V. Maus, A. P. Rapoport, B. L. Levine, L. Emery, L. Litzky, A. Bagg, B. M. Carreno, P. J. Cimino, G. K. Binder-Scholl, D. P. Smethurst, A. B. Gerry, N. J. Pumphrey, A. D. Bennett, J. E. Brewer, J. Dukes, J. Harper, H. K. Tayton-Martin, B. K. Jakobsen, N. J. Hassan, M. Kalos and C. H. June (2013). "Cardiovascular toxicity and titin cross-reactivity of affinity-enhanced T cells in myeloma and melanoma." Blood **122**(6): 863-871.

Lissat, A., M. M. Chao and U. Kontny (2012). "Targeted therapy in Ewing sarcoma." ISRN oncology **2012**: 609439.

Llombart-Bosch, A., I. Machado, S. Navarro, F. Bertoni, P. Bacchini, M. Alberghini, A. Karzeladze, N. Savelov, S. Petrov, I. Alvarado-Cabrero, D. Mihaila, P. Terrier, J. A. Lopez-Guerrero and P. Picci (2009). "Histological heterogeneity of Ewing's sarcoma/PNET: an immunohistochemical analysis of

415 genetically confirmed cases with clinical support." Virchows Archiv : an international journal of pathology **455**(5): 397-411.

Lucas, K. G., C. Schwartz and J. Kaplan (2008). "Allogeneic stem cell transplantation in a patient with relapsed Ewing sarcoma." Pediatric blood & cancer **51**(1): 142-144.

Mackintosh, C., J. Madoz-Gurpide, J. L. Ordonez, D. Osuna and D. Herrero-Martin (2010). "The molecular pathogenesis of Ewing's sarcoma." Cancer biology & therapy **9**(9): 655-667.

Madhavan, M., P. Srinivas, E. Abraham, I. Ahmed, N. R. Vijayalekshmi and P. Balaram (2002). "Down regulation of endothelial adhesion molecules in node positive breast cancer: possible failure of host defence mechanism." Pathology oncology research : POR **8**(2): 125-128.

Mahlendorf, D. E. and M. S. Staege (2013). "Characterization of Ewing sarcoma associated cancer/testis antigens." Cancer biology & therapy **14**(3): 254-261.

Malissen, M., J. Trucy, E. Jouvin-Marche, P. A. Cazenave, R. Scollay and B. Malissen (1992). "Regulation of TCR alpha and beta gene allelic exclusion during T-cell development." Immunology today **13**(8): 315-322.

Mapara, M. Y. and M. Sykes (2004). "Tolerance and cancer: mechanisms of tumor evasion and strategies for breaking tolerance." Journal of clinical oncology : official journal of the American Society of Clinical Oncology **22**(6): 1136-1151.

Marin, V., E. Cribioli, B. Philip, S. Tettamanti, I. Pizzitola, A. Biondi, E. Biagi and M. Pule (2012). "Comparison of different suicide-gene strategies for the safety improvement of genetically manipulated T cells." Human gene therapy methods **23**(6): 376-386.

Miyagawa, Y., H. Okita, H. Nakaijima, Y. Horiuchi, B. Sato, T. Taguchi, M. Toyoda, Y. U. Katagiri, J. Fujimoto, J. Hata, A. Umezawa and N. Kiyokawa (2008). "Inducible expression of chimeric EWS/ETS proteins confers Ewing's family tumor-like phenotypes to human mesenchymal progenitor cells." Molecular and cellular biology **28**(7): 2125-2137.

Moo-Young, T. A., J. W. Larson, B. A. Belt, M. C. Tan, W. G. Hawkins, T. J. Eberlein, P. S. Goedegebuure and D. C. Linehan (2009). "Tumor-derived TGF-beta mediates conversion of CD4+Foxp3+ regulatory T cells in a murine model of pancreas cancer." J Immunother **32**(1): 12-21.

Morgan, R. A., N. Chinnasamy, D. Abate-Daga, A. Gros, P. F. Robbins, Z. Zheng, M. E. Dudley, S. A. Feldman, J. C. Yang, R. M. Sherry, G. Q. Phan, M. S. Hughes, U. S. Kammula, A. D. Miller, C. J. Hessman, A. A. Stewart, N. P. Restifo, M. M. Quezado, M. Alimchandani, A. Z. Rosenberg, A. Nath, T. Wang, B. Bielekova, S. C. Wuest, N. Akula, F. J. McMahon, S. Wilde, B. Mosetter, D. J. Schendel, C. M. Laurencot and S. A. Rosenberg (2013). "Cancer regression and neurological toxicity following anti-MAGE-A3 TCR gene therapy." J Immunother **36**(2): 133-151.

Morgan, R. A., M. E. Dudley, J. R. Wunderlich, M. S. Hughes, J. C. Yang, R. M. Sherry, R. E. Royal, S. L. Topalian, U. S. Kammula, N. P. Restifo, Z. Zheng, A. Nahvi, C. R. de Vries, L. J. Rogers-Freezer, S. A. Mavroukakis and S. A. Rosenberg (2006). "Cancer regression in patients after transfer of genetically engineered lymphocytes." Science **314**(5796): 126-129.

Nauerth, M., B. Weissbrich, R. Knall, T. Franz, G. Dossinger, J. Bet, P. J. Paszkiewicz, L. Pfeifer, M. Bunse, W. Uckert, R. Holtappels, D. Gillert-Marien, M. Neuenhahn, A. Krackhardt, M. J. Reddehase, S. R. Riddell and D. H. Busch (2013). "TCR-ligand koff rate correlates with the protective capacity of antigen-specific CD8+ T cells for adoptive transfer." Science translational medicine **5**(192): 192ra187.

Neilsen, P. M., K. I. Pishas, D. F. Callen and D. M. Thomas (2011). "Targeting the p53 Pathway in Ewing Sarcoma." Sarcoma **2011**: 746939.

Niederberger, N., K. Holmberg, S. M. Alam, W. Sakati, M. Naramura, H. Gu and N. R. Gascoigne (2003). "Allelic exclusion of the TCR alpha-chain is an active process requiring TCR-mediated signaling and c-Cbl." Journal of immunology **170**(9): 4557-4563.

Ormandy, L. A., T. Hillemann, H. Wedemeyer, M. P. Manns, T. F. Greten and F. Korangy (2005). "Increased populations of regulatory T cells in peripheral blood of patients with hepatocellular carcinoma." Cancer research **65**(6): 2457-2464.

Parkhurst, M. R., J. Joo, J. P. Riley, Z. Yu, Y. Li, P. F. Robbins and S. A. Rosenberg (2009). "Characterization of genetically modified T-cell receptors that recognize the CEA:691-699 peptide in the context of HLA-A2.1 on human colorectal cancer cells." Clinical cancer research : an official journal of the American Association for Cancer Research **15**(1): 169-180.

Parkhurst, M. R., J. C. Yang, R. C. Langan, M. E. Dudley, D. A. Nathan, S. A. Feldman, J. L. Davis, R. A. Morgan, M. J. Merino, R. M. Sherry, M. S. Hughes, U. S. Kammula, G. Q. Phan, R. M. Lim, S. A. Wank, N. P. Restifo, P. F. Robbins, C. M. Laurencot and S. A. Rosenberg (2011). "T cells targeting carcinoembryonic antigen can mediate regression of metastatic colorectal cancer but induce severe transient colitis." Molecular therapy : the journal of the American Society of Gene Therapy **19**(3): 620-626.

Paulussen, M., S. Ahrens, S. Burdach, A. Craft, B. Dockhorn-Dworniczak, J. Dunst, B. Frohlich, W. Winkelmann, A. Zoubek and H. Jurgens (1998). "Primary metastatic (stage IV) Ewing tumor: survival analysis of 171 patients from the EICESS studies. European Intergroup Cooperative Ewing Sarcoma Studies." Annals of oncology : official journal of the European Society for Medical Oncology / ESMO **9**(3): 275-281.

Paulussen, M., S. Ahrens, A. W. Craft, J. Dunst, B. Frohlich, S. Jabar, C. Rube, W. Winkelmann, S. Wissing, A. Zoubek and H. Jurgens (1998). "Ewing's tumors with primary lung metastases: survival analysis of 114 (European Intergroup) Cooperative Ewing's Sarcoma Studies patients." Journal of clinical oncology : official journal of the American Society of Clinical Oncology **16**(9): 3044-3052.

Paulussen, M., S. Ahrens, J. Dunst, W. Winkelmann, G. U. Exner, R. Kotz, G. Amann, B. Dockhorn-Dworniczak, D. Harms, S. Muller-Weihrich, K. Welte, B. Kornhuber, G. Janka-Schaub, U. Gobel, J. Treuner, P. A. Voute, A. Zoubek, H. Gadner and H. Jurgens (2001). "Localized Ewing tumor of bone: final results of the cooperative Ewing's Sarcoma Study CESS 86." J Clin Oncol **19**(6): 1818-1829.

Paulussen, M., A. W. Craft, I. Lewis, A. Hackshaw, C. Douglas, J. Dunst, A. Schuck, W. Winkelmann, G. Kohler, C. Poremba, A. Zoubek, R. Ladenstein, H. van den Berg, A. Hunold, A. Cassoni, D. Spooner, R. Grimer, J. Whelan, A. McTiernan and H. Jurgens (2008). "Results of the EICESS-92 Study: two randomized trials of Ewing's sarcoma treatment--cyclophosphamide compared with ifosfamide in standard-risk patients and assessment of benefit of etoposide added to standard treatment in high-risk patients." Journal of clinical oncology : official journal of the American Society of Clinical Oncology **26**(27): 4385-4393.

Paulussen, M., A. W. Craft, I. Lewis, A. Hackshaw, C. Douglas, J. Dunst, A. Schuck, W. Winkelmann, G. Kohler, C. Poremba, A. Zoubek, R. Ladenstein, H.

van den Berg, A. Hunold, A. Cassoni, D. Spooner, R. Grimer, J. Whelan, A. McTiernan, H. Jurgens and S. European Intergroup Cooperative Ewing's Sarcoma (2008). "Results of the EICESS-92 Study: two randomized trials of Ewing's sarcoma treatment--cyclophosphamide compared with ifosfamide in standard-risk patients and assessment of benefit of etoposide added to standard treatment in high-risk patients." J Clin Oncol **26**(27): 4385-4393.

Pegram, H. J., J. C. Lee, E. G. Hayman, G. H. Imperato, T. F. Tedder, M. Sadelain and R. J. Brentjens (2012). "Tumor-targeted T cells modified to secrete IL-12 eradicate systemic tumors without need for prior conditioning." Blood **119**(18): 4133-4141.

Perez, S. A., M. V. Karamouzis, D. V. Skarlos, A. Ardavanis, N. N. Sotiriadou, E. G. Iliopoulou, M. L. Salagianni, G. Orphanos, C. N. Baxevanis, G. Rigatos and M. Papamichail (2007). "CD4+CD25+ regulatory T-cell frequency in HER-2/neu (HER)-positive and HER-negative advanced-stage breast cancer patients." Clinical cancer research : an official journal of the American Association for Cancer Research **13**(9): 2714-2721.

Piali, L., A. Fichtel, H. J. Terpe, B. A. Imhof and R. H. Gisler (1995). "Endothelial vascular cell adhesion molecule 1 expression is suppressed by melanoma and carcinoma." The Journal of experimental medicine **181**(2): 811-816.

Pinto, A., P. Dickman and D. Parham (2011). "Pathobiologic markers of the ewing sarcoma family of tumors: state of the art and prediction of behaviour." Sarcoma **2011**: 856190.

Pirson, S. (2009). "Generation of autologous and allorestricted cytotoxic T cell clones directed against Ewing Tumor antigens."

Porter, D. L., B. L. Levine, M. Kalos, A. Bagg and C. H. June (2011). "Chimeric antigen receptor-modified T cells in chronic lymphoid leukemia." The New England journal of medicine **365**(8): 725-733.

Potikyan, G., K. A. France, M. R. Carlson, J. Dong, S. F. Nelson and C. T. Denny (2008). "Genetically defined EWS/FLI1 model system suggests mesenchymal origin of Ewing's family tumors." Laboratory investigation; a journal of technical methods and pathology **88**(12): 1291-1302.

Potikyan, G., K. A. France, M. R. Carlson, J. Dong, S. F. Nelson and C. T. Denny (2008). "Genetically defined EWS/FLI1 model system suggests mesenchymal origin of Ewing's family tumors." Lab Invest **88**(12): 1291-1302.

Radvanyi, L. G., C. Bernatchez, M. Zhang, P. S. Fox, P. Miller, J. Chacon, R. Wu, G. Lizee, S. Mahoney, G. Alvarado, M. Glass, V. E. Johnson, J. D. McMannis, E. Shpall, V. Prieto, N. Papadopoulos, K. Kim, J. Homsi, A. Bedikian, W. J. Hwu, S. Patel, M. I. Ross, J. E. Lee, J. E. Gershenwald, A. Lucci, R. Royal, J. N. Cormier, M. A. Davies, R. Mansaray, O. J. Fulbright, C. Toth, R. Ramachandran, S. Wardell, A. Gonzalez and P. Hwu (2012). "Specific lymphocyte subsets predict response to adoptive cell therapy using expanded autologous tumor-infiltrating lymphocytes in metastatic melanoma patients." Clinical cancer research : an official journal of the American Association for Cancer Research **18**(24): 6758-6770.

Ramos, C. A., B. Savoldo and G. Dotti (2014). "CD19-CAR Trials." Cancer journal **20**(2): 112-118.

Rasper, M., S. Jabar, A. Ranft, H. Jurgens, S. Amler and U. Dirksen (2014). "The value of high-dose chemotherapy in patients with first relapsed Ewing sarcoma." Pediatr Blood Cancer **61**(8): 1382-1386.

Richter, G. H., S. Plehm, A. Fasan, S. Rossler, R. Unland, I. M. Bennani-Baiti, M. Hotfilder, D. Lowel, I. von Luettichau, I. Mossbrugger, L. Quintanilla-Martinez, H. Kovar, M. S. Staege, C. Muller-Tidow and S. Burdach (2009). "EZH2 is a mediator of EWS/FLI1 driven tumor growth and metastasis blocking endothelial and neuro-ectodermal differentiation." Proc Natl Acad Sci U S A **106**(13): 5324-5329.

Richter, G. H., S. Plehm, A. Fasan, S. Rossler, R. Unland, I. M. Bennani-Baiti, M. Hotfilder, D. Lowel, I. von Luettichau, I. Mossbrugger, L. Quintanilla-Martinez, H. Kovar, M. S. Staege, C. Muller-Tidow and S. Burdach (2009). "EZH2 is a mediator of EWS/FLI1 driven tumor growth and metastasis blocking endothelial and neuro-ectodermal differentiation." Proceedings of the National Academy of Sciences of the United States of America **106**(13): 5324-5329.

Riggi, N., L. Cironi, P. Provero, M. L. Suva, K. Kaloulis, C. Garcia-Echeverria, F. Hoffmann, A. Trumpp and I. Stamenkovic (2005). "Development of Ewing's sarcoma from primary bone marrow-derived mesenchymal progenitor cells." Cancer research **65**(24): 11459-11468.

Riggi, N., M. L. Suva and I. Stamenkovic (2009). "Ewing's sarcoma origin: from duel to duality." Expert review of anticancer therapy **9**(8): 1025-1030.

Riggi, N., M. L. Suva, D. Suva, L. Cironi, P. Provero, S. Tercier, J. M. Joseph, J. C. Stehle, K. Baumer, V. Kindler and I. Stamenkovic (2008). "EWS-FLI-1 expression triggers a Ewing's sarcoma initiation program in primary human mesenchymal stem cells." Cancer research **68**(7): 2176-2185.

Rill, D. R., V. M. Santana, W. M. Roberts, T. Nilson, L. C. Bowman, R. A. Krance, H. E. Heslop, R. C. Moen, J. N. Ihle and M. K. Brenner (1994). "Direct demonstration that autologous bone marrow transplantation for solid tumors can return a multiplicity of tumorigenic cells." Blood **84**(2): 380-383.

Robbins, P. F., Y. C. Lu, M. El-Gamil, Y. F. Li, C. Gross, J. Gartner, J. C. Lin, J. K. Teer, P. Cliften, E. Tycksen, Y. Samuels and S. A. Rosenberg (2013). "Mining exomic sequencing data to identify mutated antigens recognized by adoptively transferred tumor-reactive T cells." Nat Med **19**(6): 747-752.

Robbins, P. F., R. A. Morgan, S. A. Feldman, J. C. Yang, R. M. Sherry, M. E. Dudley, J. R. Wunderlich, A. V. Nahvi, L. J. Helman, C. L. Mackall, U. S. Kammula, M. S. Hughes, N. P. Restifo, M. Raffeld, C. C. Lee, C. L. Levy, Y. F. Li, M. El-Gamil, S. L. Schwarz, C. Laurencot and S. A. Rosenberg (2011). "Tumor regression in patients with metastatic synovial cell sarcoma and melanoma using genetically engineered lymphocytes reactive with NY-ESO-1." Journal of clinical oncology : official journal of the American Society of Clinical Oncology **29**(7): 917-924.

Rodriguez-Galindo, C., S. L. Spunt and A. S. Pappo (2003). "Treatment of Ewing sarcoma family of tumors: current status and outlook for the future." Medical and pediatric oncology **40**(5): 276-287.

Rosenberg, S. A. and M. E. Dudley (2009). "Adoptive cell therapy for the treatment of patients with metastatic melanoma." Curr Opin Immunol **21**(2): 233-240.

Rosenberg, S. A., J. C. Yang, R. M. Sherry, U. S. Kammula, M. S. Hughes, G. Q. Phan, D. E. Citrin, N. P. Restifo, P. F. Robbins, J. R. Wunderlich, K. E. Morton, C. M. Laurencot, S. M. Steinberg, D. E. White and M. E. Dudley (2011). "Durable complete responses in heavily pretreated patients with metastatic melanoma using T-cell transfer immunotherapy." Clinical cancer research : an

official journal of the American Association for Cancer Research **17**(13): 4550-4557.

Rosenthal, J., E. Bolotin, M. Shakhnovits, A. Pawlowska, P. Falk, D. Qian, C. Oliver, J. Sato, J. Miser and S. Forman (2008). "High-dose therapy with hematopoietic stem cell rescue in patients with poor prognosis Ewing family tumors." Bone marrow transplantation **42**(5): 311-318.

Ross, K. A., N. A. Smyth, C. D. Murawski and J. G. Kennedy (2013). "The biology of ewing sarcoma." ISRN oncology **2013**: 759725.

Sakaguchi, S., T. Yamaguchi, T. Nomura and M. Ono (2008). "Regulatory T cells and immune tolerance." Cell **133**(5): 775-787.

Sanda, M. G., N. P. Restifo, J. C. Walsh, Y. Kawakami, W. G. Nelson, D. M. Pardoll and J. W. Simons (1995). "Molecular characterization of defective antigen processing in human prostate cancer." Journal of the National Cancer Institute **87**(4): 280-285.

Scholten, K. B., D. Kramer, E. W. Kueter, M. Graf, T. Schoedl, C. J. Meijer, M. W. Schreurs and E. Hooijberg (2006). "Codon modification of T cell receptors allows enhanced functional expression in transgenic human T cells." Clinical immunology **119**(2): 135-145.

Schuck, A., J. Hofmann, C. Rube, A. Hillmann, S. Ahrens, M. Paulussen, H. Jurgens, J. Dunst and N. Willich (1998). "Radiotherapy in Ewing's sarcoma and PNET of the chest wall: results of the trials CESS 81, CESS 86 and EICESS 92." International journal of radiation oncology, biology, physics **42**(5): 1001-1006.

Schumm, M., P. Lang, W. Bethge, C. Faul, T. Feuchtinger, M. Pfeiffer, W. Vogel, V. Huppert and R. Handgretinger (2013). "Depletion of T-cell receptor alpha/beta and CD19 positive cells from apheresis products with the CliniMACS device." Cytotherapy **15**(10): 1253-1258.

Schuster, I. (2008). "Identifikation, Klonierung und retroviraler Transfer allorestringierter FMNL1-peptidspezifischer T-Zellrezeptoren für die Entwicklung adoptiver Immuntherapien gegen B-Zell-Non-Hodgkin-Lymphome."

Sharrocks, A. D. (2001). "The ETS-domain transcription factor family." Nature reviews. Molecular cell biology **2**(11): 827-837.

Sommermeyer, D. and W. Uckert (2010). "Minimal amino acid exchange in human TCR constant regions fosters improved function of TCR gene-modified T cells." Journal of immunology **184**(11): 6223-6231.

Sotomayor, E. M., I. Borrello, F. M. Rattis, A. G. Cuenca, J. Abrams, K. Staveley-O'Carroll and H. I. Levitsky (2001). "Cross-presentation of tumor antigens by bone marrow-derived antigen-presenting cells is the dominant mechanism in the induction of T-cell tolerance during B-cell lymphoma progression." Blood **98**(4): 1070-1077.

Staege, M. S., C. Hutter, I. Neumann, S. Foja, U. E. Hattenhorst, G. Hansen, D. Afar and S. E. Burdach (2004). "DNA microarrays reveal relationship of Ewing family tumors to both endothelial and fetal neural crest-derived cells and define novel targets." Cancer research **64**(22): 8213-8221.

Steinle, A., C. Reinhardt, P. Jantzer and D. J. Schendel (1995). "In vivo expansion of HLA-B35 alloreactive T cells sharing homologous T cell receptors: evidence for maintenance of an oligoclonally dominated allospecificity by persistent stimulation with an autologous MHC/peptide complex." The Journal of experimental medicine **181**(2): 503-513.

Stumpf, M., A. Hasenburg, M. O. Riener, U. Jutting, C. Wang, Y. Shen, M. Orlowska-Volk, P. Fisch, Z. Wang, G. Gitsch, M. Werner and S. Lassmann (2009). "Intraepithelial CD8-positive T lymphocytes predict survival for patients with serous stage III ovarian carcinomas: relevance of clonal selection of T lymphocytes." British journal of cancer **101**(9): 1513-1521.

Suzuki, F. (1996). "Roles of cartilage matrix proteins, chondromodulin-I and -II, in endochondral bone formation: a review." Connective tissue research **35**(1-4): 303-307.

Szymczak, A. L., C. J. Workman, Y. Wang, K. M. Vignali, S. Dilioglou, E. F. Vanin and D. A. Vignali (2004). "Correction of multi-gene deficiency in vivo using a single 'self-cleaving' 2A peptide-based retroviral vector." Nature biotechnology **22**(5): 589-594.

Takashima, Y., T. Era, K. Nakao, S. Kondo, M. Kasuga, A. G. Smith and S. Nishikawa (2007). "Neuroepithelial cells supply an initial transient wave of MSC differentiation." Cell **129**(7): 1377-1388.

Thacker, M. M., H. T. Temple and S. P. Scully (2005). "Current treatment for Ewing's sarcoma." Expert review of anticancer therapy **5**(2): 319-331.

Thiel, U., E. Koscielniak, F. Blaeschke, T. G. Grunewald, M. Badoglio, M. A. Diaz, C. Paillard, A. Prete, M. Ussowicz, P. Lang, F. Fagioli, P. Lutz, G. Ehninger, P. Schneider, A. Santucci, P. Bader, B. Gruhn, M. Faraci, P. Antunovic, J. Styczynski, W. H. Kruger, L. Castagna, P. Rohrlich, M. Ouachee-Chardin, A. Salmon, C. Peters, M. Bregni, S. Burdach, P. Solid Tumour Working, B. the Paediatric Disease Working Party of the European Group for and T. Marrow (2013). "Allogeneic stem cell transplantation for patients with advanced rhabdomyosarcoma: a retrospective assessment." Br J Cancer **109**(10): 2523-2532.

Thiel, U., S. Pirson, C. Muller-Spahn, H. Conrad, D. H. Busch, H. Bernhard, S. Burdach and G. H. Richter (2011). "Specific recognition and inhibition of Ewing tumour growth by antigen-specific allo-restricted cytotoxic T cells." British journal of cancer **104**(6): 948-956.

Thiel, U., A. Wawer, P. Wolf, M. Badoglio, A. Santucci, T. Klingebiel, O. Basu, A. Borkhardt, H. J. Laws, Y. Kodera, A. Yoshimi, C. Peters, R. Ladenstein, A. Pession, A. Prete, E. C. Urban, W. Schwinger, P. Bordigoni, A. Salmon, M. A. Diaz, B. Afanasyev, I. Lisukov, E. Morozova, A. Toren, B. Bielorai, J. Korsakas, F. Fagioli, D. Caselli, G. Ehninger, B. Gruhn, U. Dirksen, F. Abdel-Rahman, M. Aglietta, E. Mastrodicasa, M. Torrent, P. Corradini, F. Demeocq, G. Dini, P. Dreger, M. Eyrich, J. Gozdzik, F. Guilhot, E. Holler, E. Koscielniak, C. Messina, D. Nachbaur, R. Sabbatini, E. Oldani, H. Ottinger, H. Ozsahin, R. Schots, S. Siena, J. Stein, S. Sufliarska, A. Unal, M. Ussowicz, P. Schneider, W. Woessmann, H. Jurgens, M. Bregni and S. Burdach (2011). "No improvement of survival with reduced- versus high-intensity conditioning for allogeneic stem cell transplants in Ewing tumor patients." Annals of oncology : official journal of the European Society for Medical Oncology / ESMO **22**(7): 1614-1621.

Thiel, U., P. Wolf, A. Wawer, F. Blaeschke, T. G. Grunewald, I. T. von Luttichau, T. Klingebiel, P. Bader, A. Borkhardt, H. J. Laws, R. Handgretinger, P. Lang, P. G. Schlegel, M. Eyrich, B. Gruhn, G. Ehninger, E. Koscielniak, C. Klein, K. W. Sykora, E. Holler, C. Mauz-Korholz, W. Woessmann, G. H. Richter, A. H. Schmidt, C. Peters, U. Dirksen, H. Jurgens, M. Bregni and S. Burdach (2012). "Human leukocyte antigen distribution in German Caucasians with advanced Ewing's sarcoma." Klinische Padiatrie **224**(6): 353-358.

Tirode, F., K. Laud-Duval, A. Prieur, B. Delorme, P. Charbord and O. Delattre (2007). "Mesenchymal stem cell features of Ewing tumors." Cancer cell **11**(5): 421-429.

Topfer, K., S. Kempe, N. Muller, M. Schmitz, M. Bachmann, M. Cartellieri, G. Schackert and A. Temme (2011). "Tumor evasion from T cell surveillance." Journal of biomedicine & biotechnology **2011**: 918471.

Traggiai, E., L. Chicha, L. Mazzucchelli, L. Bronz, J. C. Piffaretti, A. Lanzavecchia and M. G. Manz (2004). "Development of a human adaptive immune system in cord blood cell-transplanted mice." Science **304**(5667): 104-107.

van Loenen, M. M., R. de Boer, A. L. Amir, R. S. Hagedoorn, G. L. Volbeda, R. Willemze, J. J. van Rood, J. H. Falkenburg and M. H. Heemskerk (2010). "Mixed T cell receptor dimers harbor potentially harmful neoreactivity." Proceedings of the National Academy of Sciences of the United States of America **107**(24): 10972-10977.

Viguier, M., F. Lemaitre, O. Verola, M. S. Cho, G. Gorochov, L. Dubertret, H. Bachelez, P. Kourilsky and L. Ferradini (2004). "Foxp3 expressing CD4+CD25(high) regulatory T cells are overrepresented in human metastatic melanoma lymph nodes and inhibit the function of infiltrating T cells." Journal of immunology **173**(2): 1444-1453.

Weiden, P. L., N. Flournoy, E. D. Thomas, R. Prentice, A. Fefer, C. D. Buckner and R. Storb (1979). "Antileukemic effect of graft-versus-host disease in human recipients of allogeneic-marrow grafts." N Engl J Med **300**(19): 1068-1073.

Weiden, P. L., K. M. Sullivan, N. Flournoy, R. Storb and E. D. Thomas (1981). "Antileukemic effect of chronic graft-versus-host disease: contribution to improved survival after allogeneic marrow transplantation." N Engl J Med **304**(25): 1529-1533.

Wexler, L. H., T. F. DeLaney, M. Tsokos, N. Avila, S. M. Steinberg, L. Weaver-McClure, J. Jacobson, P. Jarosinski, Y. M. Hijazi, F. M. Balis and M. E. Horowitz (1996). "Ifosfamide and etoposide plus vincristine, doxorubicin, and cyclophosphamide for newly diagnosed Ewing's sarcoma family of tumors." Cancer **78**(4): 901-911.

Wolf, A. M., D. Wolf, M. Steurer, G. Gastl, E. Gunsilius and B. Grubeck-Loebenstein (2003). "Increase of regulatory T cells in the peripheral blood of

cancer patients." Clinical cancer research : an official journal of the American Association for Cancer Research **9**(2): 606-612.

Wrzesinski, C., C. M. Paulos, A. Kaiser, P. Muranski, D. C. Palmer, L. Gattinoni, Z. Yu, S. A. Rosenberg and N. P. Restifo (2010). "Increased intensity lymphodepletion enhances tumor treatment efficacy of adoptively transferred tumor-specific T cells." Journal of immunotherapy **33**(1): 1-7.

Wu, F., W. Zhang, H. Shao, H. Bo, H. Shen, J. Li, Y. Liu, T. Wang, W. Ma and S. Huang (2013). "Human effector T cells derived from central memory cells rather than CD8(+)T cells modified by tumor-specific TCR gene transfer possess superior traits for adoptive immunotherapy." Cancer letters **339**(2): 195-207.

Xu, X. J., H. Z. Zhao and Y. M. Tang (2013). "Efficacy and safety of adoptive immunotherapy using anti-CD19 chimeric antigen receptor transduced T-cells: a systematic review of phase I clinical trials." Leukemia & lymphoma **54**(2): 255-260.

Yadav, M., S. Jhunjhunwala, Q. T. Phung, P. Lupardus, J. Tanguay, S. Bumbaca, C. Franci, T. K. Cheung, J. Fritsche, T. Weinschenk, Z. Modrusan, I. Mellman, J. R. Lill and L. Delamarre (2014). "Predicting immunogenic tumour mutations by combining mass spectrometry and exome sequencing." Nature **515**(7528): 572-576.

Yannelli, J. R., J. A. Tucker, G. Hidalgo, S. Perkins, R. Kryscio and E. A. Hirschowitz (2009). "Characteristics of PBMC obtained from leukapheresis products and tumor biopsies of patients with non-small cell lung cancer." Oncology reports **22**(6): 1459-1471.

Zhong, S., K. Malecek, L. A. Johnson, Z. Yu, E. Vega-Saenz de Miera, F. Darvishian, K. McGary, K. Huang, J. Boyer, E. Corse, Y. Shao, S. A. Rosenberg, N. P. Restifo, I. Osman and M. Krogsgaard (2013). "T-cell receptor affinity and avidity defines antitumor response and autoimmunity in T-cell immunotherapy." Proceedings of the National Academy of Sciences of the United States of America **110**(17): 6973-6978.

Zucman, J., T. Melot, C. Desmaze, J. Ghysdael, B. Plougastel, M. Peter, J. M. Zucker, T. J. Triche, D. Sheer, C. Turc-Carel and et al. (1993). "Combinatorial generation of variable fusion proteins in the Ewing family of tumours." The EMBO journal **12**(12): 4481-4487.

Zucman-Rossi, J., M. A. Batzer, M. Stoneking, O. Delattre and G. Thomas (1997). "Interethnic polymorphism of EWS intron 6: genome plasticity mediated by Alu retroposition and recombination." Hum Genet **99**(3): 357-363.

11 APPENDIX

11.1 PRIMER SEQUENCES

11.1.1 PRIMER SEQUENCES FOR VAB-REPERTOIRE ANALYSIS

P-5`αST	CTG TGC TAG ACA TGA GGT CT
P-3`αST	CTT GCC TCT GCC GTG AAT GT
3-TCα	GGT GAA TAG GCA GAC AGA CTT GTC ACT GGA
PanVα1	AGA GCC CAG TCT GTG ASC CAG S=C/G
PanVα1.1	AGA GCC CAG TCR GTG ACC CAG R=A/G
Vα2	GTT TGG AGC CAA CRG AAG GAG R=A/G
Vα3	GGT GAA CAG TCA ACA GGG AGA
Vα4	TGA TGC TAA GAC CAC MCA GC
Vα5	GGC CCT GAA CAT TCA GGA
Vα6new	GGT CAC AGC TTC ACT GTG GCT A
Vα7	ATG TTT CCA TGA AGA TGG GAG
Vα8	TGT GGC TGC AGG TGG ACT
Vα9	ATC TCA GTG CTT GTG ATA ATA
Vα10	ACC CAG CTG CTG GAG CAG AGC CCT
Vα11	AGA AAG CAA GGA CCA AGT GTT
Vα12	CAG AAG GTA ACT CAA GCG CAG ACT
Vα13	GAG CCA ATT CCA CGC TGC G
Vα14.1	CAG TCC CAG CCA GAG ATG TC
Vα14	CAG TCT CAA CCA GAG ATG TC
Vα15	GAT GTG GAG CAG AGT CTT TTC
Vα16	TCA CGC GAA GAT CAG GTC AAC
Vα17	GCT TAT GAG AAC ACT GCG T
Vα18	GCA GCT TCC CTT CCA GCA AT
Vα19	AGA ACC TGA CTG CCC AGG AA
Vα20	CAT CTC CAT GGA CTC ATA TGA
Vα21	GTG ACT ATA CTA ACA GCA TGT

Vα22	TAC ACA GCC ACA GGA TAC CCT TCC
Vα23	TGA CAC AGA TTC CTG CAG CTC
Vα24new	GAA CTG CAC TCT TCA ATG C
Vα25	ATC AGA GTC CTC AAT CTA TGT TTA
Vα26	AGA GGG AAA GAA TCT CAC CAT AA
Vα27	ACC CTC TGT TCC TGA GCA TG
Vα28	CAA AGC CCT CTA TCT CTG GTT
Vα29	AGG GGA AGA TGC TGT CAC CA
Vα30	GAG GGA GAG AGT AGC AGT
Vα31new	TCG GAG GGA GCA TCT GTG ACT A
Vα32	CAA ATT CCT CAG TAC CAG CA

P-5`βST	AAG CAG AGA TCT CCC ACA C
P-3βST	GAG GTA AAG CCA CAG TTG CT
P-3CβII	GAT GGC TCA AAC ACA GCG ACC TC
Vβ1	GCA CAA CAG TTC CCT GAC TTG GCA C
Vβ2	TCA TCA ACC ATG CAA GCC TGA CCT
Vβ3	GTC TCT AGA GAG AAG AAG GAG CGC
Vβ4	ACA TAT GAG AGT GGA TTT GTC ATT
Vβ5.1	ATA CTT CAG TGA GAC ACA GAG AAA C
Vβ5.2	TTC CCT AAC TAT AGC TCT GAG CTG
Vβ5.2T	TTC CCT AAT TAT AGC TCT GAG CTG
Vβ6.1new	GCC CAG AGT TTC TGA CTT ACT TC
Vβ6.2	ACT CTG ASG ATC CAG CGC ACA S=C/G
Vβ6.3	ACT CTG AAG ATC CAG CGC ACA
Vβ7	CCT GAA TGC CCC AAC AGC TCT C
Vβ8	ATT TAC TTT AAC AAC AAC GTT CCG
Vβ8S3	GCT TAC TTC CGC AAC CGG GCT CCT
Vβ9new	CCT AAA TCT CCA GAC AAA GCT
Vβ10	CTC CAA AAA CTC ATC CTG TAC CTT
Vβ11	TCA ACA GCT TCC AGA ATA AGG ACG
Vβ12	AAA GGA GAA GTC TCA GAT
Vβ12S3	GCA GCT GCT GAT ATT ACA GAT

Vβ13new	TCG ACA AGA CCC AGG CAT GG
Vβ13.1	CAA GGA GAA GTC CCC AAT
Vβ13.2	GGT GAG GGT ACA ACT GCC
Vβ13S5	ATA CTG CAG GTA CCA CTG GCA
Vβ14	GTC TCT CGA AAA GAG AAG AGG AAT
Vβ15	AGT GTC TCT CGA CAG GCA CAG GCT
Vβ16	AAA GAG TCT AAA CAG GAT GAG TCC
Vβ17	CAG ATA GTA AAT GAC TTT CAG
Vβ18	GAT GAG TCA GGA ATG CCA AAG GAA
Vβ19	CAA TGC CCC AAG AAC GCA CCC TGC
Vβ20	AGC TCT GAG GTG CCC CAG AAT CTC
Vβ21	AAA GGA GTA GAC TCC ACT CTC
Vβ22.1	CAT CTC TAA TCA CTT ATA CT
Vβ22.2	AAG TGA TCT TGC GCT GTG TCC CCA
Vβ22.3	CTC AGA GAA GTC TGA AAT ATT CG
Vβ23	GCA GGG TCC AGG TCA GGA CCC CCA
Vβ24new	ATC CAG GAG GCC GAA CAC TTC T

11.1.2 Primer sequences for restriction site synthesis (see 5.14.1)

EZH2_alpha_forw_NotI	TAGCGGCCGCCACCATGAAATCCTTGAGAG
EZH2_alpha_rev_EcoRI	TGGAATTCTCAGCTGGACCACAGCCGCAGC
EZH2_beta_forw_NotI	TAGCGGCCGCCACCATGAGCATCGGCCTCCTG
EZH2_beta_rev_EcoRI	TGGAATTCTCAGAAATCCTTTCTCTTGACC

EZH2_alpha_forw_EcoRI	TAGAATTCGCCACCATGAAATCCTTGAGAG
EZH2_alpha_rev_XhoI	TGCTCGAGTCAGCTGGACCACAGCCGCAGC
EZH2_beta_forw_EcoRI	TAGAATTCGCCACCATGAGCATCGGCCTCCTG
EZH2_beta_rev_XhoI	TGCTCGAGTCAGAAATCCTTTCTCTTGACC

11.1.3 Sequencing primers for pPCRScript constructs

T3	ATTAACCCTCACTAAAGGGA
T7	TAATACGACTCACTATAGGG

Primer sequences according to the manufacturer's information.

11.1.4 Sequencing primers for pMSCVneo constructs

pMSCVneo_forw	CCCTTGAACCTCCTCGTTCGACC
pMSCVneo_rev	GAGACGTGCTACTTCCATTTGTC

Primer sequences according to the manufacturer's information.

11.1.5 Sequencing primers for pMP71 constructs

Sequ_MP71_forward	TGAAAATTAGCTCGACAAAG
Sequ_MP71_reverse	GTAAATGATTGCCCCACCA

Primer design with the help of Sabine Mall, Technical University Munich.

11.1.6 Primer sequences for attachment of A- and B-chain (see 5.14.5)

EZH2_alpha_P2A_forw	TCTCTGTTAAAGCAAGCAGGAGACGTGGAAGAAAA CCCCGGTCCCATGAAATCCTTGAGAGTTTTACTGG
EZH2_beta_P2A_rev	GTCTCCTGCTTGCTTTAACAGAGAGAAGTTCGTGG CGCCGCTTCCGAAATCCTTTCTCTTGACCATGG

11.1.7 Primer Sequences for Detection of murinized and optimized transgenic TCR

EZH2_alpha_murine_forw	GTGCTGCTCGTGATCCTGT
EZH2_alpha_murine_rev	AGGGTCATCAGCAGGTTGAA
EZH2_beta_murine_forw	GTCTATCGGCCTGCTGTG

EZH2_beta_murine_rev	CCCAGCAGGATCTCGTACA
CHM1_alpha_murine_forw	CCGTGTTCATCTTCCTGT
CHM1_alpha_murine_rev	GGTCATCAGCAGATTGAA
CHM1_beta_murine_forw	GTCTCCAGATCTGCCTGA
CHM1_beta_murine_rev	ATCAGCACCAGGCCAGACA

11.2 TCR SEQUENCES

11.2.1 SEQUENCES OF EZH2-SPECIFIC TCR

UNMODIFIED SEQUENCE OF THE VARIABLE PART OF THE A-CHAIN (TRAV13-1*0).

ATGAAATCCTTGAGAGTTTTACTGGTGATCCTGTGGCTTCAGTTAAGCTGG
GTTTGGAGCCAACAGAAGGAGGTGGAGCAGGATCCTGGACCACTCAGTGT
TCCAGAGGGAGCCATTGTTTCTCTCAACTGCACTTACAGCAACAGTGCTTT
TCAATACTTCATGTGGTACAGACAGTATTCCAGAAAAGGCCCTGAGTTGCT
GATGTACACATACTCCAGTGGTAACAAAGAAGATGGAAGGTTTACAGCACA
GGTCGATAAATCCAGCAAGTATATCTCCTTGTTCATCAGAGACTCACAGCC
CAGTGATTCAGCCACCTACCTCTGTGCAATGAGCGATATAAACACCGGTAA
CCAGTTCTATTTTGGGACAGGGACAAGTTTGACGGTCATTCCAAAT

UNMODIFIED SEQUENCE OF THE VARIABLE PART OF THE B-CHAIN (TRBV6-5*01).

ATGAGCATCGGCCTCCTGTGCTGTGCAGCCTTGTCTCTCCTGTGGGCAGG
TCCAGTGAATGCTGGTGTCACTCAGACCCCAAAATTCCAGGTCCTGAAGA
CAGGACAGAGCATGACACTGCAGTGTGCCCAGGATATGAACCATGAATAC
ATGTCCTGGTATCGACAAGACCCAGGCATGGGGCTGAGGCTGATTCATTA
CTCAGTTGGTGCTGGTATCACTGACCAAGGAGAAGTCCCCAATGGCTACA
ATGTCTCCAGATCAACCACAGAGGATTTCCCGCTCAGGCTGCTGTCGGCT
GCTCCCTCCCAGACATCTGTGTACTTCTGTGCCAGCAGTTCCTACCCGGG
GCTCACTGCAACTAATGAAAAACTGTTTTTTGGCAGTGGAACCCAGCTCTC
TGTCTTGGAG

UNMODIFIED SEQUENCE OF A- AND B-CHAIN (INSERT "EZH2").

GCGGCCGCCACCATGAGCATCGGCCTCCTGTGCTGTGCAGCCTTGTCTCT
CCTGTGGGCAGGTCCAGTGAATGCTGGTGTCACTCAGACCCCAAAATTCC
AGGTCCTGAAGACAGGACAGAGCATGACACTGCAGTGTGCCCAGGATATG
AACCATGAATACATGTCCTGGTATCGACAAGACCCAGGCATGGGGCTGAG
GCTGATTCATTACTCAGTTGGTGCTGGTATCACTGACCAAGGAGAAGTCCC
CAATGGCTACAATGTCTCCAGATCAACCACAGAGGATTTCCCGCTCAGGCT
GCTGTCGGCTGCTCCCTCCCAGACATCTGTGTACTTCTGTGCCAGCAGTT
CCTACCCGGGGCTCACTGCAACTAATGAAAAACTGTTTTTTGGCAGTGGAA
CCCAGCTCTCTGTCTTGGAGGACCTGAACAAGGTGTTCCCACCCGAGGTC
GCTGTGTTTGAGCCATCAGAAGCAGAGATCTCCCACACCCAAAAGGCCAC
ACTGGTGTGCCTGGCCACAGGCTTCTTCCCTGACCACGTGGAGCTGAGCT
GGTGGGTGAATGGGAAGGAGGTGCACAGTGGGGTCAGCACGGACCCGCA
GCCCCTCAAGGAGCAGCCCGCCCTCAATGACTCCAGATACTGCCTGAGCA
GCCGCCTGAGGGTCTCGGCCACCTTCTGGCAGAACCCCCGCAACCACTT
CCGCTGTCAAGTCCAGTTCTACGGGCTCTCGGAGAATGACGAGTGGACCC
AGGATAGGGCCAAACCCGTCACCCAGATCGTCAGCGCCGAGGCCTGGGG
TAGAGCAGACTGTGGCTTTACCTCGGTGTCCTACC
AGCAAGGGGTCCTGTCTGCCACCATCCTCTATGAGATCCTGCTAGGGAAG
GCCACCCTGTATGCTGTGCTGGTCAGCGCCCTTGTGTTGATGGCCATGGT
CAAGAGAAAGGATTTCGGAAGCGGCGCCACGAACTTCTCTCTGTTAAAGC
AAGCAGGAGACGTGGAAGAAAACCCCGGTCCCATGAAATCCTTGAGAGTT
TTACTGGTGATCCTGTGGCTTCAGTTAAGCTGGGTTTGGAGCCAACAGAA
GGAGGTGGAGCAGGATCCTGGACCACTCAGTGTTCCAGAGGGAGCCATT
GTTTCTCTCAACTGCACTTACAGCAACAGTGCTTTTCAATACTTCATGTGGT
ACAGACAGTATTCCAGAAAAGGCCCTGAGTTGCTGATGTACACATACTCCA
GTGGTAACAAAGAAGATGGAAGGTTTACAGCACAGGTCGATAAATCCAGC
AAGTATATCTCCTTGTTCATCAGAGACTCACAGCCCAGTGATTCAGCCACC
TACCTCTGTGCAATGAGCGATATAAACACCGGTAACCAGTTCTATTTTGGG
ACAGGGACAAGTTTGACGGTCATTCCAAATATCCAGAACCCTGACCCTGC
CGTGTACCAGCTGAGAGACTCTAAATCCAGTGACAAGTCTGTCTGCCTATT
CACCGATTTTGATTCTCAAACAAATGTGTCACAAAGTAAGGATTCTGATGTG
TATATCACAGACAAAACTGTGCTAGACATGAGGTCTATGGACTTCAAGAGC

AACAGTGCTGTGGCCTGGAGCAACAAATCTGACTTTGCATGTGCAAACGC
CTTCAACAACAGCATTATTCCAGAAGACACCTTCTTCCCCAGCCCAGAAAG
TTCCTGTGATGTCAAGCTGGTCGAGAAAAGCTTTGAAACAGATACGAACCT
AAACTTTCAAAACCTGTCAGTGATTGGGTTCCGAATCCTCCTCCTGAAAGT
GGCCGGGTTTAATCTGCTCATGACGCTGC
GGCTGTGGTCCAGCTGAGAATTC

MURINIZED AND OPTIMIZED SEQUENCE CONTAINING A- AND B-CHAIN (INSERT "EZH2_MU_OPT").

CACTATAGGGCGAATTGGCGGAAGGCCGTCAAGGCCGCATGCGC
GGCCGCCACCATGTCTATCGGCCTGCTGTGTTGTGCCGCCCTGT
CCCTGCTGTGGGCCGGACCTGTGAATGCTGGCGTGACCCAGACC
CCCAAGTTCCAGGTGCTGAAAACCGGCCAGAGCATGACCCTGCA
GTGCGCCCAGGACATGAACCACGAGTACATGAGCTGGTACAGAC
AGGACCCCGGCATGGGCCTGCGGCTGATCCACTATTCTGTGGGA
GCCGGCATCACCGACCAGGGCGAAGTGCCCAATGGCTACAACGT
GTCCAGAAGCACCACCGAGGACTTCCCACTGCGGCTGCTGTCTG
CCGCCCCATCTCAGACCAGCGTGTACTTCTGTGCCAGCAGCAGCT
ACCCTGGCCTGACCGCCACCAACGAGAAGCTGTTCTTTGGCAGC
GGCACCCAGCTGAGCGTGCTGGAAGATCTGAGAAACGTGACCCC
CCCCAAGGTGTCCCTGTTCGAGCCTAGCAAGGCCGAGATCGCCA
ACAAGCAGAAAGCCACCCTCGTGTGCCTGGCCAGAGGCTTCTTC
CCCGACCACGTGGAACTGTCTTGGTGGGTCAACGGCAAAGAGGT
GCACAGCGGCGTGTCCACCGATCCCCAGGCCTACAAAGAGAGCA
ACTACAGCTACTGCCTGAGCAGCAGACTGCGGGTGTCCGCCACC
TTCTGGCACAACCCCCGGAACCACTTCAGATGCCAGGTGCAGTTT
CACGGCCTGAGCGAAGAGGACAAGTGGCCCGAGGGCAGCCCTAA
GCCCGTGACACAGAATATCAGCGCCGAAGCCTGGGGCAGAGCCG
ACTGTGGAATCACCAGCGCCAGCTACCATCAGGGCGTGCTGAGC
GCCACCATCCTGTACGAGATCCTGCTGGGCAAGGCCACCCTGTA
CGCCGTGCTGGTGTCTGGCCTGGTGCTGATGGCCATGGTCAAGA
AGAAGAACAGCGGCAGCGGCGCCACCAATTTCAGCCTGCTGAAA
CAGGCCGGCGACGTGGAAGAGAACCCTGGCCCTATGAAGTCCCT

GCGGGTGCTGCTCGTGATCCTGTGGCTGCAGCTGAGCTGGGTGT
GGTCCCAGCAGAAAGAGGTGGAACAGGACCCAGGCCCCCTGTCT
GTGCCTGAAGGCGCCATCGTGTCCCTGAATTGCACCTACAGCAAC
AGCGCCTTCCAGTACTTCATGTGGTACAGGCAGTACAGCCGGAAG
GGCCCCGAGCTGCTGATGTACACCTACTCCAGCGGCAACAAAGA
GGACGGCCGGTTCACAGCCCAGGTGGACAAGAGCAGCAAGTACA
TCTCCCTGTTCATCCGGGACAGCCAGCCCAGCGATAGCGCCACA
TACCTGTGCGCCATGAGCGACATCAACACCGGCAACCAGTTCTAC
TTCGGCACCGGCACCAGCCTGACCGTGATCCCCAACATCCAGAA
CCCCGAGCCCGCCGTGTATCAGCTGAAGGACCCCAGAAGCCAGG
ACAGCACCCTGTGCCTGTTCACCGACTTCGACAGCCAGATCAACG
TGCCCAAGACCATGGAAAGCGGCACCTTCATCACCGATAAGACCG
TGCTGGACATGAAGGCCATGGACAGCAAGAGCAACGGCGCCATT
GCCTGGTCCAACCAGACCAGCTTCACATGCCAGGACATCTTCAAA
GAGACAAACGCCACCTACCCCAGCAGCGACGTGCCCTGTGATGC
CACCCTGACCGAGAAGTCCTTCGAGACAGACATGAATCTGAACTT
CCAGAACCTGAGCGTGATGGGCCTGAGAATCCTGCTGCTGAAGG
TGGCCGGCTTCAACCTGCTGATGACCCTGAGACTGTGGTCCAGCT
GATGAGAATTCCGCTGGGCCTCATGGGCCTTCCGCTCACTGCCC
GCTTTCCAG

11.2.2 SEQUENCE OF CHM1-SPECIFIC TCR

UNMODIFIED SEQUENCE OF THE VARIABLE PART OF THE A-CHAIN (TRAV13-1*02).

ATGACATCCATTCGAGCTGTATTTATATTCCTGTGGCTGCAGCTGGACTTG
GTGAATGGAGAGAATGTGGAGCAGCATCCTTCAACCCTGAGTGTCCAGGA
GGGAGACAGCGCTGTTATCAAGTGTACTTATTCAGACAGTGCCTCAAACTA
CTTCCCTTGGTATAAGCAAGAACTTGGAAAAAGACCTCAGCTTATTATAGA
CATTCGTTCAAATGTGGGCGAAAAGAAAGACCAACGAATTGCTGTTACATT
GAACAAGACAGCCAAACATTTCTCCCTGCACATCACAGAGACCCAACCTGA
AGACTCGGCTGTCTACTTCTGTGCAGCAAGCGCTGGAGGAAGCCAAGGAA
ATCTCATCTTTGGAAAAGGCACTAAACTCTCTGTTAAACCAAAT

Unmodified sequence of the variable part of the B-chain (TRBV13*01).

ATGCTTAGTCCTGACCTGCCTGACTCTGCCTGGAACACCAGGCTCCTCTG
CCGTGTCATGCTTTGTCTCCTGGGAGCAGGTTCAGTGGCTGCTGGAGTCA
TCCAGTCCCCAAGACATCTGATCAAAGAAAAGAGGGAAACAGCCACTCTG
AAATGCTATCCTATCCCTAGACACGACACTGTCTACTGGTACCAGCAGGGT
CCAGGTCAGGACCCCCAGTTCCTCATTTCGTTTTATGAAAAGATGCAGAGC
GATAAAGGAAGCATCCCTGATCGATTCTCAGCTCAACAGTTCAGTGACTAT
CATTCTGAACTGAACATGAGCTCCTTGGAGCTGGGGGACTCAGCCCTGTA
CTTCTGTGCCAGCAGCTTTCTGGGGGAAAAAACTGAAGCTTTCTTTGGACA
AGGCACCAGACTCACAGTTGTAGAG

Murinized and optimized sequence containing A- and B-chain (insert “CHM1_mu_opt“).

CACTATAGGGCGAATTGGCGGAAGGCCGTCAAGGCCGCATGCGCGGCCG
CCACCATGCTGTCTCCAGATCTGCCTGACAGCGCCTGGAACACCCGGCTG
CTGTGCAGAGTGATGCTGTGCCTGCTGGGAGCCGGATCTGTGGCTGCTG
GCGTGATCCAGAGCCCCAGACACCTGATCAAAGAGAAGAGAGAGACAGC
CACCCTGAAGTGCTACCCCATCCCCAGGCACGACACCGTGTACTGGTATC
AGCAGGGCCCAGGCCAGGACCCCCAGTTCCTGATCAGCTTCTACGAGAA
GATGCAGAGCGACAAGGGCAGCATCCCCGACAGATTCAGCGCCCAGCAG
TTCAGCGACTACCACAGCGAGCTGAACATGAGCAGCCTGGAACTGGGCGA
CAGCGCCCTGTACTTCTGCGCCTCTAGCTTCCTGGGCGAGAAAACCGAGG
CATTCTTTGGGCAGGGCACCAGACTGACCGTGGTGGAAGATCTGCGGAAC
GTGACCCCCCCCCAAGGTGTCCCTGTTCGAGCCTAGCAAGGCCGAGATCG
CCAACAAGCAGAAAGCCACACTCGTGTGCCTGGCCAGAGGCTTCTTCCCC
GACCACGTGGAACTGTCTTGGTGGGTCAACGGCAAAGAGGTGCACAGCG
GCGTGTCCACCGATCCTCAGGCCTACAAAGAGAGCAACTACAGCTACTGC
CTGAGCAGCAGACTGCGG

GTGTCCGCCACCTTCTGGCACAACCCCCGGAACCACTTCAGATGCCAGGT
GCAGTTTCACGGCCTGAGCGAAGAGGACAAGTGGCCCGAGGGCAGCCCT
AAGCCCGTGACCCAGAATATCTCTGCCGAGGCCTGGGGCAGAGCCGACT
GTGGAATTACCAGCGCCAGCTACCACCAGGGCGTGCTGTCTGCCACCATC
CTGTACGAGATCCTGCTGGGCAAGGCCACCCTGTACGCCGTGCTGGTGTC
TGGCCTGGTGCTGATGGCCATGGTCAAGAAGAAGAACAGCGGCAGCGGC
GCCACCAACTTCAGCCTGCTGAAACAGGCCGGCGACGTGGAAGAGAACC
CTGGCCCTATGACCAGCATCCGGGCCGTGTTCATCTTCCTGTGGCTGCAG
CTGGACCTCGTGAACGGCGAGAACGTGGAACAGCACCCCAGCACCCTGA
GCGTGCAGGAAGGCGATAGCGCCGTGATCAAGTGCACCTACAGCGACTC
CGCCAGCAACTACTTCCCCTGGTACAAGCAGGAACTGGGAAAGCGGCCC
CAGCTGATCATCGACATCCGGTCCAACGTGGGAGAGAAGAAGGACCAGC
GGATCGCCGTGACCCTGAACAAGACCGCCAAGCACTTCTCCCTGCACATC
ACCGAGACACAGCCCGAGGACTCCGCCGTGTACTTTTGTGCCGCTTCTGC
CGGCGGATCCCAGGGCAATCTGATCTTCGGCAAGGGCACCAAGCTGAGC
GTGAAGCCCAACATCCAGAACCCCGAGCCTGCCGTGTACCAGCTGAAGGA
CCCCAGAAGCCAGGACTCCACCCTGTGCCTGTTCACCGACTTCGACAGCC
AGATCAACGTGCCCAAGACCATGGAATCCGGCACCTTCATCACCGACAAG
ACCGTGCTGGACATGAAGGCCATGGACAGCAAGAGCAACGGCGCCATTG
CCTGGTCCAACCAGACCAGCTTCACATGCCAGGACATCTTCAAAGAGACA
AACGCCACCTACCCCAGCAGCGACGTGCCCTGTGATGCCACACTGACCGA
GAAGTCCTTCGAGACAGACATGAACCTGAACTTCCAGAACCTGTCCGTGAT
GGGCCTGAGAATCCTGCTGCTGAAGGTGGCCGGCTTCAATCTGCTGATGA
CCCTGCGGCTGTGGTCCTCCTGATGAGAATTCCGCTGGGCCTCATGGGCC
TTCCGCTCACTGCCCGCTTTCCAG

12 ACKNOWLEDGEMENTS

I would like to thank the whole working group at the Laboratory for Functional Genomics and Transplantation Biology (Children's Cancer Research Center and Department of Pediatrics, Technical University Munich), especially the head of the clinic, Stefan Burdach, and the head of the laboratory Guenther Richter. My thanks go to Kristina Hauer, Melanie Thiede, Andreas Kirschner, Thomas Gruenewald, Colette Zobywalski and Stefan Pirson and especially my thesis supervisor Uwe Thiel. It was a pleasure to work with you.

I would like to thank all of our cooperating working groups: Angela Krackhardt, Richard Klar and Sabine Mall (Medizinische Klinik III, Klinikum Rechts der Isar, Technical University Munich) provided us with vectors, insert construction and transduction protocols. Markus Niemeyer (Department of Gynecology, Klinikum rechts der Isar, Technical University Munich) supplied us with cord blood samples. Dirk Busch, Bianca Weißbrich and Lunette Henkel (Institute for Medical Microbiology, Immunology and Hygiene, Technical University Munich) helped us with FACS, provided us with multimers and the according protocols. Stanley Riddell (Department of Medicine, University of Washington, Seattle, WA 98104, USA) supplied us with NSO-IL-15 cells. Wolfgang Uckert and Matthias Leisegang (Max Delbrück Center for Molecular Medicine, Berlin) helped us with murinization and codon-optimization of the TCR constructs. Katja Steiger (Institute of Pathology of the Technical University Munich) performed pathological evaluation of *in vivo* tumors.

I thank all of you for being part of this work!